The Production and Structural Behavior
of High-Strength Concrete

by

ALI NIKAEEN

B.S.C.E., Kansas State University, 1979

A MASTER'S THESIS

submitted in partial fulfillment of the

requirements for the degree

MASTER OF SCIENCE

Department of Civil Engineering

KANSAS STATE UNIVERSITY
Manhattan, Kansas

1982

Approved by:

Stuart E Swartz
Major Professor

TABLE OF CONTENTS

TABLE OF CONTENTS (continued)

TABLE OF CONTENTS (continued)

LIST OF TABLES

LIST OF TABLES (continued)

LIST OF FIGURES

LIST OF FIGURES (continued)

LIST OF FIGURES (continued)

Chapter 1

INTRODUCTION

Concrete with higher than normal strength is a part of the precast or the prestressed concrete industry, because they have special manufacturing processes such as using combined high pressure and vibration. But today, there is a growing interest in using high-strength, site-mixed concrete or ready-mixed concrete because of the availability of water-reducing agents, especially super-plasticizers, which give adequate workability for low water-cement ratio mixes. These mixes can be used in cast-in-place structures.

It has been shown that concrete having a uniaxial compressive strength from 6000 to 12000 psi (41 to 83 MPa) can be produced using conventional materials and production methods. These methods are economically and technically adequate. Concrete with strength in excess of 6000 psi is commonly called high-strength concrete.

Objective

The objective of this paper is to report on a research project on high-strength concrete at Kansas State University which was carried out in the Civil Engineering Department. The specific purposes of this paper are: a) to present results of a study of techniques for production of high-strength concrete and methods for selecting the materials and their proportions for mix design. The suitability of Kansas aggregate for producing high-strength concrete was also investigated; b) to study the compressive and flexural behavior of high-strength concrete made with Kansas aggregate in order to verify proposed stress-strain relations and to determine the shape of the compressive stress block. It was desired to determine whether the shape of the stress block is generally rectangular or triangular.

Present Usage

One of the main reasons for using high-strength concrete is that it has greater load-carrying capacity compared to normal strength concrete which means: 1) it has the potential to carry more load at lower cost; 2) the dimensions of the member reduce, therefore the dead load of the member reduces and consequently the dead load of the structure reduces. This is especially advantageous for prestressed concrete and compression members. Here it should be emphasized that high-strength concrete cannot improve all designs. For example, slabs can be made very thin by using high-strength concrete but there will be problems with excessive deflection.

Recent structures for which high-strength concrete has been used in their construction are: a) a 50-story office tower used 8000 psi (55.1 MPa) concrete (1); b) the Waterways Experiment Station (WES) developed 10000 psi (68.9 MPa) concrete for the Air Force 15 years ago to be used in underground silos (2); c) about 10 years ago 10000 psi (68.9 MPa) concrete was used in the Willows Bridge in Toronto (3); d) the O'Hare Airport terminal in Chicago used 8000 psi (55.1 MPa) concrete in prestressed roof-girders (3); e) prestressed concrete containment vessels for nuclear reactors in England and France were constructed using 9000 psi (62 MPa) concrete (3).

The most extensive use of high-strength concrete in building construction has been in the Chicago area where concrete up to

10000 psi (68.9 MPa) was in at least six different buildings (4). In 1972, 9000 psi concrete was used in 20 stories of the 50-story Mid-Continental Plaza building in Chicago. High-strength concrete has been used after that in the Chicago area building industry including the Frontier Tower, the Marriot Chicago building, the 200 W. Monroe building, and the Water Tower Place building.

Chapter 2

SELECTION OF MATERIAL

Introduction

In production of high-strength concrete, one should look for highest quality materials. From the economical point of view the suitability of locally available materials should be considered in developing the mix design. When producing good-quality, high-strength concrete, one should optimize the use of mixing materials. Once an optimum or near optimum condition is established for a material, it should be kept fixed in the mix design as the remaining variables are studied. Then one can develop an optimum mix for the available material on the basis of strength, cost and field performance.

Cement

Cement is one of the most important components of the concrete. Therefore it should be valid to say that stronger cement makes stronger concrete. In some European countries there are different grades of cement for different strength ranges from which a concrete producer can choose (3). In North America, even though there are not different grades of cement for normal Portland cement, there are differences in cement strength from plant to plant due to the lack of uniformity of production.

Walker and Bloem presented values of compressive strength for concrete from different cement suppliers and offered the following conclusions (See Ref. 3):

a) Average strength for different cement varied substantially.

b) At least one-half of the individual cement differs from shipment to shipment sufficiently to have an effect on uniformity of concrete strength.

c) There is a need for better control of uniformity of the cement production within individual sources.

There are a few factors that are considered in choosing the right grade of cement; type, chemical composition, fineness and cube strength (by ASTM Standard Method of Test C-109 [22]). Compatability of cement with the admixture should be checked by testing for false and flash set. In general, the selection of cement for high-strength concrete should be based on comparative strength test of trial mixes. Research done at Portland Cement Association laboratories has indicated that the chemical composition and fineness of cement significantly influence the strength in the concrete (21). But there is no certain rule in the United States that classifies the cements according to strength-producing capabilities. The only guideline which is available today has been provided by ASTM C-150 (19), which separates the cement into different types. Therefore the mix-designer should develop certain limits on the composition of the cement. Several studies (3,5) show that even within one type of cement, due to nonuniformity, the differences in water requirements can be as large as that between different types of cement. Tests at Cornell University show up to 22 percent difference in concrete strength using Type I cement and the same workability (3). This is also shown in Figure 2.1 (5). In Figure 2.2, Blick (6) shows the effect of different types of cement on concrete compressive strength based on mixes that have the same workability. Figure 2.2 shows that Type I cement gives highest compressive strength at all ages. Concrete made with Type I and Type II cements yield higher strength than Type III cement because of the increase in water requirement for the same workability. As the water-cement ratio and workability decrease to an allowable minimum, Type I and Type II cements prove to be more suitable for higher strength concrete than any other type.

It is recommended that the final decision on the brand of cement always be based on strength-producing capability in concrete mixture of the same workability at ages 28, 56 and 91 days. In the present investigation, Type I cement was used.

Coarse Aggregate

The selection of coarse aggregate for high strength concrete is the next most important item after choosing cement. The behavior of coarse aggregate has a great influence on concrete strength. Kaplan (23) has reported that the use of different type of coarse aggregate in a given concrete mixture resulted in variation in the compressive of as much as 29 percent.

The strength up to 5000 psi (34.5 MPa) depends essentially on the quality of the hardened cement paste that holds the aggregate particles together. The aggregate at this strength level and above always has a much greater strength than the cement paste. It is important to consider the following factors when selecting a coarse aggregate for high-strength concrete:

a) strength

b) maximum size and gradation

c) particle shape and surface texture

d) cleanliness

e) mineralogy and formation

f) aggregate-cement bond.

Strength

The aggregate chosen for high-strength concrete should have a crushing strength at least equal to the hardened cement paste. Because most good quality aggregate has a crushing strength in excess of 12000 psi (83 MPa), this factor is not a major problem for the production of high-strength concrete.

Maximum Size and Gradation

Several researchers (7,8,9) have shown that in high-strength concrete the compressive strength increases when the maximum size of aggregate decreases. However, it is obvious that there should be some limitation in order to keep drying shrinkage and creep to a reasonable and practical value. A maximum size of 0.4 in. (10 mm) is recommended for most cases (10). Figures 2.3 and 2.4 show the size effect of coarse aggregate on compressive strength. In Figure 2.4 it is indicated that the smaller size aggregate provides the most efficient use of cement in high-strength concrete. This higher strength efficiency which is obtained when using smaller aggregate is due to greater bond between the cement and coarse aggregate because of the increase in the surface area. However there is a different optimum size for each aggregate and for each level of strength desired, depending on the economics of the situation. Therefore trial batching for each job is highly recommended.

Particle Shape and Surface Texture

In a research done by Carrasquillo (3), he indicated that the ideal coarse aggregate for high-strength concrete appears to be a clean, cubical, angular, 100 percent crushed stone with minimum flat size and elongated particles. He also said if all other factors are equal, crushed stone coarse aggregate produces higher strength concrete than does a rounded aggregate. In Figures 2.5 and 2.6, the compressive strength of concrete using different types of coarse aggregate is shown.

Cleanliness

Coarse aggregate used in high-strength concrete should be free of dust coating, because the dust content causes an increase in the fines, and consequently an increase in the water requirement of the resulting concrete mixture. Hence, the water-cement ratio increases and the strength decreases. Washing the crushed stone coarse aggregate may not always be necessary, but is always recommended (11).

Mineralogy and Formation

As discussed above, the compressive strength of concrete increases when using crushed stone as the coarse aggregate. This is not only because of the shape of the aggregate but also due to its mineralogy. The Waterways Experiment Station has done some work on the effect of mineralogy on concrete strength. They achieved 17000 psi (117 MPa) using granite rock (2).

Aggregate-Paste Bond

When high-strength concrete is desired, the aggregate-paste bond should be strong; a good quality aggregate with a suitable surface texture should be used.

The aggregate-paste bond is known to decrease with increasing water-cement ratio and increasing the size of aggregate. Alexander (12) found that the cement-aggregate bond to a 3 inch particle was almost 1/10 of that to a corresponding 1/2 inch particle.

In this investigation based on the availability of certain coarse aggregates, two types of coarse aggregates were chosen:

1. Limestone with 3/8 inch maximum size from Lenexa, Kansas.
2. Quartzite stone with 3/4 inch maximum size from Lincoln, Kansas.

Both types of coarse aggregates were made as dust free as possible by washing them. A sieve analysis on both types of coarse aggregates was done. The results are given in Tables 2.1 and 2.2. The values in Tables 2.1 and 2.2 are shown graphically in Figures 2.7 and 2.8 for limestone and quartzite, respectively, in order to get a relationship between the percent passing and the size of particle.

Fine Aggregate

The gradation and particle shape of fine aggregate are very important factors in production of high-strength concrete. Fine aggregate has a great effect on the water requirement and consequently the strength of the concrete mix. In sand of the same grading, a 1 percent increase in fine aggregate voids may cause a 1 gallon per cubic yard increase in water demand (13).

One of the important functions of fine aggregate in conventional concrete is its role in providing workability and good surface finishing. Since high-strength concrete contains large amounts of cement paste, the role of fine aggregate in providing workability and good finishing is not so crucial. Fine aggregates with a fineness modulus between 2.7 and 3.2 have been most satisfactory (15). Blick (6) reported that fine aggregate with fineness modulus below this range might produce low-strength and "sticky" mixes. A reduction of the amount passing the No. 50 and No. 100 sieve on the lower side of the specification limit from ASTM C-33 is suggested. Such reductions have shown increase in compressive strength of 500 to 1000 psi (3.5 to 7.0 MPa) (14).

In this investigation, Kaw River sand with a maximum sieve size of No. 4 was used. The sieve analysis was done on fine aggregate and results are in Table 2.3 and Figure 2.9.

Table 2.4 shows a comparison between recommended fine aggregate gradation for high-strength concrete, the recommended gradation given in ASTM C-33 and the fine aggregate gradation used in this investigation.

Water

Studies (5,13) have shown that water meeting specification ASTM C-94 (19) has no harmful effect on high-strength concrete. Therefore, water meeting ASTM C-94 is adequate.

Admixture

Due to low water-cement ratio, high-strength concrete has low slump and workability is not adequate. A chemical admixture called superplasticizer or "super water reducer" can be used to improve workability and slump. This admixture actually reduces the angle between the water and surface of contact and causes the mix to be more workable. It is important to note that this effect is for a limited time and the mix changes to its original property after a short time. Therefore, superplasticizer increases the slump within a limited time without altering the compressive strength, because the slump will go back to original position as if no admixture was used in the mix. Figure 2.10 shows the effect of superplasticizer on the slump versus time on a mix with water-cement ratio of 0.35. It is believed to have similar effect on all other mixes. Twelve fluid ounces of admixture per sack of cement were used. Usually the manufacturing company gives certain limits as to how many fluid ounces of dosage should be used. With a trial mix using different amounts of superplasticizer within the limit, one can optimize the use of superplasticizer. In this investigation, the brand of superplasticizer used was Sikament. When other brands are used, trial mixing is recommended. As is shown in Figure 2.10, the slump decreases very rapidly with time, therefore it is important to consider this effect on the job site.

Chapter 3

PROPORTIONING, MIXING, TESTING

Introduction

The objective of proportioning the high-strength concrete is to obtain a material that not only possesses the desired plastic properties (workability, finishability, etc.), but also achieves the desired strength at lowest cost possible. Careful proportioning is more critical for high-strength concrete than for normal-strength concrete, since optimum performance is required from each component used. Of course, in the present investigation, the cost effect is not of great concern.

Proportioning

In order to obtain the weight of components (coarse aggregate, fine aggregate, cement, water, etc.) the unit volume method with two different approaches is used.

Approach I - In this approach the amount of fine aggregates is a percent of total aggregates, namely 25 percent, 50 percent and 75 percent. For every water-cement ratio different sand contents are used. The workability is the basis for comparison. The slump is kept between 2 1/2 inches to 3 1/2 inches for this purpose. The details of calculation are given in Appendix II-A for one value of sand content, others are similar.

Approach II - Actually, Approach II is a special case of Approach I. In this approach the sand content is being optimized. It is understood that the more dense the concrete, the higher is the value of strength. Since aggregate particles occupy a large portion of the volume in a mix, they have the most effect on the density of the concrete. In this investigation, the ratio of fine to coarse aggregate is optimized in order to get the densest value of combined aggregate possible (Figures 3.1 and 3.2 show the optimization of limestone and quartzite stone with fine aggregate, respectively). From the graph for optimum density one can read the percent fine aggregate of the total aggregate. Knowing this value and the specific gravity for both fine and coarse aggregate, the volume occupied by total aggregate can be determined. Assuming a unit volume for the mix, the volume of paste (i.e., the volume of water + volume of cement) can be determined. Knowing the volumes, the specific gravities and water-cement ratio, the weight of all the components can be determined (Appendix II-B shows the details of calculation with an example). A few trials need to be done in order to achieve the desired workability. The reason for this is due to the assumption that no air voids exist which is incorrect.

Water-Cement Ratio

To obtain high-strength concrete, using a given set of materials, the lowest possible water-cement ratio should be used together with a minimum amount of mixing water (3). Blick (6) states that the water-cement ratio is the next most important factor affecting the producibility of high-strength concrete, after the selection of the optimum strength-producing materials has been made.

In this investigation, water-cement ratios of 0.4, 0.35, and 0.3 were tried. The slump of mixes was between 2 1/2 inches to 3 1/2 inches. The mix details are given in Tables 3.1 and 3.2 for limestone and quartzite, respectively. The components were mixed together, and after the cement was wet, superplasticizer was added to the mix. The time from starting of mixing action to measuring the slump was approximately the same for all mixes.

Casting and Testing

The cylinder samples were cast by rodding three layers for every cylinder and vibrating them for 30 seconds. They were taken out of the mold and were put in the curing room one day after they were poured. Compressive tests were done at 7, 14 and 28 days. The results are given in Tables 3.3 to 3.5 for Approach I (in Approach I only limestone was used) and in Tables 3.6 and 3.7 for limestone and quartzite, respectively, for Approach II.

Graph 3.3 indicates the effect of water-cement ratio on strength of concrete. The lower the water-cement ratio the stronger the mix. Figure 3.4 shows how sand content effects the compressive strength of concrete. This figure indicates that sand content affects mixes differently as water-cement ratio changes. The effect is not linear.

Chapter 4

LITERATURE SURVEY FOR COMPRESSIVE STRESS BLOCK

Introduction

The equivalent rectangular stress block permitted by American Concrete Institute Code "ACI 318-77" (20) was based on beam tests with concrete strengths in the range of 3000 psi (21 MPa) to 6000 psi (41 MPa). For beams with concrete strength in excess of 21000 psi (145 MPa), the current Code provisions would call for a zero-depth rectangular stress block, an obvious fallacy ($a = \beta_1 c$ - in 1975 a lower limit of β_1 equal to 0.65 was adopted for concrete strength greater than 8000 psi). Therefore, there is a very strong need to evaluate the concept of the rectangular stress block for high-stress concrete.

Objective

The publications concerning high-strength concrete are not only limited but also they contradict each other. For example, in the work done by Leslie, Rajagopalan and Everard (15), they recommended:

"1. The ACI building code rectangular stress block does not predict the behavior of beams with f'_c above 8000 psi (55 MPa).

2. Further research is warranted with respect to maximum strain in the concrete for f'_c exceeding 8000 psi (55 MPa).

3. Pending further tests, a triangular stress block with the extreme fiber stress at f'_c and zero stress at neutral axis is recommended as a conservative model for predicting the behavior of beam with f'_c above 8000 psi (55 MPa)."

But in the work done by Wang, Shah, Naaman (16), they concluded:

"1. Rectangular stress distribution gives sufficiently accurate prediction of the ultimate loads and moments of reinforced concrete beams and columns made with high-strength concrete.

2. The value of the maximum concrete compressive strain at ultimate was always higher than 0.003 in."

Therefore more tests with application of different methods should be done in order to check which theory is valid. In other words, to check if the ACI Code is valid for high-strength concrete or not.

Choosing the Method

In 1955, Hognestad, Hanson and McHenry (17) worked on a research project in order to formulate a ultimate strength design criterion for concrete. In their work, they derived some equations and used a special c-shape structural element. They had an important role in developing the ultimate design theory and their work was one of the main bases for developing the ACI Code for ultimate strength theory. They formulated stress in concrete fibers as a function of strain in those fibers. They also showed that stress-strain relationships for concrete in concentric compression are indeed applicable to flexure (Figure 4.1 shows this fact). They defined K_1, K_2 and K_3 as ultimate strength coefficients (Shown in Figure a, Appendix II-E). In their paper they developed equations which permitted stress to be expressed in terms of measured strain and other known parameters:

$$f_c = \varepsilon_c \frac{df_o}{d\varepsilon_c} + f_o \quad \text{------------------------------------} \quad (4.1)$$

$$f_c = \varepsilon_c \frac{dm_o}{d\varepsilon_c} + 2\, m_o \quad \text{----------------------------------} \quad (4.2)$$

$$f_o = \frac{P_1 + P_2}{bc} \qquad (4.3)$$

$$m_o = \frac{P_1a_1 + P_2a_2}{bc^2} \qquad (4.4)$$

where

f_c = concrete compressive stress in outer fiber of the beam

ε_c = concrete strain in outer fiber of the beam

P_1 = major thrust

P_2 = minor thrust

a_1 and a_2 are lever arms

b is width and c is depth of testing region

The details are shown in Figures 4.2 and 4.3.

In this investigation, their method and analogy are applied very closely in order to investigate the behavior and shape of the stress block in high-strength concrete beam sections.

Structural Element

The shape of the structural elements are similar to those used by McHenry (i.e., c-shape structural element) as shown in Figures 4.2 and 4.3. Suitable shear, bending and diagonal tension reinforcement was placed in the end bracket to obtain failure in the central unreinforced test region. The test region was 16 inches long and such reinforcement ended at the beginning of the test region. The detail of reinforcement design is shown in Appendix II-C and Figures 4.4 to 4.7. Due to limiting capacity of the testing machine, the cross-section of the test region for the higher strength mix was reduced. The depth changed from 8 in. to 5 in. The cross sections were 5 x 8 in. for Specimen I and 5 x 5 in. for Specimen II. The test prisms were 5 x 8 x 16 in. and 5 x 5 x 16 in., correspondingly.

Chapter 5

EXPERIMENTAL WORK AND RESULTS

Casting

The specimens were cast horizontally on a level surface. Vibration was used to consolidate the concrete. The surface was finished (high-strength concrete is more diffficult to finish than normal strength concrete because the superplasticizer made the concrete very cohesive). The minimum cover was 3/8 in. The mix designs 2 and 3 of Table 3.2 were used for Specimen I and Specimen II, respectively. Some 3 x 6 in. cylinders were cast at the same time with each mix.

Curing

The elements were taken out of the mold after twenty-four hours. They were placed in a 100% humidity curing room. Specimen I was in the curing room for 32 days and Specimen II was in the curing room for 37 days. The specimens were taken out of the curing room and were kept in a 50 percent humidity environment for 15 and 10 days in order to prepare them for the test. Table 5.1 shows the details. Cylinders corresponding to each specimen were taken out at the same time with corresponding specimen.

Instrumentation and Apparatus

Ten 2.4 in. long electrical resistance strain gages were used to measure the strain in the test region. Their location can be seen in Figures 4.2 and 4.3. A data acquisition system consisting of a switch balance unit and transducer strain indicator Model HW1-D was used to measure the strain in all the strain gages.

The major load P_1, Figures 4.2 and 4.3, is applied by a 300,000 lb. testing machine through a system of bearing plate and rollers. The minor load P_2 is applied by a hydraulic jack through a steel frame shown in Appendix II-D. The load was controlled by a pressure gage system which was calibrated prior to the test. The test set-up is shown in Figure 5.20.

Test Procedure

The objective was to load in a manner such that the neutral axis coincided with the outside face of the specimens as shown in Figures 4.2 and 4.3. After each increment of the major thrust P_1, the minor thrust P_2 was adjusted so that the average strain across the neutral surface was approximately zero (as measured). Load and strain at each level were recorded and the procedure repeated up to failure. The approximate zero strain surface represents the neutral axis of a flexural member while the opposite side of the cross-section represents the extreme compressive surface. The recorded data for Specimen I are shown in Table 5.5. In this table the load and strain for each strain gage are given. The average strain at each level is given as a function of load in Table 5.6. Two strain gages were mounted on two 3 x 6 in. cylinders corresponding to Specimen I and strain was recorded as a function of load up to failure. The data are given in Tables 5.3 and 5.4. Also, six 3 x 6 in. cylinders corresponding to Specimen I were tested on the same day that the structural element was tested in order to determine the strength of the mix. The results are given in Table 5.2 where it is indicated that the strength of the mix corresponding to Specimen I is f'_c = 8400 psi (58 MPa).

The corresponding data for Specimen II are given in Tables 5.7 to 5.10. As it is indicated in Table 5.7, the strength of the mix related to Specimen II is f'_c = 9400 psi (65 MPa).

Results and Discussion of the Results

The average values of cylinder stress-strain data of Tables 5.3 and 5.4 plotted in Figure 5.1 correspond to Specimen I. In the same manner, values of Table 5.8 are plotted in Figure 5.2 for Specimen II. The stress value at each level of the test Specimen I can be determined directly by using the strain values for flexural test which are indicated in Table 5.6 and Figure 5.1 (for each strain value, from the cylinder stress-strain curve, one can read a stress value [17]). The shape of the stress block for each increment of load can be determined for Specimen II by using Table 5.10 and Figure 5. The shape of stress block is shown in Figure 5.3 and 4 for various load increments for test Specimens I and II. The strain variation along the depth of test specimen can be shown for each load increment by plotting depth versus strain. The strain variations along the depth are shown in Figures 5.5 and 5.6 for Specimens I and II, using Tables 5.6 and 5.10, respectively. The values of the flexural strains for Specimen I are plotted in Figures 5.7 to 5.11 for every two gages that are in the same level using Table 5.5. This was done in order to check the accuracy of the test set-up. The graphs show that near failure, the strain reading in the gages diverge at each level. This is believed to be due to a twisting action which is introduced by set-up error. It was tried to prevent or improve this error for test Specimen II. These graphs are not shown for Specimen II, but it is believed that they would be very similar in nature.

To determine the ultimate strength factor, K_1, K_2, K_3, the equilibrium concept is used. The detail is shown in Appendix II-E. By equilibrium of forces and moment from Figure 5.16, K_1K_3 and K_2 can be determined.

$$K_1K_3 = \frac{C}{bc\ f_c'} = \frac{P_1 + P_2}{bc\ f_c'} \quad \text{------------------------} \quad (5.1)$$

$$K_2 = 1 - \frac{P_1a_1 + P_2a_2}{(P_1 + P_2)c} \quad \text{------------------------} \quad (5.2)$$

The values of K_1K_3, K_2 and $\frac{K_2}{K_1K_3}$ can be directly measured from zero up to failure. The individual value of the coefficient K_3 is the ratio of maximum compressive stress in the beam (i.e., $f_{c\ max}$ flexural test) to the corresponding average cylinder strength f_c'. To calculate K_1, which is the shape factor, one should evaluate K_1K_3 and K_2. The values of ultimate strength factors are given in Tables 5.11 and 5.12 for Specimens I and II. The ultimate strength factor K_2 is the position of resultant reaction force which is produced by concrete. The ultimate strength factors and other properties at ultimate condition for both specimens are given in Table 5.13.

Figures 5.12 and 5.13 show the values of K_1K_3 and K_2 computed by Equations (5.1) and (5.2) as a function of the strain ε_c at the compression face for Specimens I and II. K_2 is the position of resultant force in the concrete from the outer fiber of the beam. Figure 5.12 shows that the position of resultant force at low load is 0.33, corresponding to triangular stress distribution. But at higher loads the K_2 changes from 0.31 to 0.41 at ultimate condition, which means even at ultimate condition, the stress distribution is not rectangular

(rectangular stress block corresponds to $K_2 = 1/2 = 0.5$). The variation of K_2 is smaller for Specimen II which has higher strength (i.e., $f'_c = 9400$ psi, 65 MPa). Figure 5.13 shows K_2 varies from 0.32 to 0.37 for Specimen II. Therefore the higher the strength, the more the stress block distribution appears to be of the triangular type. Figures 5.14 and 5.15 show the values of K_1, K_2 versus the concrete strength. These graphs also prove the above fact about the stress distribution is correct. The rectangular and triangular conditions and ACI limit are also plotted on the same figure for comparison purpose. In calculating the values of ultimate strength factors, the actual area is used rather than nominal area (the areas were measured carefully using Verinier calipers, for Specimen I, area = 40.47 in^2, for Specimen II, area = 25 in^2). The outer fiber stress in the beam is also calculated using Equations (4.1) and (4.2), for both specimens. The results are given in Tables 5.14, 5.15 and 5.16, 5.17 for Specimens I and II. A computer program was used to determine the differential parts (the detail of computer program is given in Appendix II-E). In Tables 5.15 and 5.17, flexural stress is given using both methods of Equations 4.1, 4.2 and cylinder stress-strain curve, for comparison purposes for Specimens I and II, respectively. By comparing the results, it is observed that stress for Specimen I using Equations 4.1 and 4.2 does not seem to be correct and is very different with the result from stress-strain curve. There may be a source of error in calculation, because when Equations 4.1 and 4.2 are used for finding the stresses, at some levels of loading the stresses were greater than the cylinder strength which is obviously wrong. But the corresponding results for Specimen II are close enough. A typical shape of stress block at the ultimate condition is shown in Figure 5.16.

Strain Behavior

From the test data in Table 5.13, the strain at ultimate condition for flexural test of Specimen I is 0.002 in/in. The maximum cylinder strain at ultimate condition are 0.002395 in/in. and 0.002100 in/in. for cylinders corresponding to Specimen I. The strain at ultimate condition for Specimen II is 0.00311 in/in. and the maximum cylinder strain at ultimate condition is 0.00294 in/in. for cylinder corresponding to this specimen. Some cylinders corresponding to Specimen II were tested at ages other than test day. They showed a reduction of strain with increasing ultimate strength at older ages. In other words, the strain decreases while strength increases due to age. This is due to an increase in the modulus of elasticity E_c, because the stress-strain curve becomes steeper. Table 5.18 shows the results of cylinder tests corresponding to older ages than test day. As it is indicated in Table 5.18 and Figures 5.18-5.19, the value of strain at ultimate condition is 0.0025 in/in. at 72 days, 0.00209 at 85 days and 0.00200 at 120 days old. Therefore the value of strain is either less than 0.003 in/in. which is proposed by ACI Code or it decreases to become less than ACI proposed value. Therefore a more conservative value of 0.002 in/in. is recommended. References (15) and (18) have noticed the same problem with strain. Reference (18) has suggested a more conservative value of 0.0025 in/in.

Chapter 6

SUMMARY AND CONCLUSION

Summary

A mix design for high-strength concrete was developed. Numerous cylinder tests were involved in order to determine the strength of concrete. A superplasticizer was used in all the mixes in order to improve the workability. A total of four flexural specimens were made in order to verify the shape of the stress block. Only two of the specimens were tested successfully. One was broken without gaining any results due to malfunction of ramp pressure gage. The other one did not have adequate strength in order to satisfy the purpose of this investigation. From the test results and analogy of them it is possible to conclude some points.

Conclusions:

1. Superplasticizers are helpful if the right amounts are used. Too much superplasticizer decreases the strength and also segregates the mix.
2. High-strength concrete has a brittle mode of failure. There was no crack observed before failure and it has a sudden failure. This is true for both compressive and flexural tests. Unlike the normal strength concrete, the failure line passes through the stone rather than interface of mortar and stone (this is observed by other investigators [18]). Due to this action the surface of high-strength concrete is smoother than normal concrete for both compressive and flexural tests. Figure 5.21 shows the type of failure.

3. Stress-strain is almost linear up to failure and there is no descending part due to brittle failure.
4. The shape of the stress block changes from rectangular to triangular type as the strength increases, because of the fact that the position of the concrete internal reaction force is $K_2 = 0.37$ at ultimate condition for higher strength mix (i.e., $f'_c = 9400$ psi, 65 MPa). This value is very close to $1/3 \simeq 0.33$ which is the center of gravity of a triangular stress block rather than 0.5 which is the center of gravity of a rectangular stress block.
5. The strain behavior in high-strength concrete is different from normal strength concrete, because either strain at ultimate condition is less than 0.003 in/in. proposed by ACI Code or it might be greater than ACI proposed, but it decreases with time drastically. Therefore, a more conservative value of 0.002 in/in. is recommended.
6. Since high-strength concrete pick up strength efficiently up to 90 days, a 28-day strength test is not adequate for high-strength concrete. A 56-day strength is recommended. recommended.

Recommendation for Future Work

High-strength concrete can be considered as a material that can replace normal-strength concrete. Therefore it must be compared to normal concrete in all aspects. Yet, intensive research is required to bring about all the theories and specifications for high-strength concrete. Because as the strength increases, the K_2 value gets very close to triangular shape stress distribution, therefore tests with higher-strength concrete are desired in order to formulate a sound theory. Since higher-strength test specimens (i.e., 13000 psi - 15000 psi, 97-103 MPa) will answer the questions more clearly than those in the range of 8000 - 9000 psi (55-62 MPa), mix design for that range of strength is desired. A large number of beam test and column test data is necessary in order to formulate that theory. A large number of accurate strain tests are essential in order to determine a good approximation value for strain at ultimate strength.

APPENDIX I

REFERENCES

1. "New York City Gets its First High-Strength Concrete Tower," Engineering News-Record, Vol. 201, No. 18, November 2, 1978, p. 22.

2. Saucier, Kenneth L., "High-Strength Concrete, Past, Present, Future," Concrete International, American Concrete Institute, Vol. 2, No. 6, June 1980, pp. 46-50.

3. Carrasquillo, Ramon L., Nilson, A. H., and Slate, Floyd O., "The Production of High-Strength Concrete," Research Report No. 78-1, Department of Structural Engineering, Cornell University, Ithaca, May 1978, p.2.

4. "High-Strength Concrete in Chicago High-Rise Buildings," Task Force Report No. 5, Chicago Committee on High-Rise Buildings, Feb. 5, 1977.

5. "High-Strength Concrete," First Edition, Manual of Concrete Materials-Aggregates, National Crushed Stone Association, January 1975, p. 16.

6. Blick, Ronald L., "Some Factors Influencing High-Strength Concrete," Modern Concrete, April 1973.

7. Bloem, D. L. and Gaynor, R. D., "Effect of Aggregates Properties on Strength of Concrete," American Concrete Institute Journal, Vol. 60, October 1963, pp. 1429-1455.

8. Burgess, A. J., Ryell, J. and Bunting, J., "High-Strength Concrete for the Willows Bridge," American Concrete Institute Journal, Vol. 67, No. 8, August 1970, p. 611.

9. Mather, Katherine, "High-Strength Concrete, High Density Concrete," (ACI Summary Paper), American Concrete Institute Journal, Proceedings, Vol. 62, No. 8, August 1965, pp. 951-962.

10. Tentative Interim Report on High-Strength Concrete, American Concrete Institute Journal, Proceedings, Vol. 64, No. 9, September 1967, pp. 556-557.

11. "High Strength Concrete--Crushed Stone Makes the Difference," Third Draft, presented at the January 1975 National Crushed Stone Association Convention in Florida, November 1974, p. 31.

12. Alexander, K. M., "Factors Controlling the Strength and the Shrinkage of Concrete," Construction Review, Vol. 33, No. 11, Nov. 1960, pp. 19-29.

13. Freedman, Sidney, "High-Strength Concrete," Publication No. 1S176, Portland Cement Association, 1971 (Reprint from Modern Concrete, 1970-1971), p. 19.

14. Smith, E. F., Tynees, W. O. and Saucier, K. L., "High Compressive-Strength Concrete, Development of Concrete Mixtures," Technical Documentary Report No. TDR 63-3114, U. S. Army Engineer Waterways Experiment Station, Vicksburg, Mississippi, February 1964, p. 44.

15. Leslie, Keith E., Rajagopalan, K. S., and Everard, Noel J., "Flexural Behavior of High-Strength Concrete Beams," ACI Journal, September 1976, pp. 517-521.

16. Wang, Pao-Tsan, Shah, Surendra P., Naaman, Antonie E., "High-Strength Concrete in Ultimate Strength Design," Journal of the Structural Division, ASCE, No. 1978, pp. 1761-1773.

17. Hognestad, Eivid, Hanson, N. W., and McHenry, Douglas, "Concrete Stress Distribution in Ultimate Strength Design," Journal of the American Concrete Institute, Dec. 1955, pp. 455-479.

18. Nilson, Arthur H., Slate, Floyd O., "Structural Properties of Very High-Strength Concrete," Second Progress Report ENG 76-08752, Department of Structural Engineering, Cornell University, Ithaca, New York, January 1979.

19. "Concrete and Mineral Aggregates (including Manual of Concrete Testing)," Annual Book of ASTM Standard, Part 14, 1974.

20. "Building Code Requirement for Reinforced Concrete (ACI 318-77)," American Concrete Institute, 1977.

21. Perenchio, W. F., "An Evaluation of Some of the Factors Involved in Producing Very High-Strength Concrete," Bulletin No. RD014, Portland Cement Association, 1973.

22. "Cement; Lime; Ceilings and Walls (including Manual of Cement Testing)", Annual Book of ASTM Standard, Part 13, 1976.

23. Kaplan, M. F., "Flexural and Compressive Strength of Concrete as Affected by the Properties of Coarse Aggregate," American Concrete Institute Journal, Vol. 55, May 1959, pp. 1193-1208.

APPENDIX II

A. Detailed calculation for mix design approach I for 25 percent sand in total aggregate.

$$V_s = \frac{W_s}{\gamma_s} \qquad \text{(A.1)}$$

$$W_s = 0.25\ W_T$$

$$W_s = 0.25\ (W_s + W_a)$$

$$0.75\ W_s = 0.25\ W_a$$

$$W_s = \frac{1}{3} W_a$$

$$V_s = \frac{\frac{1}{3} W_a}{\gamma_s}$$

Based on cubic yard = 27 ft^3

$$V_a = 27\ ft^3 - V_W - V_c - V_A - V_s$$

$$V_a = 27 - V_W - V_c - V_A - \frac{\frac{1}{3} W_a}{\gamma_s}$$

$$V_a + \frac{\frac{1}{3} W_a}{\gamma_s} = 27 - V_W - V_c - V_A$$

$$V_a = \frac{W_a}{\gamma_a}$$

$$\frac{W_a}{\gamma_a} + \frac{\frac{1}{3} W_a}{\gamma_s} = 27 - V_W - V_c - V_A$$

$$W_a + \frac{\frac{1}{3} W_a \gamma_a}{\gamma_s} = [27 - V_W - V_c - V_A]\gamma_a$$

$$W_a \left(1 + \frac{1}{3}\frac{\gamma_a}{\gamma_s}\right) = (27 - V_W - V_c - V_A)\gamma_a \text{ --------------- (A.2)}$$

For 50 percent sand in total aggregate this becomes

$$W_a \left(1 + \frac{\gamma_a}{\gamma_s}\right) = (27 - V_W - V_c^* - V_A^\dagger)\gamma_a \text{ ---------------- (A.3)}$$

For 75 percent sand in total aggregate

$$W_a \left(1 + \frac{3\gamma_a}{\gamma_s}\right) = (27 - V_W - V_c - V_A)\gamma_a \text{ --------------- (A.4)}$$

where

W_s = weight of sand

W_w = weight of water

W_a = weight of coarse aggregate

γ_a = density of coarse aggregate

γ_s = density of sand

V_W = volume of water

V_c = volume of cement

V_A = volume of air content

V_s = volume of sand

V_a = volume of air

*water-cement ratio is given (i.e., 0.4, 0.35, 0.3).

†volume of air entrapped is assumed to be 2 percent by volume.

B. Mix design calculation and detail for approach II.

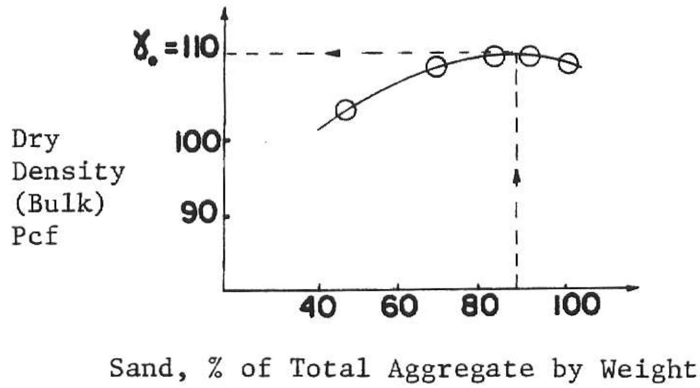

γ_o = 110 pcf, % sand = 85 by weight

$\frac{W}{c} = 0.4$

Material	SP. G.	Wt/ft^3	Absolute Volume/ft^3
Cement	3.15		
Rock	2.54	(0.15)(110) = 16.50	0.104
Sand	2.63	(0.85)(110) = 93.50	0.570
Water	1.00		

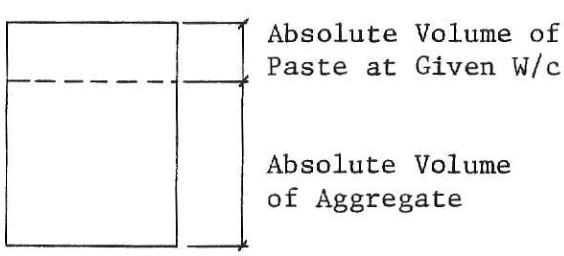

$V_{aggregate} = 0.104 + 0.57 = 0.674 \text{ ft}^3$

$V_{paste} = 1-0.674 = 0.326 \text{ ft}^3$

If there are no air voids

$V_{paste} = V_{cement} + V_{water} = 0.326$

$$V_{cement} = \frac{W_{cement}}{(3.15)(62.4)}$$

$$V_{water} = \frac{W_{water}}{62.4} = \frac{0.4\ W_{cement}}{62.4}$$

$$\frac{W_{cement}}{62.4}\left(\frac{1}{3.15} + 0.4\right) = 0.326$$

$$W_{cement} = \frac{(0.326)(62.4)(3.15)}{1 + 0.4(3.15)} = \underline{\underline{28.35\ \text{lb.}}}$$

$$W_{water} = 0.4(28.35) = \underline{\underline{11.34\ \text{lb.}}}$$

C. Design of Steel Reinforcement.

Longitudinal Reinforcement

By inspection, Section A-A (Figure 4.2) is the weakest section, therefore Section A-A will govern the design. To be on the safe side, assume P_2 = 30,000 lb. for design purposes.

P_2 = 30,000 lb.

a = 14"

$P_2 \cdot a = M$

M = 420,000 lb-in.

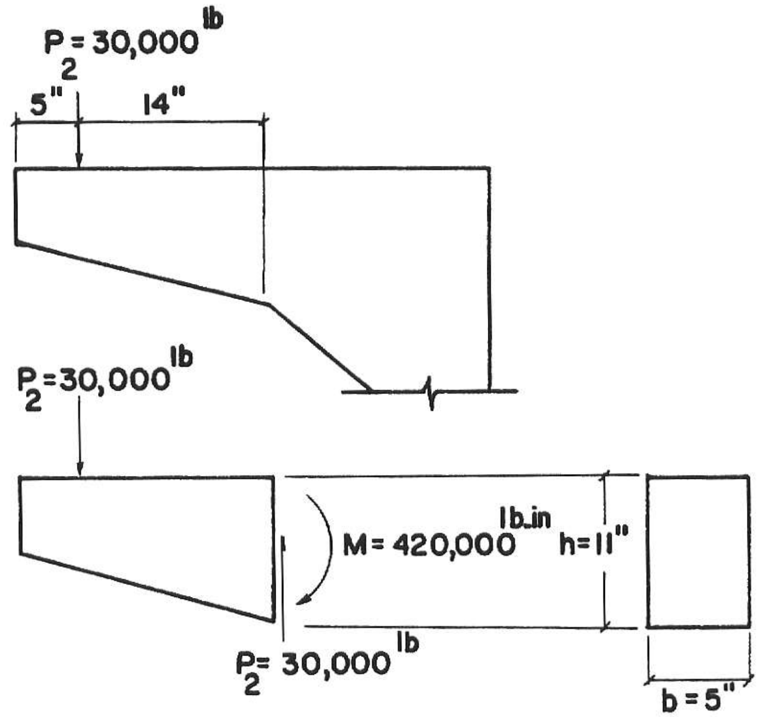

Assumptions:

1. Concrete will take 85 percent of its ultimate strength,
2. A triangular stress block with zero at neutral axis and maximum at its outermost fiber.
3. Assume steel will take up stresses to its ultimate value.

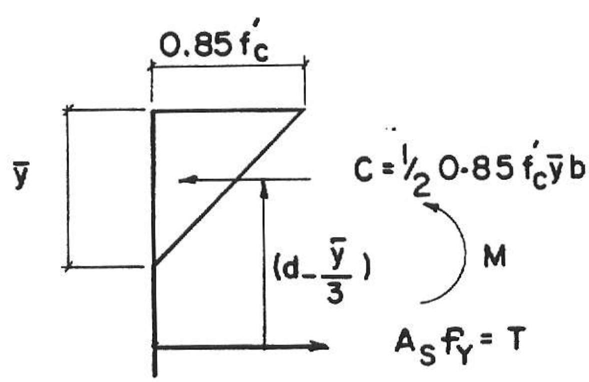

$$\Sigma F_x = 0 \overset{+}{\rightarrow} T - C = 0 \rightarrow T = C \quad \text{------------------------} \quad (C.1)$$

Therefore:

$$A_s f_y = \frac{1}{2} b \, \bar{y} \, (0.85 \, f'_c) \quad \text{------------------------------} \quad (C.2)$$

$$M = A_s f_y \left(d - \frac{\bar{y}}{3}\right) \quad \text{--------------------------------} \quad (C.3)$$

From Equation (C.2), $\bar{y}$ can be determined:

$$\bar{y} = \frac{A_s f_y}{\frac{0.85}{2} f'_c \, b}$$

Substitute $\bar{y}$ in Equation (C.3)

$$M = A_s f_y \left(d - \frac{\frac{A_s f_y}{\frac{0.85}{2} f'_c \, b}}{3}\right)$$

$$M = A_s f_y \left(d - \frac{A_s f_y}{(\frac{0.85}{2})(3) f'_c \, b}\right) \quad \text{----------------------} \quad (C.4)$$

$M = 420{,}000$ lb-in.

$b = 5''$

$d = 9.25''$

$f_y = 40000$ psi (est.)

$f'_c = 12000$ psi (est.)

Substitute the given values in Equation (C.4), therefore

$$420{,}000 = A_s \, (40000) \left[9.25 - \frac{A_s \, (40000)}{(\frac{0.85}{2})(3)(12000)(5)} \right]$$

$$A_s^2 - 17.6906 \, A_s + 20.08125 = 0.$$

$$A_s = \frac{-(-17.6906) \pm \sqrt{(-17.6906)^2 - 4(20.08125)}}{2}$$

$$A_s = \frac{17.6906 \pm 15.252}{2} \qquad \begin{matrix} A_s = 16.47 \text{ in}^2 \\ \\ A_s = 1.22 \text{ in}^2 \end{matrix}$$

Use 6 #4 in two rows → $A_s = 1.18 \simeq 1.2 \simeq 1.22$ O.K.

Length of each reinforcement is equal to 31 in.

Design of Shear Reinforcement

From ACI Code:

$$s = \frac{\phi A_v \, fy \, d}{V_u - \phi V_c}$$ for stirrups normal to beam axis

$$s = \frac{\phi A_v \, fy \, d \, (\text{Sin } \alpha + \text{Cos } \alpha)}{V_u - \phi V_c}$$ for inclined stirrups at and α to beam axis

Assumptions:

1. Concrete will not take any force.
2. Steel rebars will be placed at 45° angle
3. Using #3 bars, A 0.11, $A_v = 2 \times 0.11 = .22$,

   $f_y = 40000$ psi.

$V_u = P_2 = 30000$ lb. and V_c assumed = 0.

* $$s = \frac{(0.85)(0.22)(40000)(\text{Sin } 45° + \text{Cos } 45°)(9.25)}{30000} = 3.26 \text{ in.}$$

$$\simeq 3.3 \text{ in.}$$

* Using #3 bars at 3.3 in. for stirrup.

Length of each leg of stirrups are calculated as shown below:

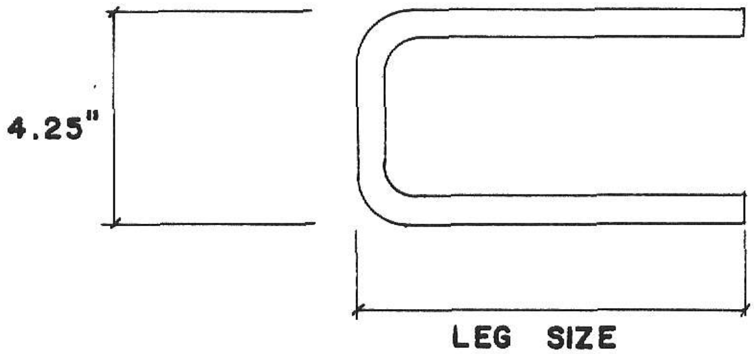

Figure II-C Picture of each Stirrup

A total of nine stirrups are placed with a 45° angle:

#1) $5 + 0\,\frac{6}{19} = 5 \times \frac{1}{\text{Cos } 45°} = 7.02 - (0.375 \times 2)^{*} = 6.32 \simeq 6\,\frac{5}{16}$ in.

#2) $5 + 3.3\,(\frac{6}{19}) = 6.04 \times \frac{1}{\text{Cos } 45°} = 8.54 - (0.375 \times 2) = 7.79 \simeq 7\,\frac{6}{8}$ in.

#3) $5 + 2 \times 3.3\,(\frac{6}{19}) = 7.08 \times \frac{1}{\text{Cos } 45°} = 10.02 - (0.375 \times 2) = 9.27 \simeq 9\,\frac{2}{8}$ in.

#4) $5 + 3 \times 3.3\,(\frac{6}{19}) = 8.13 \times \frac{1}{\text{Cos } 45°} = 11.49 - (0.75) = 10.74 \simeq 10\,\frac{6}{8}$ in.

#5) $5 + 4(3.3)(\frac{6}{19}) = 9.16\,\frac{1}{\text{Cos } 45°} = 12.97 - (0.75) = 12.22 \simeq 12\,\frac{2}{8}$ in.

#6) $5 + 5(3.3)(\frac{6}{19}) = 10.21\,\frac{1}{\text{Cos } 45°} = 14.44 - 0.75 = 13.69 \simeq 13\,\frac{11}{16}$ in.

#7) $5 + 6(3.3)(\frac{6}{19}) = 11.25 \times \frac{1}{\text{Cos } 45°} = 15.91 - 0.75 = 15.16 \simeq 15\,\frac{3}{16}$ in.

#8) $5 + 7(3.3)(\frac{6}{19}) = 12.29 \times \frac{1}{\text{Cos } 45°} = 17.39 - 0.75 = 16.64 \simeq 16\,\frac{10}{16}$ in.

#9) $5 + 8(3.3)(\frac{6}{19}) = 13.34 \times \frac{1}{\text{Cos } 45°} = 18.86 - 0.75 = 18.11 \simeq 18\,\frac{1}{8}$ in.

0.375 in. = $\frac{3}{8}$ is cover for bars on each side.

Column Reinforcement

Using #4 steel, two on each face

Length of each rebar is 16 1/2 in. long.

Using 1/8 in. diameter wire for column ties.

The details are shown in Figures 4.6 and 4.7 for Specimen I and Specimen II, respectively. A complete bar set up is shown in Figure 4.4, together with Figures 4.5, 4.6 and 4.7.

D. Design of Testing Frame.

The expected load for frame is 22 kips. But to be more conservative, it is assumed to be 30 kips. Also using a factor of safety of 1.5

$$30\ K \times 1.5 = 45000\ lb. = 45\ K$$

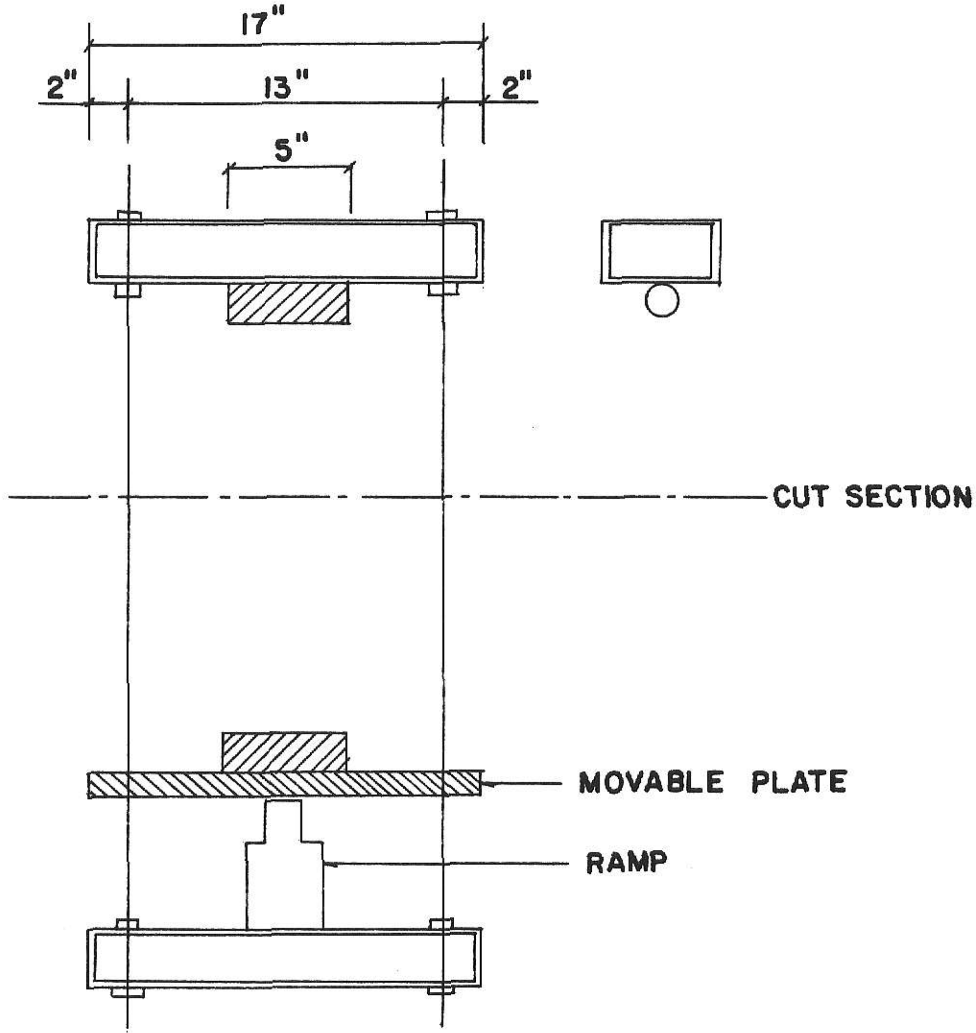

Design the rods

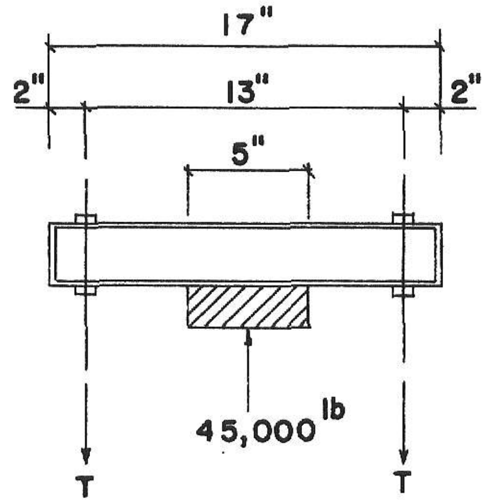

$\Sigma F_y = 0$

$2T = 45000$

$T = 22500$ lb.

Using plastic analysis

$A_s F_y = T$

$F_y = 36000$ psi

$A_s (36000 \text{ psi}) = 22500$ lb.

$A_s = 0.625 \text{ in}^2$

$A = \pi r^2 \rightarrow A_s = A = 0.625 = \pi r^2$

$r = 0.446$ in.

using $r = 0.5$ in.

$D = 2 \times 4 = 1$ in. diameter

E. Derivation of Ultimate Strength Factors K_1K_3, K_2

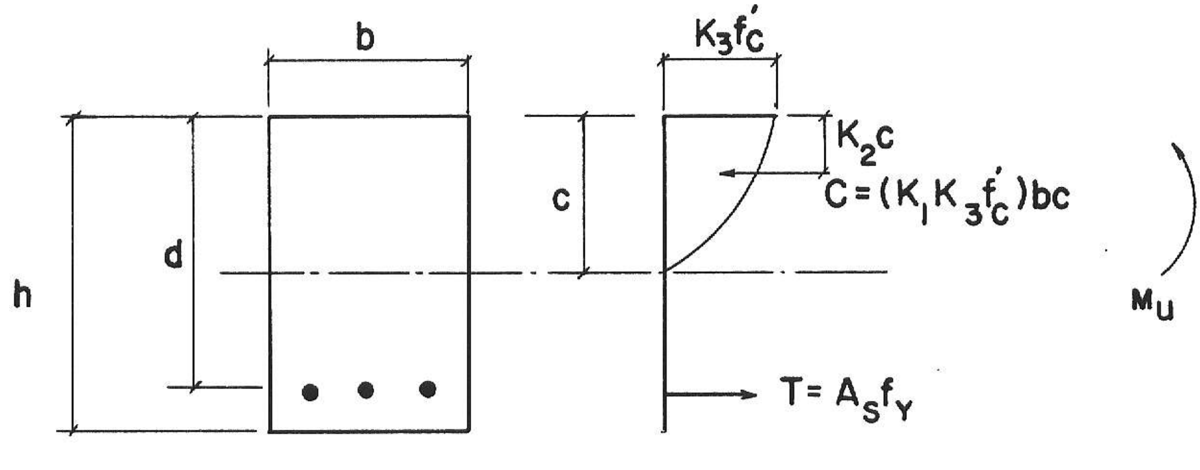

Figure a: Force Couple System

without any assumption we obtain the equilibrium equation of force and moment:

$$\Sigma F_x = 0 \quad T = C \rightarrow T = K_1K_3\ f_c'\ bc$$

$$K_1K_3 = \frac{T}{f_c'\ bc} \qquad \text{(I.1)}$$

$$\Sigma M = 0 \quad T(d-K_2c) = C(d-K_2c) = Mu$$

$$K_2 = \frac{d}{c} - \frac{Mu}{TC} = \frac{d}{c} - \frac{Mu}{Cc} \qquad \text{(I.2)}$$

Applying the same concept to the test specimen shown in Figure 5.17, we have

$$C = P_1 + P_2$$

Substitute in Equation (I.1) we obtain

$$K_1K_3 = \frac{P_1 + P_2}{bc\ f_c'} \qquad \text{(I.3)}$$

where f_c' is the cylinder compressive strength.

$$Mu = P_1a_1 + P_2a_2$$

Substitute in Equation (I.2)

$$K_2 = \frac{d}{c} - \frac{P_1a_1 + P_2a_2}{(P_1 + P_2)c}$$

$d = c$ for test specimen

Therefore:

$$K_2 = 1 - \frac{P_1a_1 + P_2a_2}{(P_1 + P_2)c}$$

F. Computer program for calculating $\frac{dm_o}{dt_c}$, $\frac{df_o}{d\varepsilon_c}$.

```
5  INPUT "NO. OF DATA POINTS N=?";N
10  DIM X(N),Y(N),A(3),DY(N)
15 N2 = N - 2
20  DIM B(5,3),BB(3,3),BF(3)
22  FOR I = 1 TO N
24  PRINT "DATA POINT NO.";I
25  INPUT "X(I)=?";X(I)
26  INPUT "Y(I)=?";Y(I)
27  NEXT I
30  FOR I = 3 TO N2
35  FOR J = 1 TO 5
40 B(J,1) = 1
45 IJ = I - 3 + J
50 B(J,2) = X(IJ) - X(I)
55 B(J,3) = B(J,2) ↑ 2
60  NEXT J
65  FOR J = 1 TO 3
70  FOR K = 1 TO 3
75 BB(J,K) = 0
80  FOR L = 1 TO 5
85 BB(J,K) = BB(J,K) + B(L,J) * B(L,K)
90  NEXT L,K,J
95  FOR J = 1 TO 3
100 BF(J) = 0
105  FOR K = 1 TO 5
107 IK = I - 3 + K
110 BF(J) = BF(J) + B(K,J) * Y(IK)
115  NEXT K,J
120 D = BB(1,1) * (BB(2,2) * BB(3,3) - BB(2,3) * BB(3,2)) - BB(1,2) * BB(
     2,1) * BB(3,3)
121 D = D + BB(1,2) * BB(2,3) * BB(3,1) + BB(1,3) * (BB(3,2) * BB(2,1) -
     BB(2,2) * BB(3,1))
125 E = BB(1,1) * (BF(2) * BB(3,3) - BB(2,3) * BF(3)) - BF(1) * (BB(2,1) *
     BB(3,3) - BB(2,3) * BB(3,1))
130 E = E + BB(1,3) * (BB(2,1) * BF(3) - BF(2) * BB(3,1))
135 C(2) = E / D
140 E = BB(1,1) * (BB(2,2) * BF(3) - BF(2) * BB(3,2)) - BB(1,2) * (BB(2,1
     ) * BF(3) - BF(2) * BB(3,1))
145 E = E + BF(1) * (BB(2,1) * BB(3,2) - BB(2,2) * BB(3,1))
150 C(3) = E / D
155  IF I = 3 THEN 250
160  IF I = N2 THEN 300
170 DY(I) = C(2)
180  GOTO 327
250 DY(I - 2) = C(2) + 2 * C(3) * (X(1) - X(3))
251 D$ = ""
252  PRINT D$; PR# 1
```

```
255  PRINT "DY/DX(1)=";DY(1)
256  PRINT D$: PR# 0
260 DY(2) = C(2) + 2 * C(3) * (X(2) - X(3))
261  PRINT D$: PR# 1
265  PRINT "DY/DX(2)=";DY(2)
266  PRINT D$: PR# 0
270 DY(I) = C(2)
280  GOTO 327
300 DY(I) = C(2)
310 DY(I + 1) = C(2) + 2 * C(3) * (X(I + 1) - X(I))
311  PRINT D$: PR# 1
315  PRINT "DY/DX(";I + 1;")=";DY(I + 1)
316  PRINT D$: PR# 0
320 DY(I + 2) = C(2) + 2 * C(3) * (X(I + 2) - X(I))
321  PRINT D$: PR# 1
325  PRINT "DY/DX(";I + 2;")=";DY(I + 2)
326  PRINT D$: PR# 0
327  PRINT D$: PR# 1
350  PRINT "DY/DX(";I;")=";DY(I)
351  PRINT D$: PR# 0
360  NEXT I
370  END
```

APPENDIX III

TABLES AND FIGURES

Table 2.1: Sieve Analysis of Limestone

U.S. Sieve No.	Retained			Percent Retained	Σ% Retained	Σ% Passing
	Wt. Sample + Sieve (lb)	Wt. Sieve (lb)	Wt. Sample (lb)			
3/8	1.635	1.48	0.155	7.03	7.03	92.97
4	2.810	1.550	1.260	57.12	64.15	35.85
8	1.86	1.140	0.72	32.64	96.79	3.21
16	1.165	1.105	0.06	2.72	99.51	0.49
30	0.997	0.994	0.003	0.14	99.65	0.35
50	1.031	1.030	0.001	0.05	99.70	0.30
100	0.893	0.891	0.002	0.09	99.79	0.21
Passing No. 100	0.870	0.865	0.005	0.23	100.02	-0.02

Σ of % Retained Wt. 567 Fineness 5.67 $\gamma = 97.16\ lb/ft^3$

Table 2.2: Sieve Analysis of Quartzite Stone

U.S. Sieve No.	Retained			Percent Retained	Σ% Retained	Σ% Passing
	Wt. Sample + Sieve (1b)	Wt. Sieve (1b)	Wt. Sample (1b)			
3/4	--	--	4.400	--	--	100
1/2	5.038	3.340	1.698	38.50	38.50	61.50
3/8	4.785	2.960	1.825	41.38	79.88	20.12
4	3.882	3.100	0.782	17.73	97.61	2.39
8	2.340	2.280	0.060	1.36	98.97	1.03
16	2.225	2.209	0.016	0.36	99.33	0.67
30	1.990	1.988	0.002	0.05	99.38	0.62
50	2.064	2.060	0.004	0.09	99.47	0.53
100	1.788	1.783	0.005	0.11	99.58	0.42
Passing No. 100	1.748	1.730	0.018	0.41	99.99	0.01

Σ of % Retained Wt. 713 Fineness 7.13 γ = 96.01 pcf

Table 2.3: Sieve Analysis of Sand

U.S. Sieve No.	Retained			Percent Retained	Σ% Retained	Σ% Passing
	Wt. Sample + Sieve (lb)	Wt. Sieve (lb)	Wt. Sample (lb)			
4	1.575	1.552	0.023	2.09	2.09	97.91
8	1.250	1.140	0.110	10.01	12.10	87.90
16	1.350	1.105	0.245	22.29	34.39	65.61
30	1.313	0.995	0.318	28.94	63.33	36.67
50	1.345	1.031	0.314	28.67	91.90	8.10
100	0.977	0.892	0.085	7.73	99.63	0.37
Passing No. 100	0.869	0.865	0.004	0.36	99.99	0.01

Σ of % Retained 303 Fineness Modulus 3.03 $\gamma_s = 112.81$

Table 2.4: Fine Aggregate Gradation for High-Strength Concrete (5)
% retained

Sieve Size	ASTM C-33	Recommended for High-Strength Concrete	Gradation Used in This Investigation
3/8"		100	100
No. 4	95-100	95-100	98
No. 8	80-100	80-100	88
No. 16	50-85	50-85	66
No. 30	25-60	25-60	37
No. 50	10-30	5-20	8
No. 100	2-10	0-5	0.5

Table 3.1: Properties of Fresh Concrete Using Limestone and Mix Approach II**

Mix No.	Water to mix (lb)	Water Net* (lb)	W/c	Slump (in)	Air %	C.F. Sack/cubic yard	Remarks
L-1	6.28	6.16	0.3	9 1/2	4.3	11.50	Slump, high, used 140 mℓ of superplasticizer. Cast 12 3x6 in. and 1 6x12 in. cylinder. The mix is based on 1/2 cubic ft.

*use absorption of aggregate = 0.2 percent by weight of aggregate.

**sand-aggregate ratio of 58 percent by weight is used.

Table 3.2: Properties of Fresh Concrete Using Quartzite Stone and Mix Approach II**

Mix No.	Water		W/c	Slump (in)	Air %	Unit Weight pcf	C.F. Sack/ cubic yard	Remarks
	to mix (lb)	Net* (lb)						
1R	5.38	5.27	0.38	2	-	-	-	Too dry. N.G.
1	5.60	5.5	0.4	3 1/8	2.6	148.76	7.86	OK. Cast 12 3x6 in. cylinders and 1 6x12 in. cylinder
2	5.48	5.35	0.34	2 6/8	4.4	148.20	7.92	Used 2 fl. oz. (59 mℓ) super-plasticizer. OK Cast 12 3x6 in cylinders and 1 6x12 in. cylinders.
2R	5.48	5.35	0.34	9 2/8	2.2	151.24	8.1	Slump too high, used 4 fl. oz. (118 mℓ) of super-plasticizer.
3	5.46	5.33	0.29	4 1/8	3.6	151.12	9.1	OK Cast 12 3x6 in. cylinders. All the mixes are based on 1/2 cubic ft.

*use absorption of aggregate = 0.2 percent by weight of aggregate.

**sand-aggregate ratio of 55 percent by weight is used.

Table 3.3: Cylinder Test Data Using Mix of Approach I, $\frac{W}{c} = 0.4$
3 x 6 in. cylinder* A = 7.07 in^2, Limestone Aggregate

Sample Subscript	No. of Days in Curing Room	No. of Days Air Dried	Sand Content % of Total Aggregate	Cement-Aggregate Ratio by Weight	Slump (in)	Stress (psi)	Average Stress (psi)
1-A	28	7	0	0.26	0.00	5107	
2-A	28	7	0	0.26	0.00	4300	
							4703
1-B	28	7	0	0.43	1 1/2	6436	
2-B	28	7	0	0.43	1 1/2	6366	
							6401
1-C	28	7	0	0.50	3 1/4	6380	
2-C	28	7	0	0.50	3 1/4	7215	
3-C	28	7	0	0.50	3 1/4	5036	
4-C	28	7	0	0.50	3 1/4	7172	
							6450
1-D	28	7	25	0.46	7.00	7186	
2-D	28	7	25	0.46	7.00	8063	
							7624

*all the samples have been in the mold for 2 days.

Table 3.3 continued

Sample Subscript	No. of Days in Curing Room	No. of Days Air Dried	Sand Content % of Total Aggregate	Cement-Aggregate Ratio by Weight	Slump (in)	Stress (psi)	Average Stress (psi)
1-E	28	7	25	0.38	3.00	6097	
2-E	28	7	25	0.38	3.00	7497	
3-E	28	7	25	0.38	3.00	7978	
4-E	28	7	25	0.38	3.00	7356	
							7232
1-F	28	7	50	0.4	8 1/4	7653	
2-F	28	7	50	0.4	8 1/4	7540	
							7596
1-G	28	7	50	0.31	1 3/4	7950	
2-G	28	7	50	0.31	1 3/4	7356	
							7653
1-H	28	7	50	0.33	3 1/4	8063	
2-H	28	7	50	0.33	3 1/4	7837	
3-H	28	7	50	0.33	3 1/4	7498	
4-H	28	7	50	0.33	3 1/4	7950	
							7837

Table 3.3 continued

Sample Subscript	No. of Days in Curing Room	No. of Days Air Dried	Sand Content % of Total Aggregate	Cement-Aggregate Ratio by Weight	Slump (in)	Stress (psi)	Average Stress (psi)
1-I	28	7	75	0.26	0.00	6918	
2-I	28	7	75	0.26	0.00	6890	
							6904
1-J	28	7	75	0.31	2.00	7357	
2-J	28	7	75	0.31	2.00	7158	
							7257
1-L	28	7	75	0.33	1/2	7088	
2-L	28	7	75	0.33	1/2	7286	
							7187
1-M	28	7	75	0.35	2 3/4	7795	
2-M	28	7	75	0.35	2 3/4	7583	
3-M	28	7	75	0.35	2 3/4	7569	
4-M	28	7	75	0.35	2 3/4	7441	
							7597

Table 3.4: Cylinder Test Data Using Mix of Approach I, $\frac{W}{c} = 0.35$

3 x 6 in. cylinder A = 7.07 in^2, Limestone Aggregate

Sample Subscript	No. of Days in Curing Room	No. of Days Air Dried	Sand Content % of Total Aggregate	Cement-Aggregate Ratio by Weight	Slump (in)	Stress (psi)	Average Stress (psi)
1-A	28	7	0	0.29	0.00	3621	
2-A	28	7	0	0.29	0.00	3635	
							3628
1-B	28	7	0	0.39	0.00	8431	
2-B	28	7	0	0.39	0.00	9054	
							8742
1-C	28	7	0	0.51	2.00	8700	
2-C	28	7	0	0.51	2.00	8884	
							8792
1-D	28	7	0	0.54	2.5	7922	
2-D	28	7	0	0.54	2.5	8205	
							8063
1-E	28	7	0	0.55	2.75	8092	
2-E	28	7	0	0.55	2.75	7950	

Table 3.4 continued

Sample Subscript	No. of Days in Curing Room	No. of Days Air Dried	Sand Content % of Total Aggregate	Cement-Aggregate Ratio by Weight	Slump (in)	Stress (psi)	Average Stress (psi)
3-E	28	7	0	0.55	2.75	8049	
4-E	28	7	0	0.55	2.75	8021	
							8028
1-F	28	7	25	0.44	3.25	8063	
2-F	28	7	25	0.44	3.25	7738	
3-F	28	7	25	0.44	3.25	7215	
4-F	28	7	25	0.44	3.25	8346	
							7840
1-G	28	7	50	0.38	2.00	8417	
2-G	28	7	50	0.38	2.00	8205	
							8311
1-H	28	7	50	0.40	2.75	7639	
2-H	28	7	50	0.40	2.75	7597	
3-H	28	7	50	0.40	2.75	7795	
4-H	28	7	50	0.40	2.75	7710	
							7685

Table 3.4 continued

Sample Subscript	No. of Days in Curing Room	No. of Days Air Dried	Sand Content % of Total Aggregate	Cement-Aggregate Ratio by Weight	Slump (in)	Stress (psi)	Average Stress (psi)
1-I	28	7	75	0.41	2.5	8048	
2-I	28	7	75	0.41	2.5	8302	
							8175
1-J	28	7	75	0.42	2.1	8090	
2-J	28	7	75	0.42	2.1	8119	
							8104
1-K	28	7	75	0.44	3.25	7425	
2-K	28	7	75	0.44	3.25	8204	
3-K	28	7	75	0.44	3.25	8175	
4-K	28	7	75	0.44	3.25	7851	
							7913

Table 3.5: Cylinder Test Data Using Mix of Approach I, $\frac{W}{c} = 0.30$

3 x 6 in. cylinder $A = 7.07\ in^2$, Limestone Aggregate

Sample Subscript	No. of Days in Curing Room	No. of Days Air Dried	Sand Content % of Total Aggregate	Cement-Aggregate Ratio by Weight	Slump (in)	Stress (psi)	Average Stress (psi)
1-A	28	7	0	0.67	0.75	8628	
2-A	28	7	0	0.67	0.75	8388	
							8508
1-B	28	7	0	0.77	1.00	8175	
2-B	28	7	0	0.77	1.00	7496	
							7835
1-C	28	7	0	0.88	2.75	7850	
2-C	28	7	0	0.88	2.75	7850	
3-C	28	7	0	0.88	2.75	7638	
4-C	28	7	0	0.88	2.75	7468	
							7701
1-D	28	7	25	0.54	0.50	8670	
2-D	28	7	25	0.54	0.50	8897	
							8783

Table 3.5 continued

Sample Subscript	No. of Days in Curing Room	No. of Days Air Dried	Sand Content % of Total Aggregate	Cement-Aggregate Ratio by Weight	Slump (in)	Stress (psi)	Average Stress (psi)
1-E	28	7	25	0.63	1.25	8458	
2-E	28	7	25	0.63	1.25	8373	
							8415
1-F	28	7	25	0.70	2.5	7115	
2-F	28	7	25	0.70	2.5	7992	
							7553
1-G	28	7	25	0.76	3.00	8685	
2-G	28	7	25	0.76	3.00	8826	
3-G	28	7	25	0.76	3.00	8402	
4-G	28	7	25	0.76	3.00	9151	
							8766
1-H	28	7	50	0.58	2.00	8812	
2-H	28	7	50	0.58	2.00	8501	
							8656
1-I	28	7	50	0.62	2.10	8925	
2-I	28	7	50	0.62	2.10	10438	
							9681

Table 3.5 continued

Sample Subscript	No. of Days in Curing Room	No. of Days Air Dried	Sand Cont nt % of Total Agtregate	Cement-Aggregate Ratio by Weight	Slump (in)	Stress (psi)	Average Stress (psi)
1-J	28	7	50	0.67	3.1	8543	
2-J	28	7	50	0.67	3.1	8006	
3-J	28	7	50	0.67	3.1	8204	
4-J	28	7	50	0.67	3.1	8133	
							8221
1-K	28	7	75	0.61	2.75	7440	
2-K	28	7	75	0.61	2.75	8359	
3-K	28	7	75	0.61	2.75	8345	
4-K	28	7	75	0.61	2.75	7539	
							7921

Table 3.6: Cylinder Compressive Strength, Using Limestone Aggregate and Mix Approach II

Mix Subscript	Strength psi			
	3 x 6 in.*			6 x 12 in.
	3 days	7 days	28 days	
L-1	6870	790	8610	6825

*average of 3 cylinders.

3 x 6 in. $A = 7.07\ in^2$

6 x 12 in. $A = 28.27\ in^2$

Table 3.7: Cylinder Compressive Strength of Concrete Using Quartzite Stone Aggregate and Mix Approach II

Mix Subscript	Strength psi				
	3 x 6 in.*				6 x 12 in.
	3 days	7 days	28 days (14 days in curing room, 14 days in water pressure vessel of 50 psi)	Steam Cured	28 days
1	4450	5690	6700	7040	5890
2	5990	6750	7980	8000	7140
3	6980	7630	8520	9320	--

*average of 3 cylinders.

Table 5.1: Information About the Test Specimens

Specimen Subscript	Water-cement Ratio	Mix Design	Casting Date	No. of Days in Curing Room	No. of Days in 50% Humidity	Age (days)	Average f'_c psi
Specimen I	0.34	2	Feb. 12-81	Feb. 13-81 to March 16-81	March 17-81 to March 31-81	47	8400
Specimen II	0.29	3	July 18-81	July 19-81 to Aug. 24-81	Aug. 25-81 to Sep. 3-81	47	9400

Table 5.2: Test Cylinders for Specimen I

Cylinder	3 x 6 Area (in^2)	Load (lb)	Stress lb/in^2	Added More Superplasticizer (mℓ)
1	7.07	58000	8204	10
2	7.07	53700	7595	10
3	7.07	58700	8303	10
4	7.07	62700	8868	0
5	7.07	62400	8826	0
6	7.07	62400	8826	0
f'_c average $= \frac{\Sigma f'_c}{\Sigma}$			8437 ≃ 8400	

Table 5.3: Stress-Strain Relation for Cylinder #1*
Corresponding to Specimen I

Load (lb)	Stress (psi)	Strain Reading in Gage #1 ($\mu\varepsilon$)	Strain Reading in Gage #2 ($\mu\varepsilon$)	Average ($\mu\varepsilon$)
4000	566	88	112	100
8000	1132	180	234	207
12000	1697	267	348	307
16000	2263	351	452	402
20000	2829	438	550	494
24000	3395	528	668	598
28000	3960	622	792	707
32000	4526	724	957	841
36000	5092	818	1080	949
40000	5658	930	1224	1077
44000	6223	1044	1392	1218
48000	6789	1188	1580	1384
52000	7355	1350	1790	1570
54000	7638	1470	1980	1725
55000	7779	1536	2122	1829
56000	7920	1578	2212	1895
56500	7992	1644	2395	2020

*added 10 mℓ more superplasticizer.

Table 5.4: Stress-Strain Relation for Cylinder #2 Corresponding to Specimen I

Load (lb)	Stress (psi)	Strain Reading in Gage #1 (με)	Strain Reading in Gage #2 (με)	Average (με)
4000	566	112	80	96
8000	1132	222	173	198
12000	1697	322	264	293
16000	2263	416	358	387
20000	2829	508	446	477
24000	3395	608	541	575
28000	3960	710	634	672
32000	4526	820	738	779
36000	5092	950	850	900
40000	5658	1070	960	1015
44000	6223	1220	1078	1149
48000	6789	1306	1222	1264
52000	7355	1584	1364	1474
54000	7638	1726	1448	1587
55000	7779	1810	1508	1659
56000	7920	1902	1572	1737
57000	8062	2020	1650	1835
58000	8204	2210	1805	2008

Table 5.5: Load-Strain Data for Flexural Test of Structural Specimen I

P_1 Axial Load Machine* (ib)	Ram Pressure (psi)	P_2 Eccentric Load Ram Load (lb)	Strain Reading in ($\mu\varepsilon$)									
			Gage #1	Gage #2	Gage #3	Gage #4	Gage #5	Gage #6	Gage #7	Gage #8	Gage #9	Gage #10
27000	165	1600	+22	+27	0.00	-42	-64	-87	-94	-68	-50	-30
42000	310	2900	+18	+29	-33	-71	-115	-154	-164	-120	-86	-48
61250	435	4080	-4	+24	-50	-114	-176	-234	-248	-185	-135	-76
81250	588	5500	-19	-5	-75	-158	-233	-304	-322	-242	-180	-108
102000	775	7200	-19	-4	-99	-204	-308	-401	-422	-319	-232	-139
120250	925	8600	-23	0.00	-116	-246	-372	-482	-511	-388	-282	-164
140000	1050	9700	-34	0.00	-142	-294	-446	-575	-611	-467	-342	-207
160000	1160	10700	-43	-2	-167	-343	-515	-666	-709	-549	-404	0247
170000	1225	11300	-43	0.00	-176	-369	-556	-723	-768	-596	-440	-265
180000	1260	11650	-53	0.00	-188	-395	-594	-770	-819	-637	-473	-287
189000	1350	12450	-55	0.00	-205	-438	-663	-860	-914	-716	-528	-324
198500	1315	12150	-66	0.00	-217	-456	-688	-890	-948	-743	-553	-342
201000	1325	12200	-66	0.00	-222	-469	-711	-916	-977	-766	-570	-352
209000	1350	12450	-76	0.00	-234	-489	-742	-956	-1020	-802	-600	-374

*There was an initial load of 6000 lbs. on the beam, corresponding to a uniform stress of 148 psi, when the gages were balanced. Gage factor 2.03.

Table 5.5 continued

P_1 Axial Load Machine (lb)	Ram Pressure (psi)	P_2 Eccentric Load Ram Load (lb)	Strain Reading in ($\mu\varepsilon$)									
			Gage #1	Gage #2	Gage #3	Gage #4	Gage #5	Gage #6	Gage #7	Gage #8	Gage #9	Gage #10
218500	1400	12900	-78	0.00	-244	-516	-784	-1014	-1084	-852	-640	-396
229000	1425	13100	-88	- 6	-260	-551	-834	-1079	-1162	-916	-702	-429
238500	1410	13000	-107	+33	-280	-585	-877	-1137	-1230	-974	-752	-469
248000	1410	13000	-110	00	-285	-625	-945	-1242	-1360	-1068	-823	-502
256000	1275	11800	-150	00	-320	-685	-1010	-1330	-1467	-1184	-930	-590
263500	1248	11550	-166	+28	-332	-711	-1040	-1377	-1532	-1248	-982	-631
268000	1180	10900	-178	0.00	-332	-726	-1058	-1418	-1768	-1338	-1040	-670
272500	1020	11250	-237	+42	-340	-744	-1061	-1442	-1918	-1482	-1162	-764
280000	950	8800	-268						-2000			

Table 5.6: Load and Average Strain at Each Level, for Flexural Test of Specimen I

P_1 Axial Load Machine Load (lb)	Ramp Pressure	P_2 Eccentric Load Ramp Load (lb)	Strain Reading (με)				
			Average Gage #1 & #2 at the Surface	Average Gage #3 & #10 at 2" Depth	Average Gage #4 & #9 at 4" Depth	Average Gage #5 & #8 at 6" Depth	Average Gage #6 & #7 at 8" Depth
27000	165	1600	+25	-15	-46	-66	-91
42000	310	2900	+24	-41	-79	-118	-159
61250	435	4080	+10	-63	-125	-181	-241
81250	588	5500	-12	-92	-169	-238	-313
102000	775	7200	-12	-119	-218	-314	-412
120250	925	8600	-12	-140	-246	-380	-497
140000	1050	9700	-17	-175	-318	-457	-593
160000	1160	10700	-23	-207	-374	-532	-688
170000	1225	11300	-22	-221	-405	-576	-746
180000	1260	11650	-27	-238	-434	-616	-795
189000	1350	12450	-28	-265	-483	-690	-887
198500	1315	12150	-33	-280	-505	-716	-919
201000	1325	12200	-33	-287	-520	-739	-947
209000	1350	12450	-38	-304	-545	-772	-988

Table 5.6 continued

P_1 Axial Load Machine Load (lb)	Ramp Pressure	P_2 Eccentric Load Ramp Load (lb)	Strain Reading (με)				
			Average Gage #1 & #2 at the Surface	Average Gage #3 & #10 at 2" Depth	Average Gage #4 & #9 at 4" Depth	Average Gage #5 & #8 at 6" Depth	Average Gage #6 & #7 at 8" Depth
218500	1400	12900	-39	-320	-578	-820	-1049
229000	1425	13100	-44	-345	-627	-875	-1121
238500	1410	13000	-57	-375	-669	-926	-1184
248000	1410	13000	-38	-394	-724	-1007	-1301
256000	1275	11800	-75	-455	-808	-1097	-1399
263500	1248	11550	-83	-482	-847	-1144	-1455
268000	1180	10900	-75	-501	-883	-1198	-1593
272500	1020	11250	-119	-552	-953	-1272	-1680
280000	950	8800	-113				-2000

Table 5.7: Cylinder Data Corresponding to Structural Specimen II

No. of Cylinders	3 x 6 in. Area in^2	Load lb	Stress psi
1	7.07	65500	9264
2	7.07	65000	9194
3	7.07	64000	9052
4	7.07	70500	9971
5	7.07	66700	9434

$$f'_c \text{ average} = \frac{\Sigma f'_c}{\Sigma} = \frac{46915}{5} = 9383 \text{ psi}$$

$$\simeq 9400 \text{ psi}$$

Table 5.8: Stress-Strain Data of Cylinder Test Corresponding to Structural Specimen II

Load (lb)	3 x 6 in. Cylinder Area (in^2)	Stress (psi)	Strain Reading in Gage #1 ($\mu\varepsilon$)	Strain Reading in Gage #2 ($\mu\varepsilon$)	Average Strain ($\mu\varepsilon$)
4000	7.07	566	-65	-100	-83
8000	7.07	1132	-135	-182	-159
12000	7.07	1697	-218	-272	-245
16000	7.07	2263	-298	-370	-334
20000	7.07	2829	-384	-464	-424
24000	7.07	3395	-480	-560	-520
29000	7.07	4102	-600	-680	-640
32000	7.07	4526	-670	-790	-730
36000	7.07	5092	-812	-904	-858
40000	7.07	5658	-923	-1053	-988
44000	7.07	6223	-1062	-1218	-1140
48000	7.07	6789	-1240	-1424	-1332
52000	7.07	7355	-1451	-1645	-1548
56000	7.07	7921	-1732	-1836	-1784
60000	7.07	8487	-1950	-2180	-2065
62000	7.07	8769	-2116	-2348	-2232
64000	7.07	9052	-2276	-2621	-2448
66000	7.07	9335	-2594	-2890	-2742
66700	7.07	9434	--	-2940	-2940

Table 5.9: Load-Strain Data for Flexural Test of Structural Specimen II

P_1 Axial Load (machine load) (lb)	Ramp Pressure	P_2 Eccentric Load Ramp Load (lb)	Strain Reading (με)									
			Gage #1	Gage #2	Gage #3	Gage #4	Gage #5	Gage #6	Gage #7	Gage #8	Gage #9	Gage #10
0	0		0	0	0	0	+600-600* = 0	0	0	0	0	0
23000	75	700	-14	-108	-162	-234	+247-600 = -353	-335	-278	-164	-98	-43
44500	170	1600	0	-120	-231	-398	0-600 = -600	-698	-620	-373	-226	-74
61000	255	2300	-8	-168	-316	-555	-172-600 = -772	-950	-843	-516	-315	-97
71000	290	2680	0	-168	-344	-640	-298-600 = -898	-1122	-1000	-618	-369	-106
85250	335	3100	0	-197	-414	-768	-488-600 = -1088	-1378	-1227	-772	-472	-140
100000	400	3680	0	-207	-474	-913	-708-600 = -1308	-1686	-1502	-952	-578	-159
110000	420	3880	0	-222	-523	-1018	-861-600 = -1461	-1883	-1676	-1080	-655	-186
119750	430	3950	-5	-254	-584	-1131	-1016-600 = -1616	-2098	-1864	-1218	-749	-222

Table 5.9 continued

P_1 Axial Load (machine load) (lb)	Ramp Pressure	P_2 Eccentric Load Ramp Load (lb)	Strain Reading (με)									
			Gage #1	Gage #2	Gage #3	Gage #4	Gage #5	Gage #6	Gage #7	Gage #8	Gage #9	Gage #10
124750	425	3900	0	-250	-606	-1210	-1140-600 = -1740	-2289	-2022	-1321	-798	-217
129500	450	4120	0	-260	-641	-1280	-1239-600 = -1839	-2422	-2132	-1404	-851	-240
134500	450	4120	0	-282	-686	-1356	-1352-600 = -1952	-2577	-2250	-1500	-911	-263
138500	453	4150	-3	-293	-715	-1436	-1480-600 = -2080	-2774	-2401	-1613	-974	-272
144750	453	4150	0	-300	-760	-1529	-1630-600 = -2230	-3012	-2576	-1742	-1062	-304
150000	450	4120	0	-278	-802	-1685	-1888-600 = -2488	-3317	-2900	-1970	-1176	-258

*Subtract 600 from all values of Gage #5 in order to correct that gage.

Table 5.10: Load and Average Strain at Each Level for Flexural Test of Specimen II

P_1 Axial Load (machine load) (lb)	Ramp Pressure Reading	P_2 Eccentric Load Ramp Load	Strain Reading in ($\mu\varepsilon$) Average Gage #1 & #2 at the Surface	Average Gage #3 & #10 at 3/4 in.	Average Gage #4 & #9 at 2 1/4 in.	Average Gage #5 & #8 at 3 1/2 in.	Average Gage #6 & #7 at 5 in.
0	0	0	0	0	0	0	0
23000	75	700	-61	-103	-166	-259	-307
44500	170	1600	-60	-153	-312	-487	-659
61000	255	2300	-88	-207	-435	-644	-897
71000	290	2680	-84	-225	-505	-758	-1061
85250	335	3100	-99	-277	-620	-930	-1303
100000	400	3680	-104	-317	-746	-1130	-1594
110000	420	3880	-111	-355	-837	-1271	-1780
119750	430	3950	-130	-403	-940	-1417	-1981
124750	425	3900	-125	-412	-1004	-1531	-2156
129500	450	4120	-130	-441	-1066	-1622	-2277
134500	450	4120	-141	-475	-1134	-1726	-2414
138500	453	4150	-148	-494	-1205	-1847	-2588
144750	453	4150	-150	-532	-1296	-1986	-2794
150000	450	4120	-139	-530	-1431	-2229	-3109

Table 5.11: Load and Ultimate Strength Factors for Specimen I

P_1 Major Thrust (lb)	P_2 Minor Thrust (lb)	ε_c at Comp. Face $\mu\varepsilon$	f_c psi	K_1	K_2	K_3 f_{max}/f'_c	K_1K_3	$\frac{K_2}{K_1K_3}$	f_o^* psi	m_o^* psi
27000	1600	-91	475	1.5	0.34	$\frac{475}{8437}$ = .056	0.084	4.04	707	467
42000	2900	-159	850	1.31	0.32	$\frac{850}{8437}$ = .101	0.132	2.42	1109	760
61250	4080	-241	1300	1.25	0.32	$\frac{1300}{8437}$ = 0.154	0.192	1.67	1614	1097
81250	5500	-313	1700	1.27	0.32	$\frac{1700}{8437}$ = 0.201	0.255	1.25	2144	1463
102000	7200	-412	2260	1.2	0.31	$\frac{2260}{8437}$ = 0.268	0.321	0.97	2698	1861
120250	8600	-497	2750	1.16	0.31	$\frac{2750}{8437}$ = 0.326	0.379	0.82	3184	2203
140000	9700	-593	3300	1.12	0.31 ≃ 0.32	$\frac{3300}{8437}$ = 0.391	0.44	0.73	3699	2539
160000	10700	-688	3825	1.11	0.32	$\frac{3825}{8437}$ = 0.453	0.502	0.64	4218	2869
170000	11300	-746	4100	1.09	0.32	$\frac{4100}{8437}$ = .485	0.533	0.60	4480	3043

Table 5.11 continued

P_1 Major Thrust (lb)	P_2 Minor Thrust (lb)	ε_c at Comp. Face $\mu\varepsilon$	f_c psi	K_1	K_2	K_3 f_{max}/f'_c	K_1K_3	$\frac{K_2}{K_1K_3}$	f_o psi	m_o psi
180000	11650	-795	4350	1.09	0.33 ≃ 0.32	$\frac{4350}{8437}$ = 0.516	0.564	0.59	4736	3195
189000	12450	-887	4800	1.04	0.32	$\frac{4800}{8437}$ = 0.569	0.593	0.54	4978	3373
198500	12150	-919	4950	1.06	0.33	$\frac{4950}{8437}$ = 0.587	0.620	0.53	5025	3467
201000	12200	-947	5100	1.04	0.34	$\frac{5100}{8437}$ = 0.604	0.627	0.54	52680*	3500
209000	12450	-988	5325	1.03	0.34	$\frac{5325}{8437}$ = 0.631	0.651	0.52	5472	3620
218500	12900	-1049	5550	1.04	0.34	$\frac{5550}{8437}$ = 0.658	0.681	0.50	5718	3775
229000	13100	-1121	5825	1.03	0.34	$\frac{5825}{8437}$ = 0.690	0.712	0.48	5982	3922
238500	13000	-1184	6100	1.02	0.35	$\frac{6100}{8437}$ = 0.723	0.740	0.47	6214	4031
248000	13000	-1301	6525	0.99	0.36	$\frac{6525}{8437}$ = .773	0.767	0.47	6449	4148

Table 5.11 continued

P_1 Major Thrust (lb)	P_2 Minor Thrust (lb)	ε_c at Comp. Face $\mu\varepsilon$	f_c psi	K_1	K_2	K_3 f_{max}/f'_c	K_1K_3	$\frac{K_2}{K_1K_3}$	f_o psi	m_o psi
256000	11800	-1399	6850	0.971	0.37	$\frac{6850}{8437}$ = 0.812	0.788	0.47	6617	4147
263500	11550	-1455	7025	0.973	0.38	$\frac{7025}{8437}$ = 0.833	0.810	0.47	6796	4219
268000	10900	-1593	7380	0.937	0.39	$\frac{7380}{8437}$ = 0.875	0.820	0.47	6892	4220
272500	11250	-1680	7065	0.997	0.39	$\frac{7065}{8437}$ = 0.837	0.835	0.47	7011	4305
280000	8800	-2000	7990	0.898	0.41	$\frac{6935}{8437}$ = 0.947	0.850	0.48	7136	4193

Table 5.12: Load and Ultimate Strength Factors for Specimen II

P_1 Axial Load (machine load) (lb)	P_2 Minor Thrust	ε_c at Comp. Face ($\mu\varepsilon$)	K_1	K_2	K_3 f_{max}/f'_c	K_1K_3	$\frac{K_2}{K_1K_3}$	f_c psi
23000	700	-307	0.452	0.36	$\frac{2100}{9400} = 0.223$	0.101	3.56	2100
44500	1600	-659	0.441	0.33	$\frac{4175}{9400} = 0.444$	0.196	1.68	4175
61000	2300	-897	0.482	0.32	$\frac{5250}{9400} = 0.559$	0.269	1.19	5250
71000	2680	-1061	0.498	0.32	$\frac{5925}{9400} = 0.630$	0.314	1.02	5925
85250	3100	-1303	0.520	0.33	$\frac{6800}{9400} = 0.723$	0.376	0.878	6800
100000	3680	-1594	0.537	0.33	$\frac{7725}{9400} = 0.822$	0.441	0.748	7725
110000	3880	-1780	0.558	0.33	$\frac{8175}{9400} = 0.870$	0.485	0.680	8175
119750	3950	-1981	0.575	0.34	$\frac{8600}{9400} = 0.915$	0.526	0.646	8600
124750	3900	-2156	0.578	0.35	$\frac{8900}{9400} = 0.947$	0.547	0.640	8900
129500	4120	-2277	0.589	0.35	$\frac{9075}{9400} = 0.965$	0.569	0.615	9075
134500	4120	-2414	0.571	0.35	$\frac{9225}{9400} = 0.981$	0.560	0.625	9225
138500	4150	-2588	0.609	0.36	$\frac{9375}{9400} = 0.997$	0.607	0.590	9375

Table 5.12 continued

P_1 Axial Load (machine load) (lb)	P_2 Minor Thrust	ε_c at Comp. Face ($\mu\varepsilon$)	K_1	K_2	K_3 f_{max}/f'_c	K_1K_3	$\frac{K_2}{K_1K_3}$	f_c psi
144750	4150	-2794	0.632	0.36	$\frac{9425}{9400} = 1.00$	0.634	0.569	9425
150000	4120	-3109	0.653	0.37	$\frac{9450}{9400} = 1.01$	0.656	0.564	9450

Table 5.13: Values of Coefficients at Ultimate Condition

Specimen Subscript	f'_c (psi)	f_{max} (psi)	K_1	K_2	K_3	K_1K_3	$\frac{K_2}{K_1K_3}$	ε_{cu} (in/in)
Specimen I	8400	7990	0.895	0.41	0.95	0.850	0.48	0.00200
Specimen II	9400	9500	0.650	0.37	1.01	0.656	0.564	0.00311

Table 5.14: Load and Stress Data for Flexural Test of Specimen I Using Equations (4.1), (4.2)

Net Major Thrust P_1 (lb)	Minor Thrust P_2 (lb)	Strain at Comp. Face ε_c ($\mu\varepsilon$)	f_o* (psi)	m_o** (psi)	$\frac{df_o}{d\varepsilon_c}$	$\frac{dm_o}{d\varepsilon_c}$	$f_c = \varepsilon_c \frac{df_o}{d\varepsilon_c} + f_o$ Eq. (4.1) (psi)	$f_c = \varepsilon_c \frac{dm_o}{d\varepsilon_c} + 2\, m_o$ Eq. (4.2) (psi)	f_c Average of Eq. (4.1) & Eq. (4.2) (psi)
21000	1600	-91	558	393	6.384	4.379	1139	1185	1162
36000	2900	-159	961	687	6.347	4.379	1970	2070	2020
55250	4080	-241	1466	1023	6.302	4.379	2985	3101	3043
75250	5500	-313	1995	1388	6.238	4.332	3947	4132	4039
96000	7200	-412	2550	1787	6.876	4.089	4971	5259	5115
114250	8600	-497	3036	2129	5.536	3.759	5787	6126	5956
134000	9700	-593	3551	2464	5.342	3.494	6708	7000	6854
154000	10700	-688	4070	2795	5.087	3.240	7570	7819	7694
164000	11300	-746	4332	2969	4.332	2.822	7564	8043	7803
174000	11650	-795	4587	3121	4.103	2.580	7849	8293	8071

$^*f_o = \frac{P_1 + P_2}{bc}$ $a_1 = 4$ in., $a_2 = 27$ in.

$^{**}m_o = \frac{P_1 a_1 + P_2 a_2}{bc^2}$ $bc = 40.47$ in.^{2}, $c = 8$ in.

Table 5.14 continued

Net Major Thrust P_1 (lb)	Minor Thrust P_2 (lb)	Strain at Comp. Face ε_c ($\mu\varepsilon$)	f_o * (psi)	m_o ** (psi)	$\frac{df_o}{d\varepsilon_c}$	$\frac{dm_o}{d\varepsilon_c}$	$f_c = \varepsilon_c \frac{df_o}{d\varepsilon_c} + f_o$ Eq. (4.1) (psi)	$f_c = \varepsilon_c \frac{dm_o}{d\varepsilon_c} + 2\ m_o$ Eq. (4.2) (psi)	f_c Average of Eq. (4.1) & Eq. (4.2) (psi)
183000	12450	-887	4830	3299	3.814	2.009	8213	8380	8296
192500	12150	-919	5057	3391	4.268	2.291	8979	8887	8933
195000	12200	-947	5120	3427	4.656	2.389	9529	9116	9322
203000	12450	-988	5324	3546	4.012	2.399	9287	9462	9374
212500	12900	-1049	5570	3701	4.032	2.333	9800	9850	9825
223000	13100	-1121	5834	3848	3.387	1.848	9631	9768	9699
232500	13000	-1184	6066	3957	2.895	1.399	9494	9570	9532
242000	13000	-1301	6301	4074	2.243	0.737	9219	9106	9162
250000	11800	-1399	6469	4073	1.676	0.427	8814	8738	8776
257500	11550	-1455	6648	4145	1.602	0.342	8979	8788	8883
262000	10900	-1593	6743	4146	1.107	0.311	8504	8787	8645
266500	11250	-1680	6863	4231	0.859	0.110	8306	8646	8476
274000	8800	-2000	6988	4119	-0.048	-0.630	6893	6978	6935

Table 5.15: Load and Stress Data for Flexural Test of Specimen I Using Eq. 4.1 & 4.2 and Cylinder Stress-Strain Curve

Net Major Thrust P_1 (lb)	Minor Thrust P_2 (lb)	Strain at Compression Face ε_c ($\mu\varepsilon$)	f_c Average of Eq. (4.1) and Eq. (4.2) (psi)	f_c Reading using Cylinder Stress-Strain Curve (psi)
21000	1600	-91	1162	475
36000	2900	-159	2020	850
55250	4080	-241	3043	1300
75250	5500	-313	4039	1700
96000	7200	-412	5115	2260
114250	8600	-497	5956	2750
134000	9700	-593	6854	3300
154000	10700	-688	7694	3825
164000	11300	-746	7803	4100
174000	11650	-795	8071	4350
183000	12450	-887	8296	4800
192500	12150	-919	8933	4950
195000	12200	-947	9322	5100
203000	12450	-988	9374	5325

Table 5.15 continued

Net Major Thrust P_1 (lb)	Minor Thrust P_2 (lb)	Strain at Compression Face ε_c ($\mu\varepsilon$)	f_c Average of Eq. (4.1) and Eq. (4.2) (psi)	f_c Reading using Cylinder Stress-Strain Curve (psi)
212500	12900	-1049	9825	5550
223000	13100	-1121	9699	5825
232500	13000	-1184	9532	6100
242000	13000	-1301	9162	6525
250000	11800	-1399	8776	6850
257500	11550	-1455	8883	7025
262000	10900	-1593	8645	7380
266500	11250	-1680	8476	7065
274000	8800	-2000	6935	7990

Table 5.16: Load-Stress Data for Flexural Test of Specimen II Using Eq. (4.1), (4.2)

Major Thrust P_1 (lb)	Minor Thrust P_2 (lb)	Strain at Comp. Face ε_c ($\mu\varepsilon$)	f_o* (psi)	m_o** (psi)	$\frac{df_o}{d\varepsilon_c}$	$\frac{dm_o}{d\varepsilon_c}$	$f_c = \varepsilon_c \frac{df_o}{d\varepsilon_c} + f_o$ Eq. (4.1) (psi)	$f_c = \varepsilon_c \frac{dm_o}{d\varepsilon_c} + 2\ m_o$ Eq. (4.2) (psi)	f_c Average of Eq. (4.1) & Eq. (4.2) (psi)
23000	700	-307	948	611	2.723	1.955	1784	1822	1803
44500	1600	-659	1844	1236	2.650	1.840	3591	3685	3638
61000	2300	-897	2532	1717	2.601	1.763	4866	5015	4941
71000	2680	-1061	2947	1999	2.532	1.711	5633	5814	5724
85250	3100	-1303	3534	2375	2.301	1.513	6532	6721	6627
100000	3680	-1594	4147	2795	2.130	1.317	7543	7689	7616
110000	3880	-1780	4555	3038	1.873	1.081	7889	8001	7945
119750	3950	-1981	4948	3248	1.640	0.915	8196	8309	8253
124750	3900	-2156	5146	3337	1.478	0.831	8333	8466	8400
129500	4120	-2277	5345	3480	1.298	0.729	8301	8620	8461
134500	4120	-2414	5545	3580	1.299	0.740	8681	8947	8814
138500	4150	-2588	5706	3666	1.090	0.553	8526	8764	8645
144750	4150	-2794	5956	3791	0.888	0.439	8437	8809	8623
150000	4120	-3109	6165	3890	0.580	0.264	7968	8602	8285

*$f_c = \frac{P_1 + P_2}{bc}$ **$m_o = \frac{P_1 a_1 + P_2 a_2}{bc^2}$ $bc = 25\ in^2$, $a_1 = 2.5$ in., $a_2 = 27$ in., $c = 5$ in.

Table 5.17: Load-Stress Data for Flexural Test of Specimen II Using Eq. 4.1 & 4.2 and Cylinder Stress-Strain Curve

Major Thrust P_1 (lb)	Minor Thrust P_2 (lb)	Strain at Compression Face ε_c ($\mu\varepsilon$)	f_c Average of Eq. (4.1) and Eq. (4.2) (psi)	f_c Reading using Cylinder Stress-Strain Curve (psi)
23000	700	-307	1803	2100
44500	1600	-659	3638	4175
61000	2300	-897	4941	5250
71000	2680	-1061	5724	5925
85250	3100	-1303	6627	6800
100000	3680	-1594	7616	7725
110000	3880	-1780	7945	8175
119750	3950	-1981	8253	8600
124750	3900	-2156	8400	8900
129500	4120	-2277	8461	9075
134500	4120	-2414	8814	9225
138500	4150	-2588	8645	9375
144750	4150	-2794	8623	9425
150000	4120	-3109	8283	9450

Table 5.18: Ultimate Strain at Different Ages

Age (day)	Strain in/in
47	0.002940
72	0.00250
85	0.00209
120	0.00200

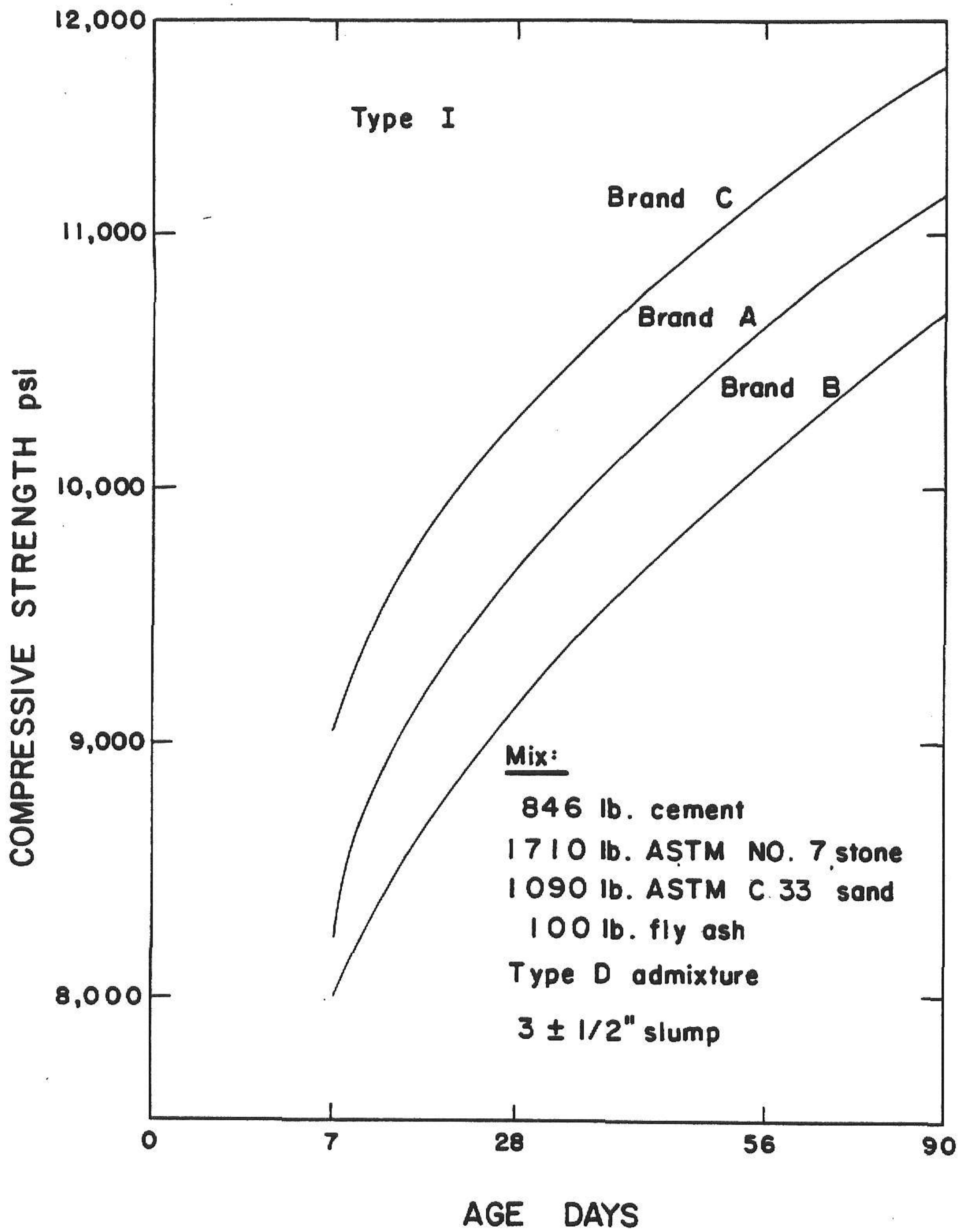

Figure 2.1: Effect of Various Brands of Type I Cement on Concrete Compressive Strength (5)

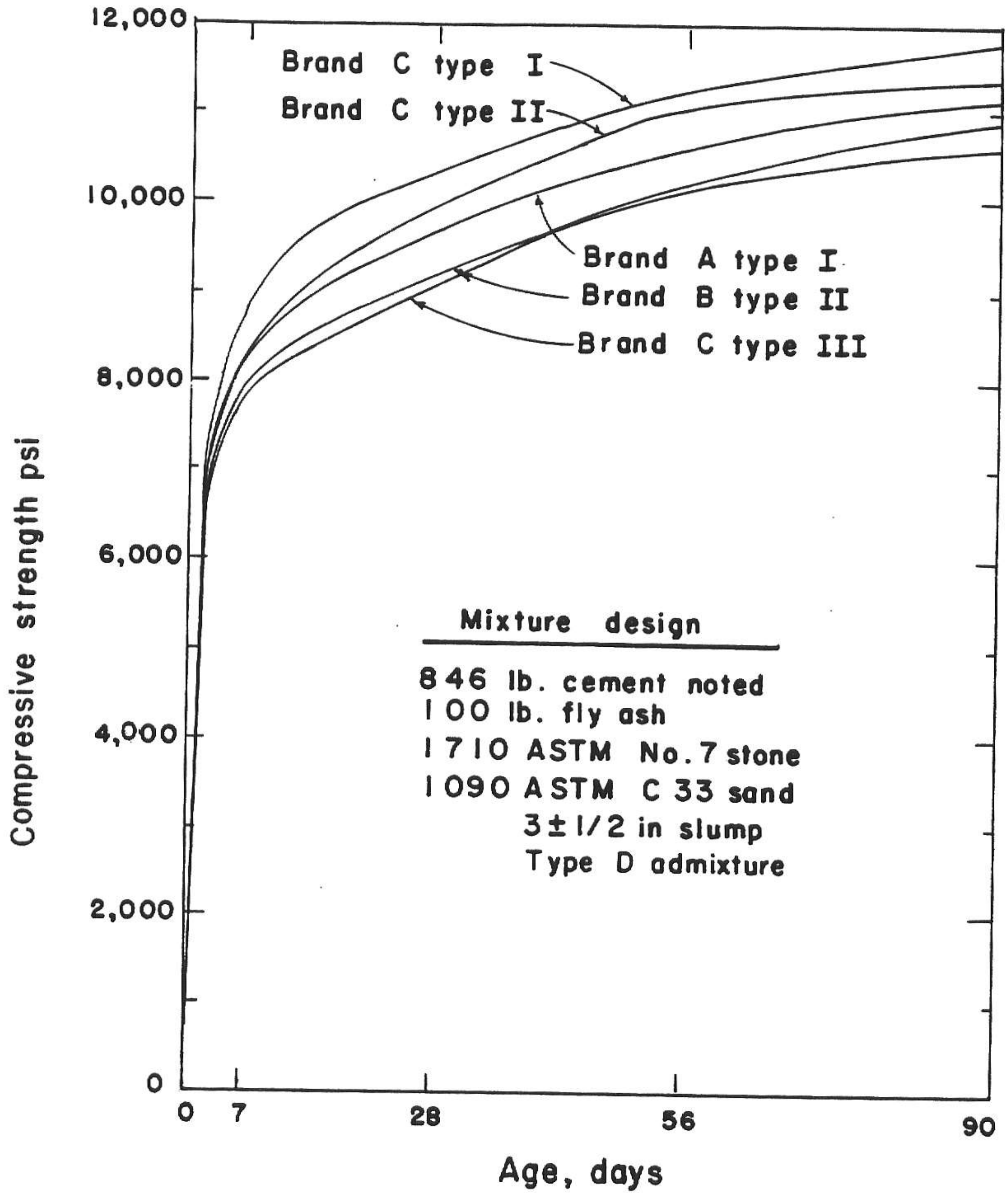

Figure 2.2: Effect of Various Cements on Concrete Compressive Strength (6)

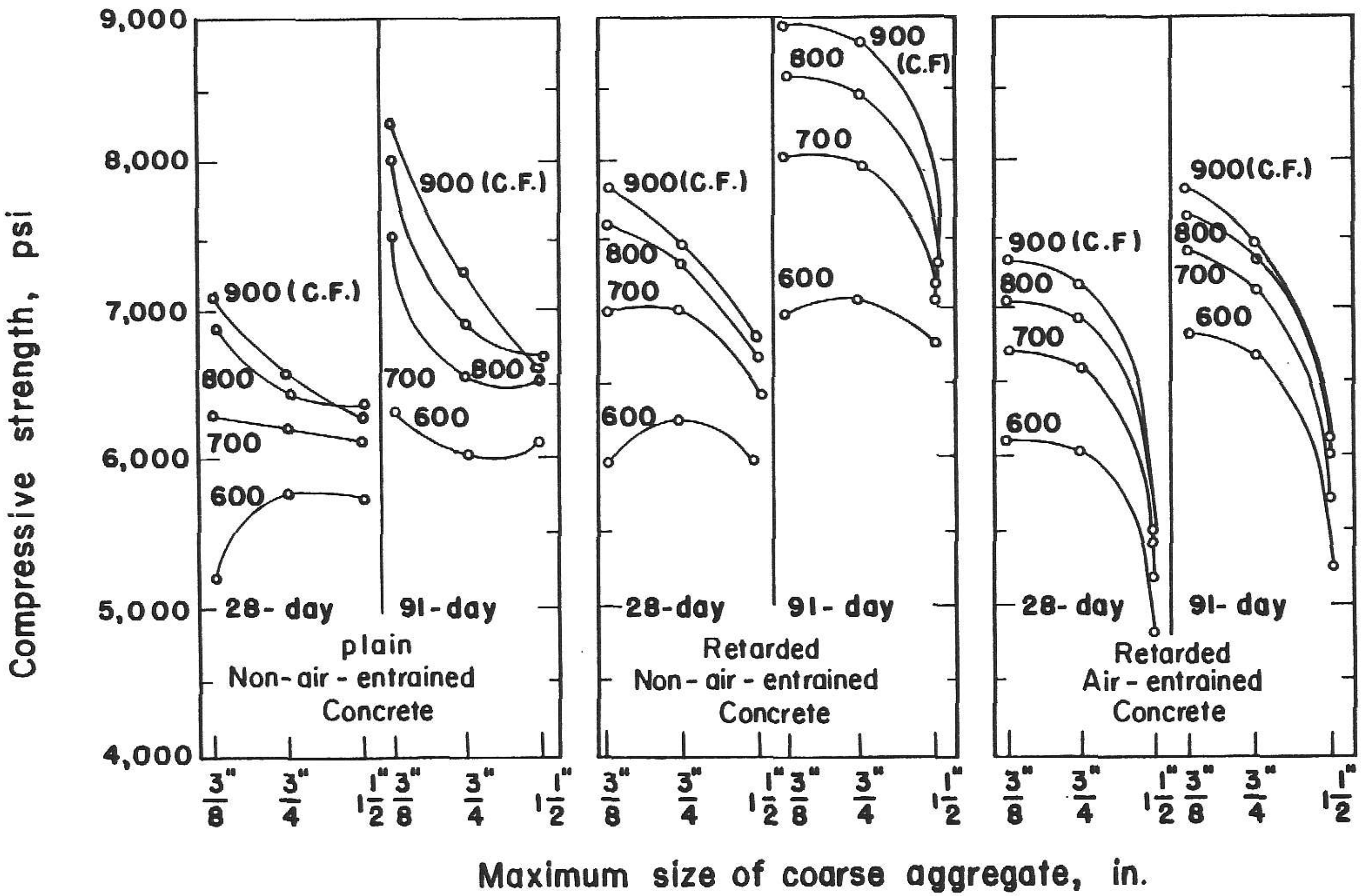

Figure 2.3: Effect of Size of Coarse Aggregate on Compressive Strength in Different Types of Concrete (adapted from Ref. 3)

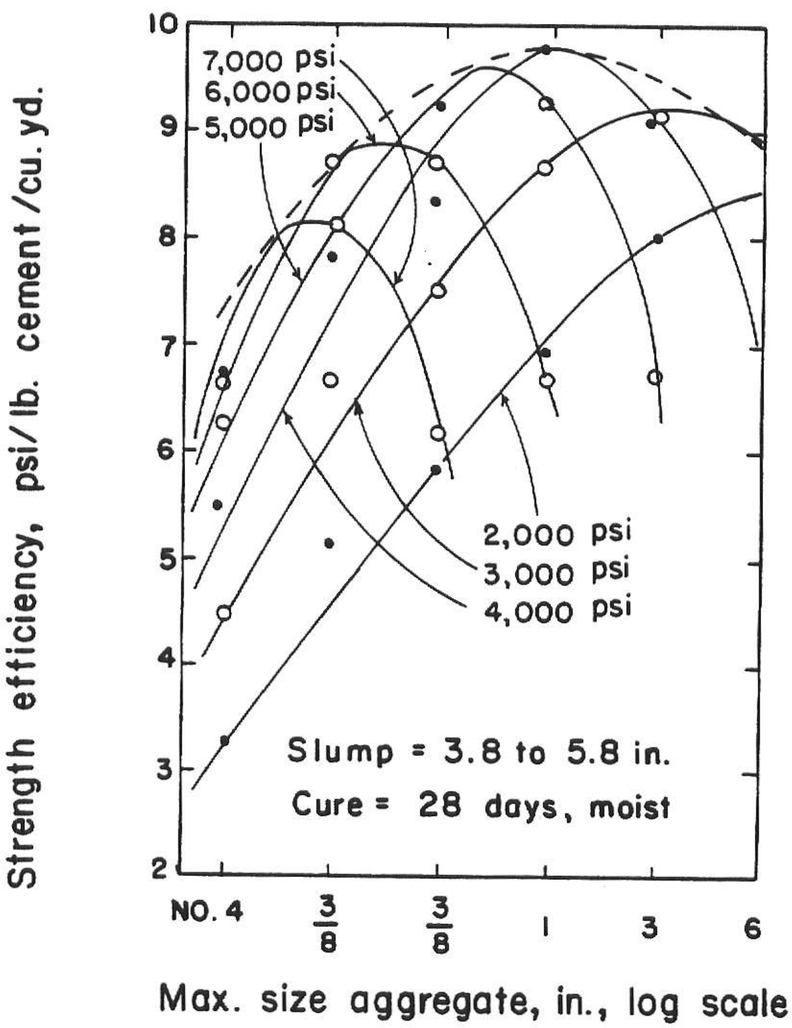

Figure 2.4: Maximum Size Aggregate for Strength Efficiency Envelope (14)

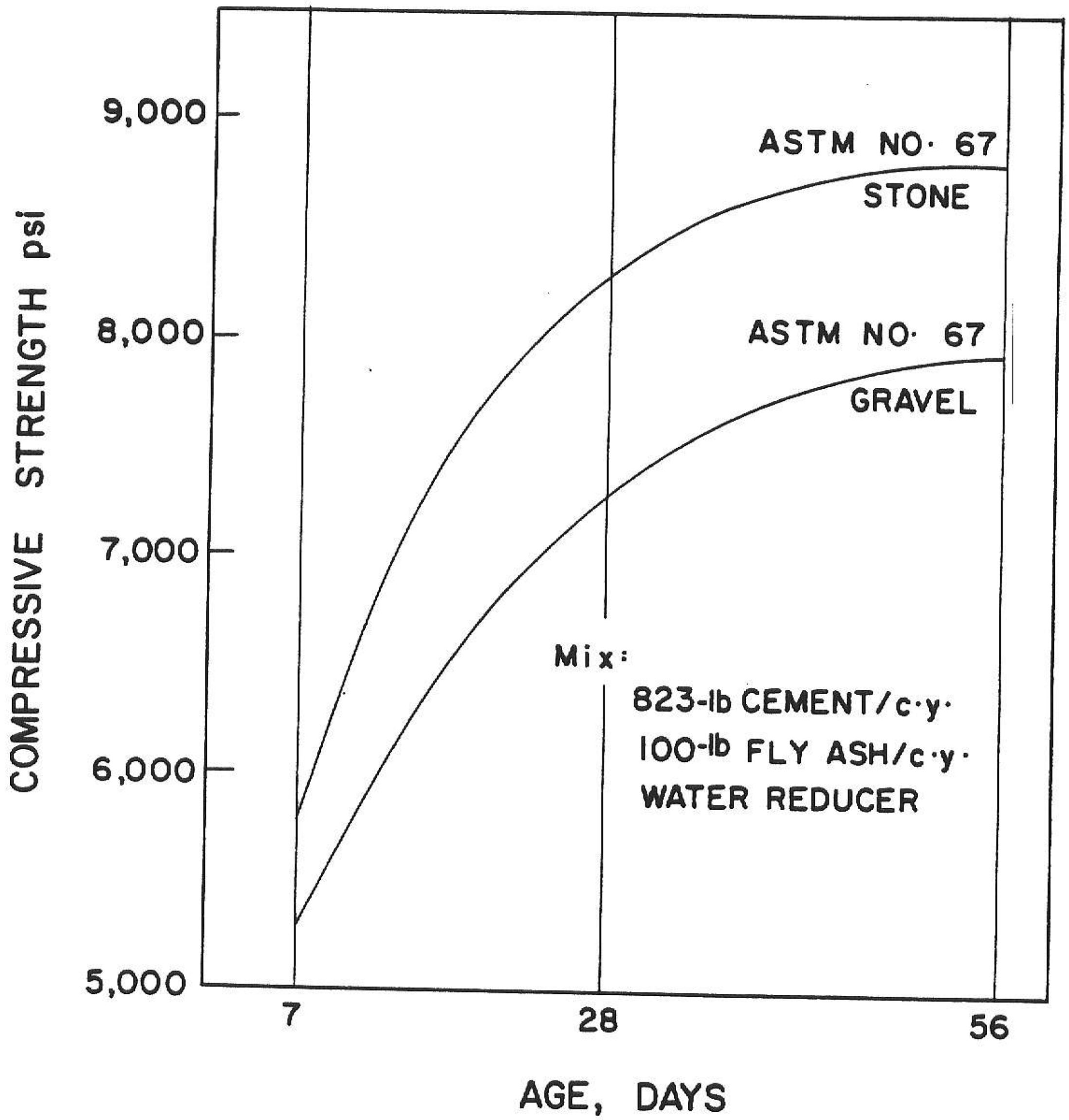

Figure 2.5: Compressive Strength of Concrete Using Two Sizes and Types of Coarse Aggregate for 7,500 psi Concrete (12)

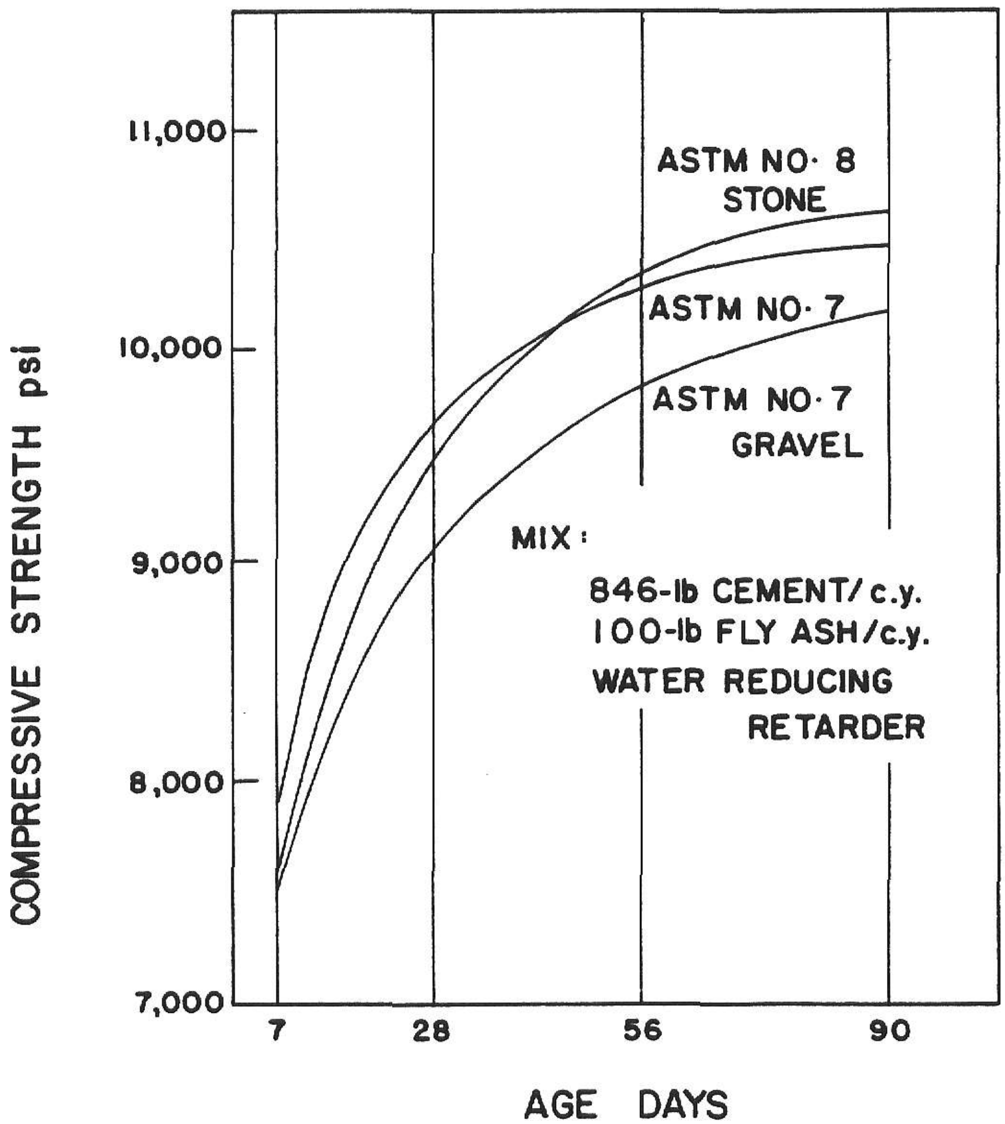

Figure 2.6: Compressive Strength of High-Strength Concrete Using Three Sizes and Types of Coarse Aggregate

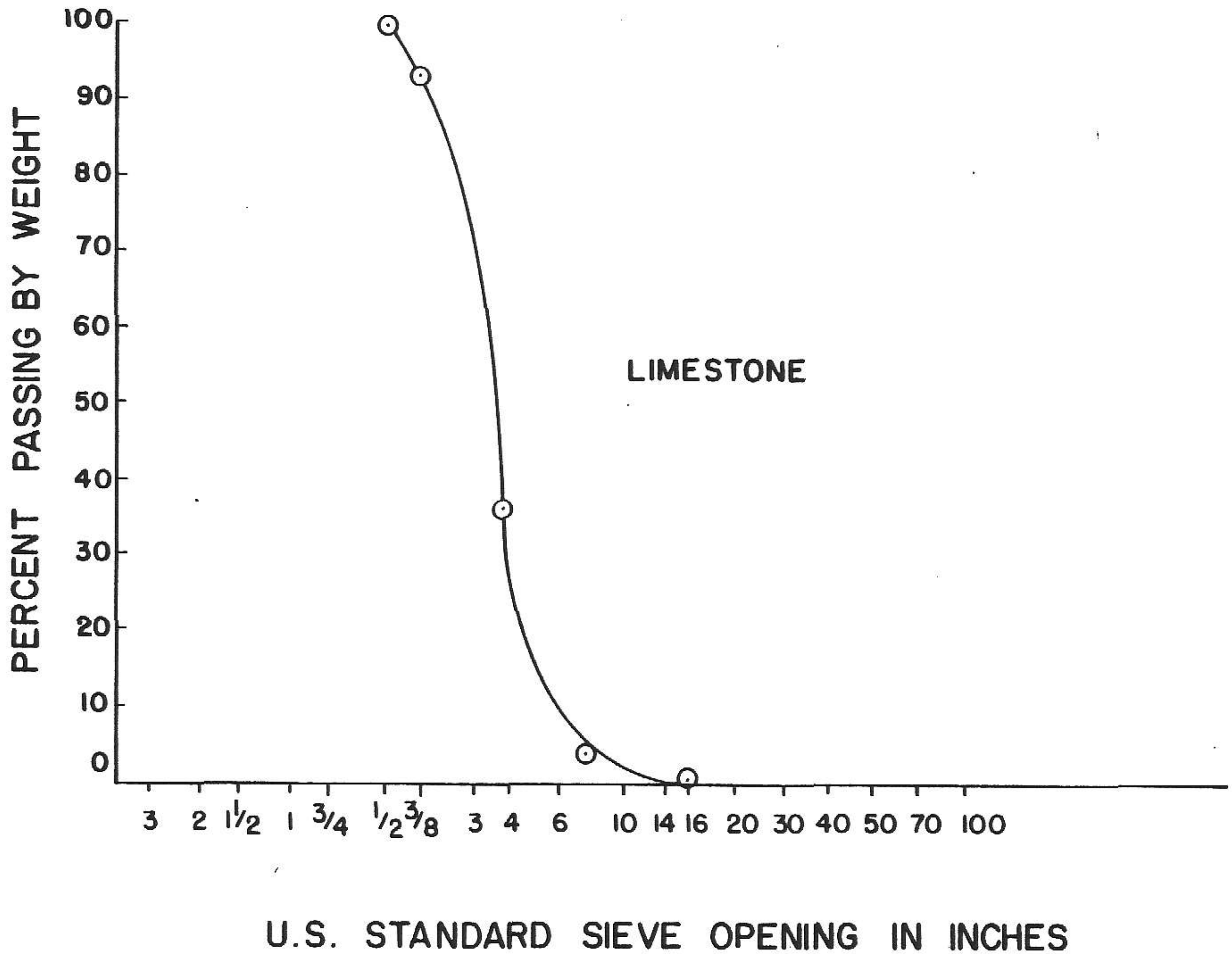

Figure 2.7: Size of Aggregate vs. Percent Passing, Limestone

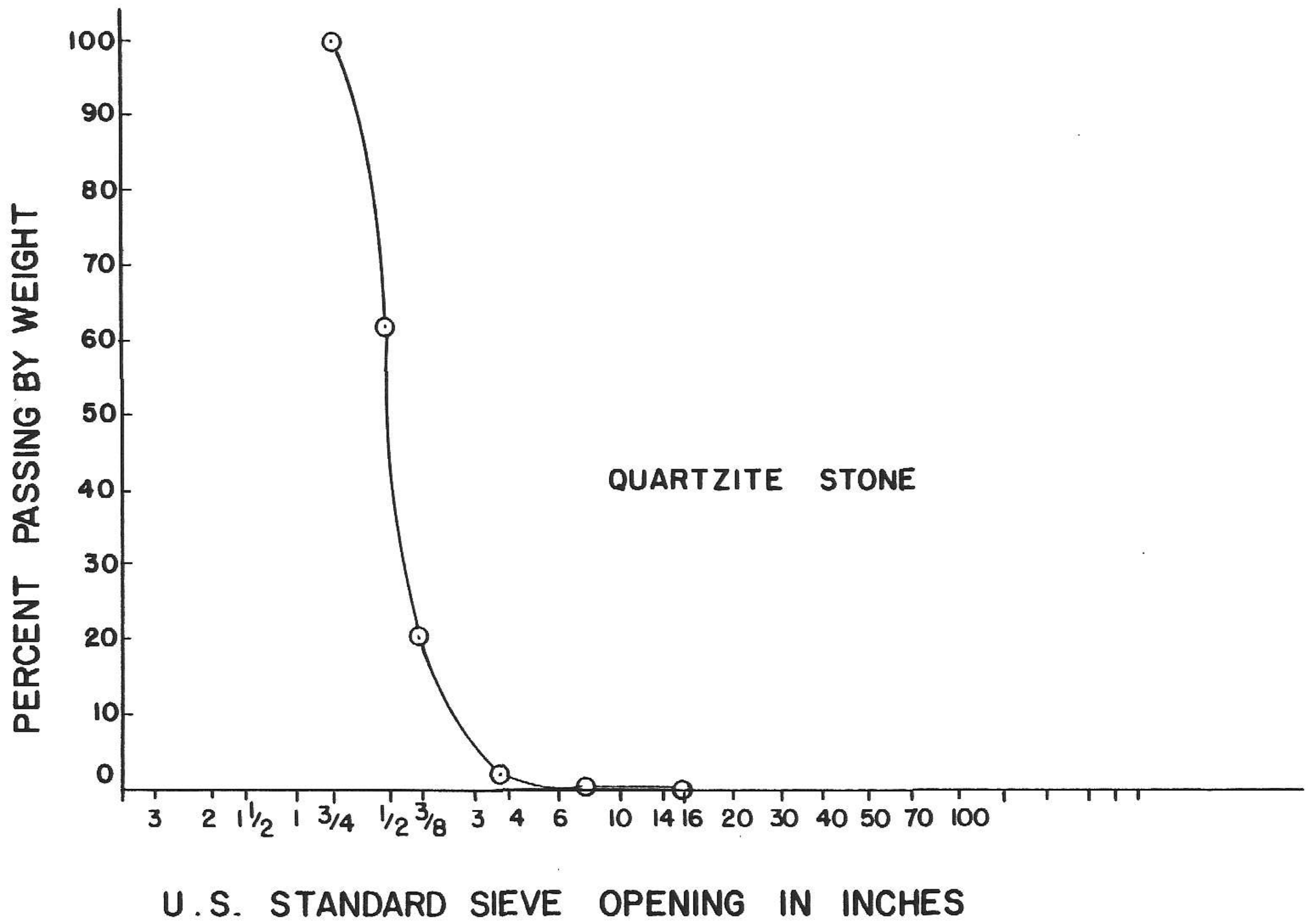

Figure 2.8: Size of Aggregate vs. Percent Passing, Quartzite

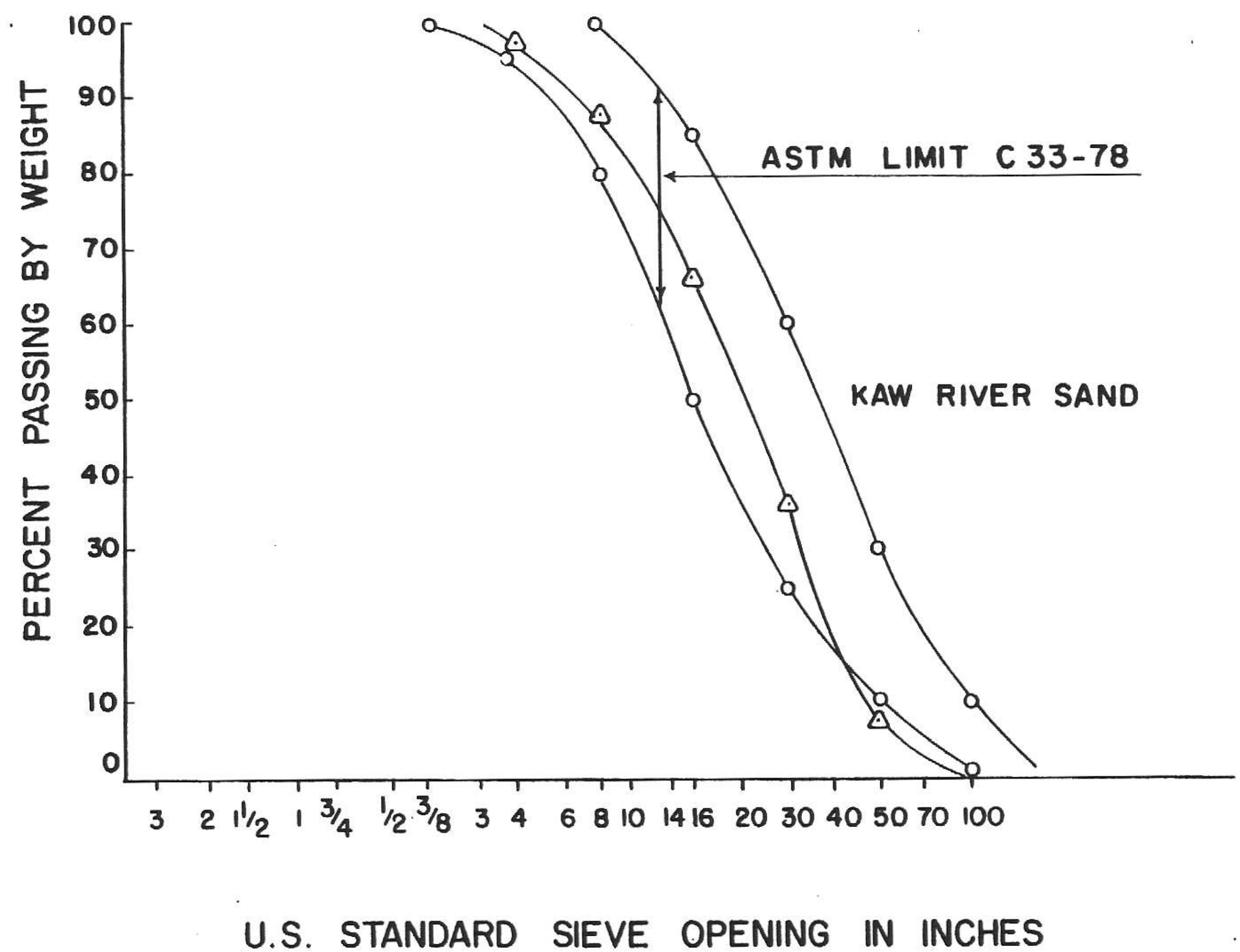

Figure 2.9: Sand Sieve Analysis - Percent Passing vs. Sieve Size

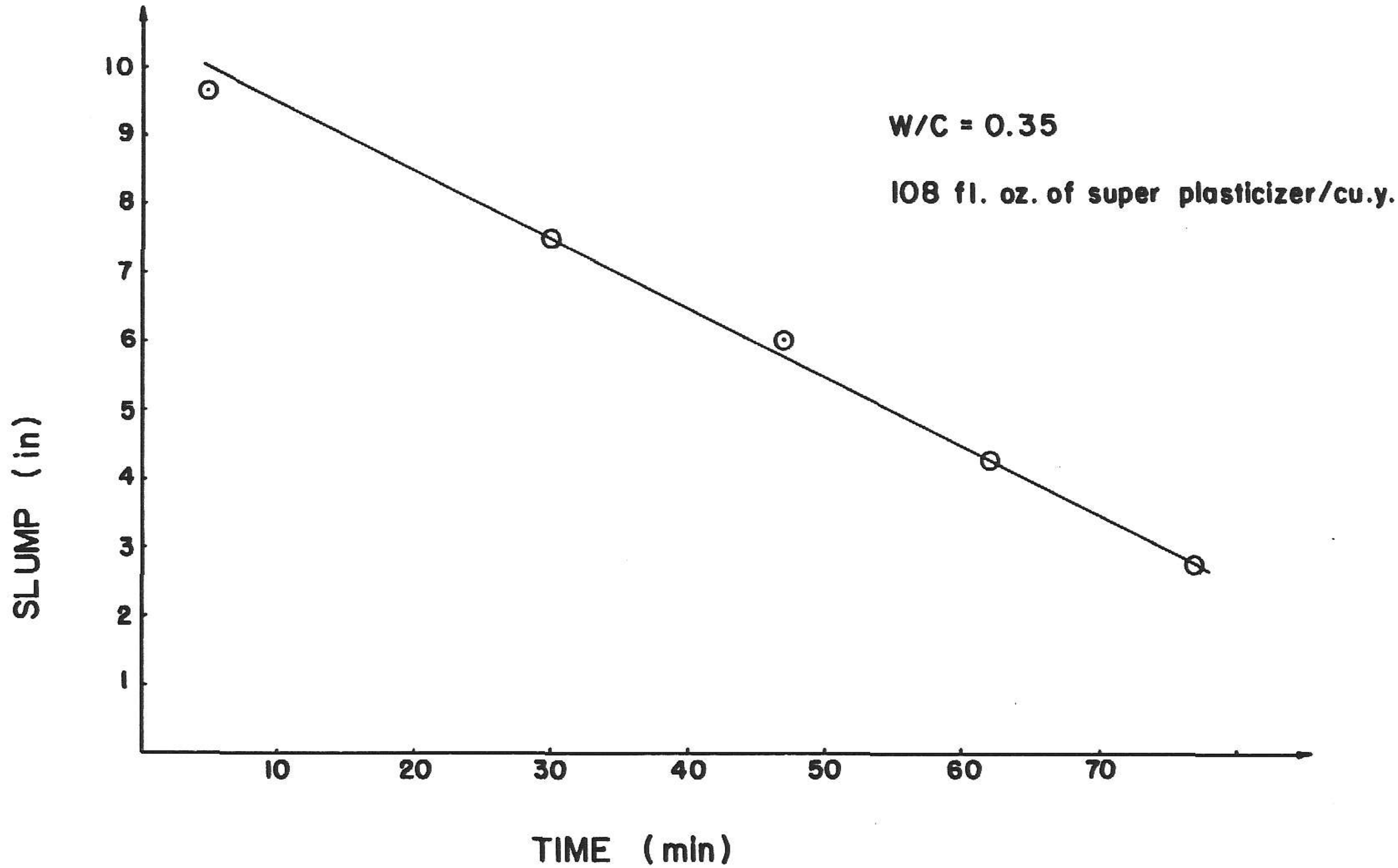

Figure 2.10: Slump vs. Time When Using Superplasticizer

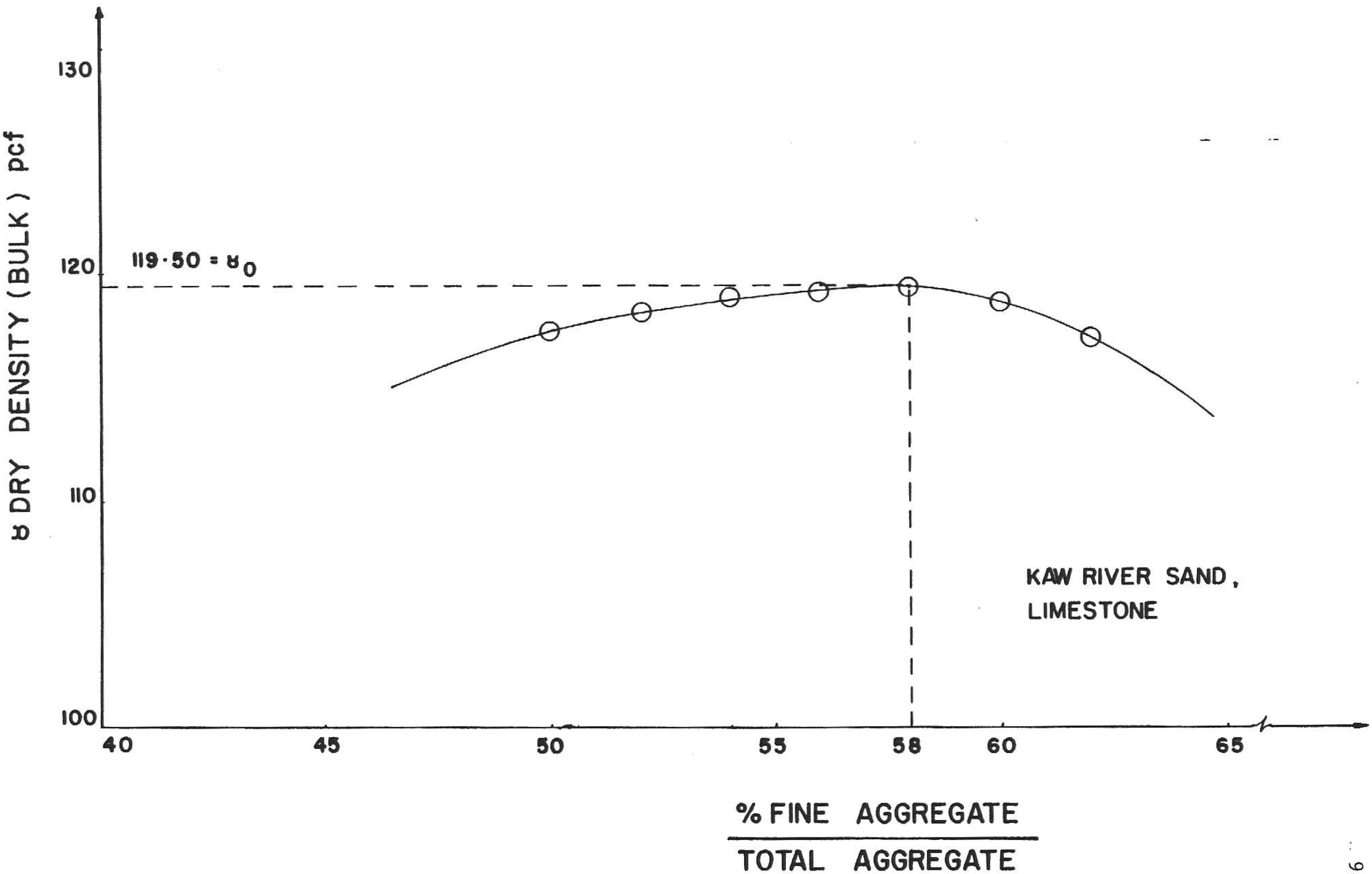

Figure 3.1: Dry Density vs. Percent $\frac{\text{Fine Aggregate}}{\text{Total Aggregate}}$

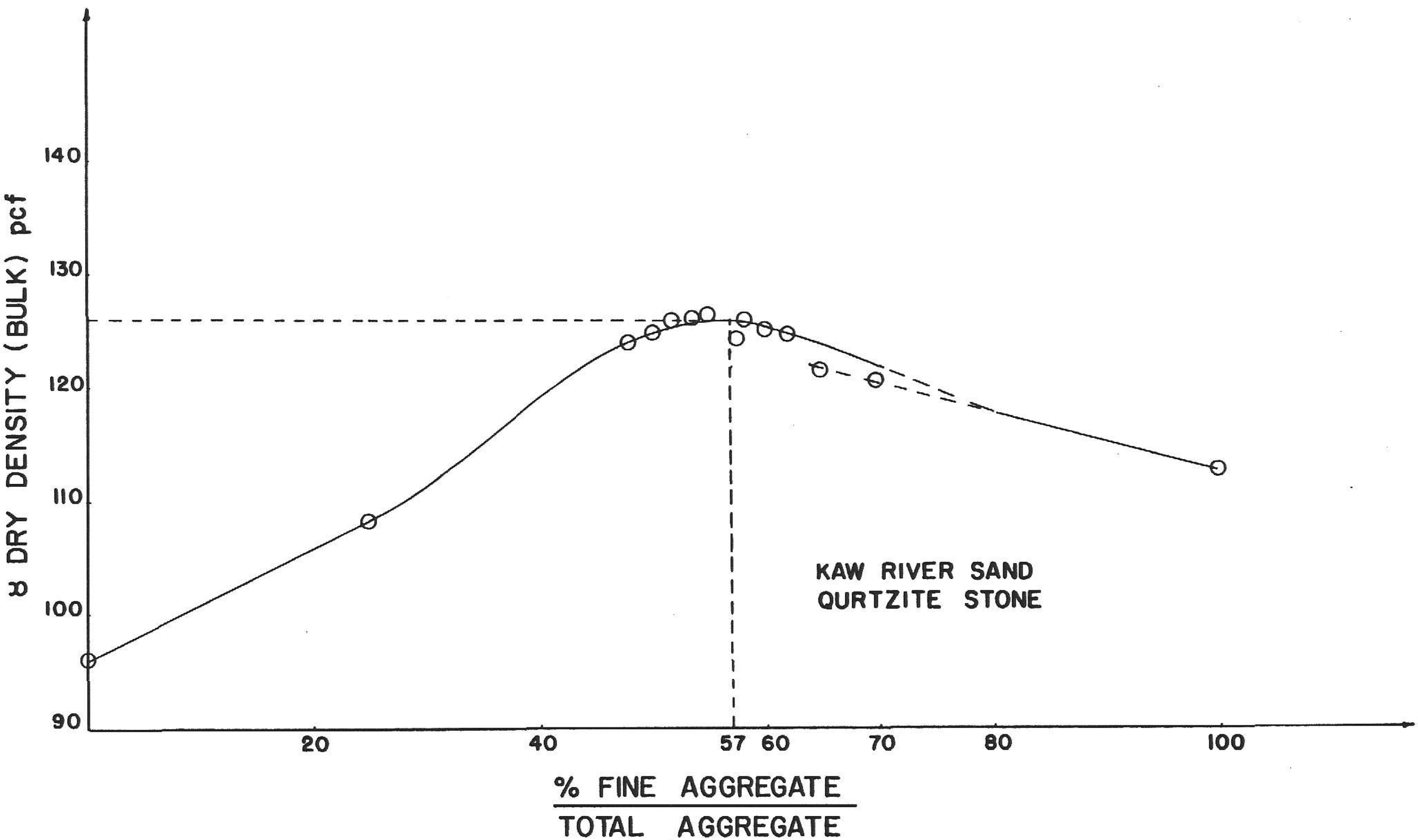

Figure 3.2: Dry Density vs. Percent $\frac{\text{Fine Aggregate}}{\text{Total Aggregate}}$

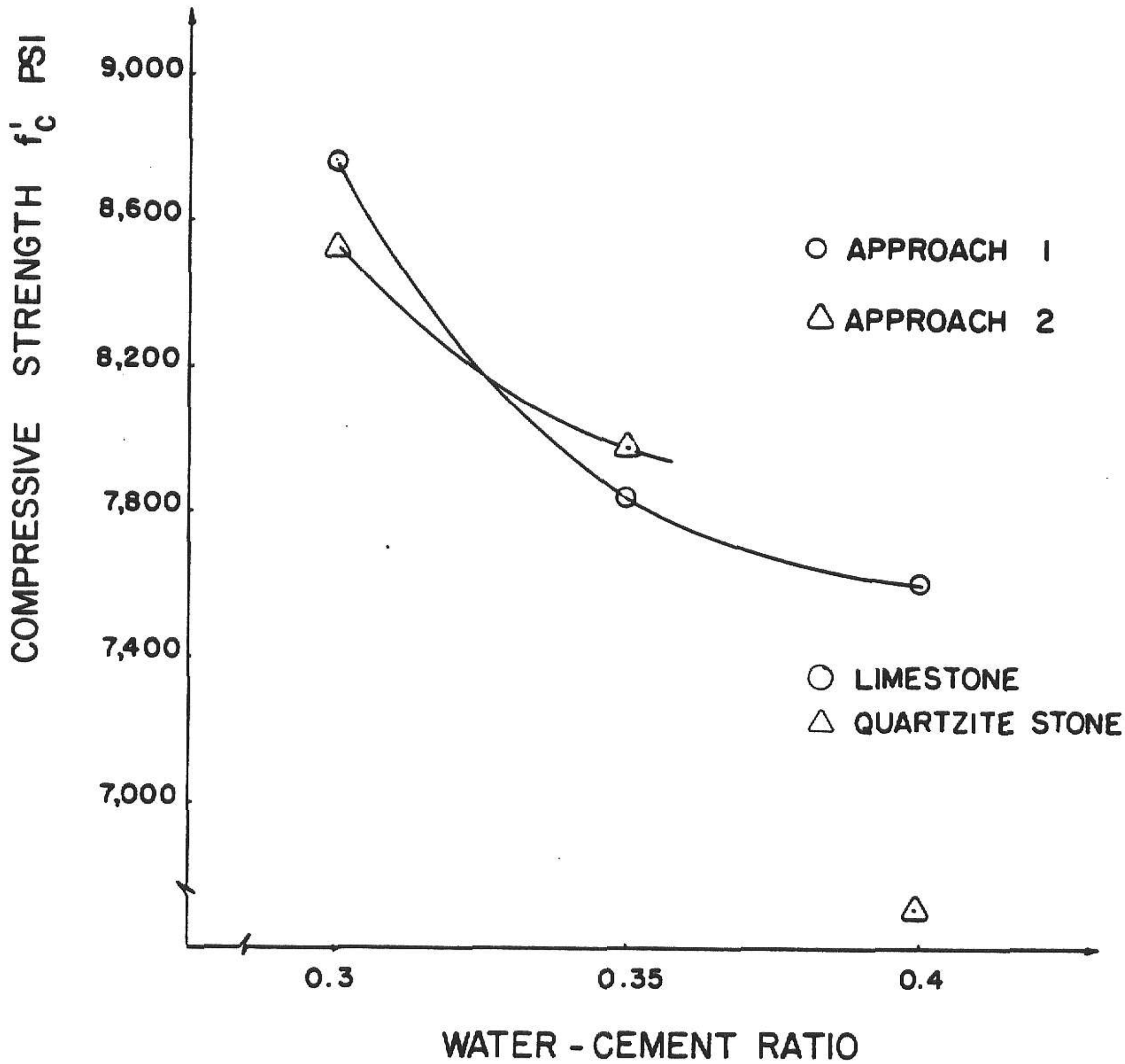

Figure 3.3: f'_c vs. Water-Cement Ratio

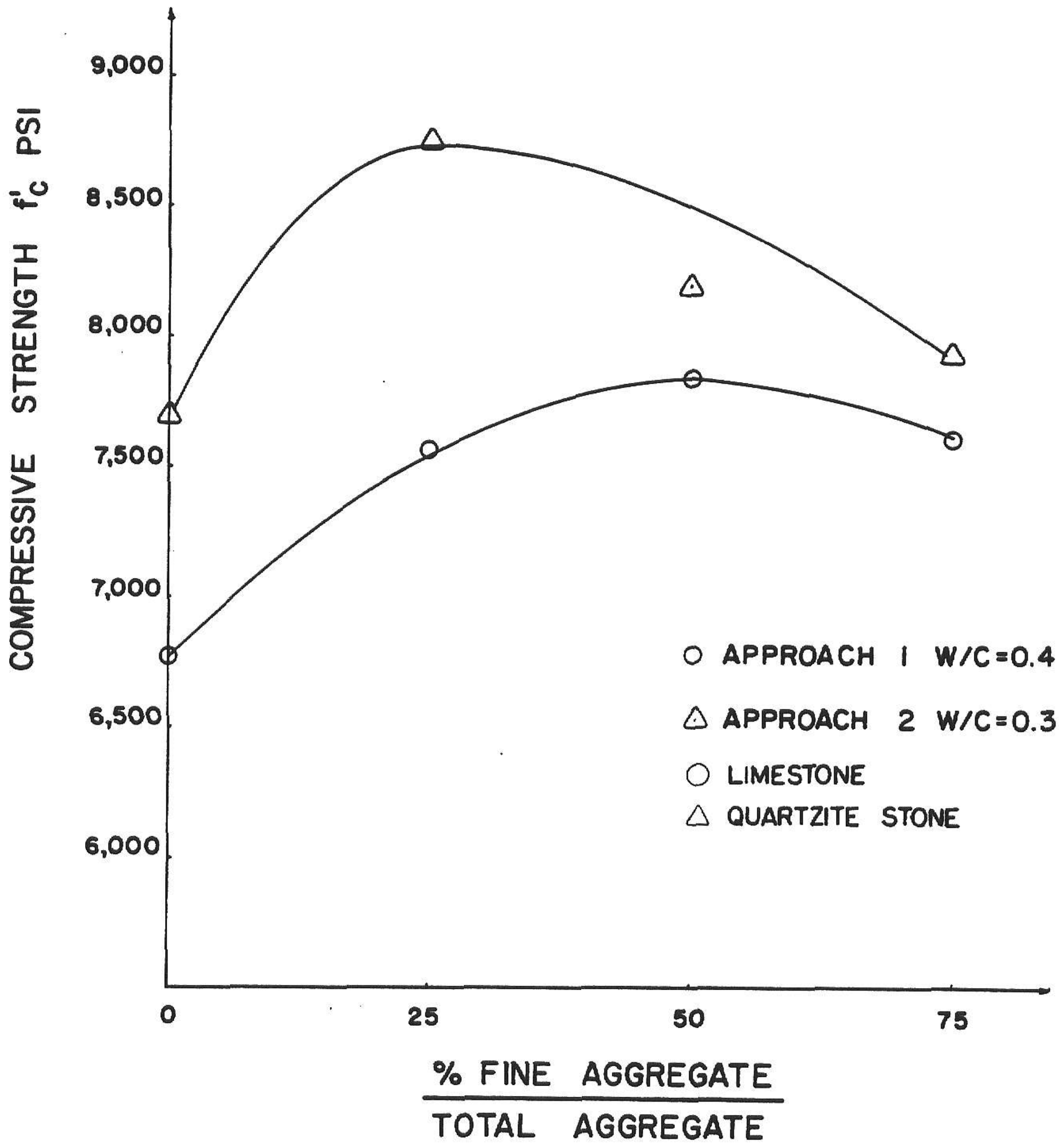

Figure 3.4: f'_c vs. Percent Fine Aggregate of Total Aggregate

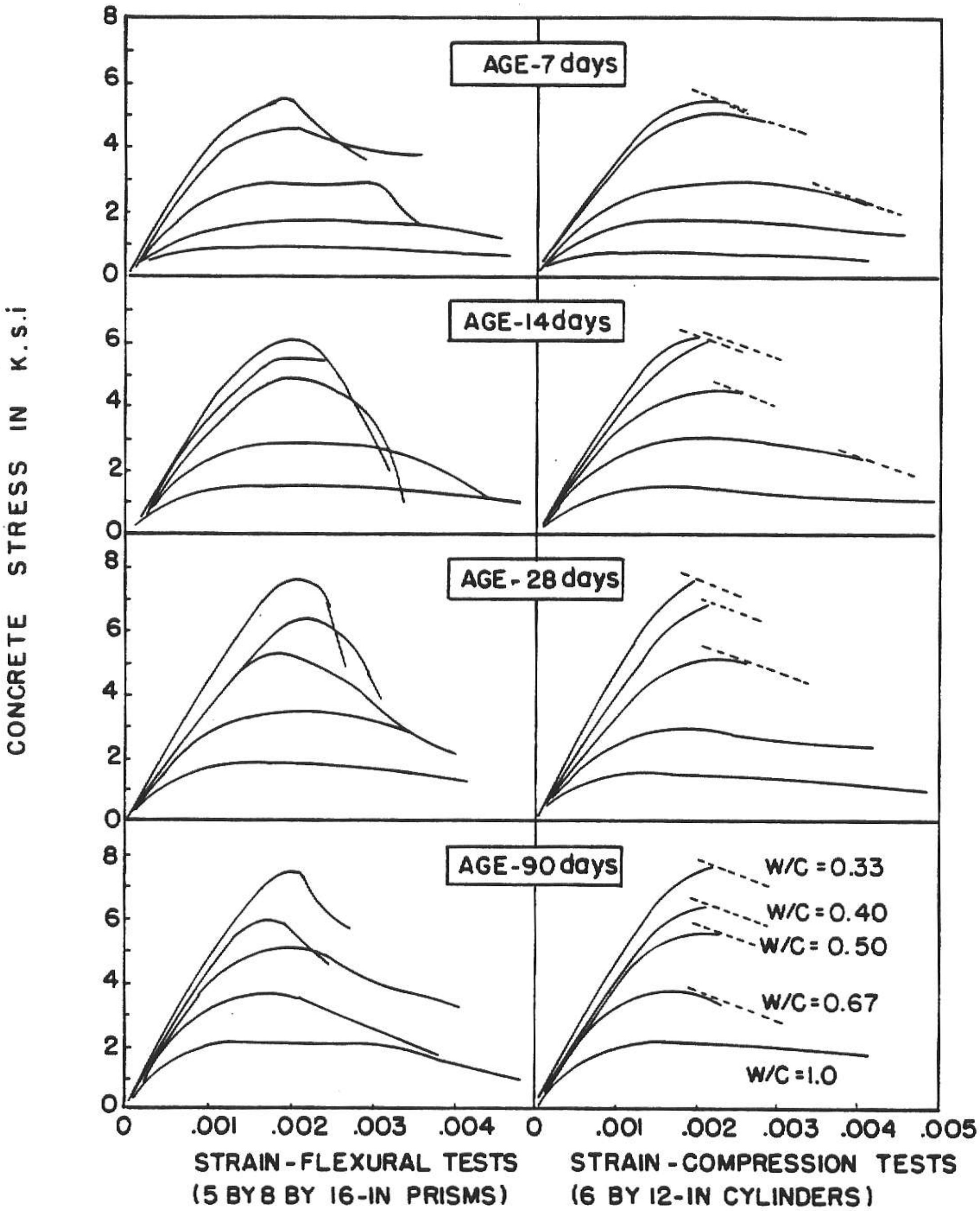

Figure 4.1: Concrete Stress-Strain Relations (17)

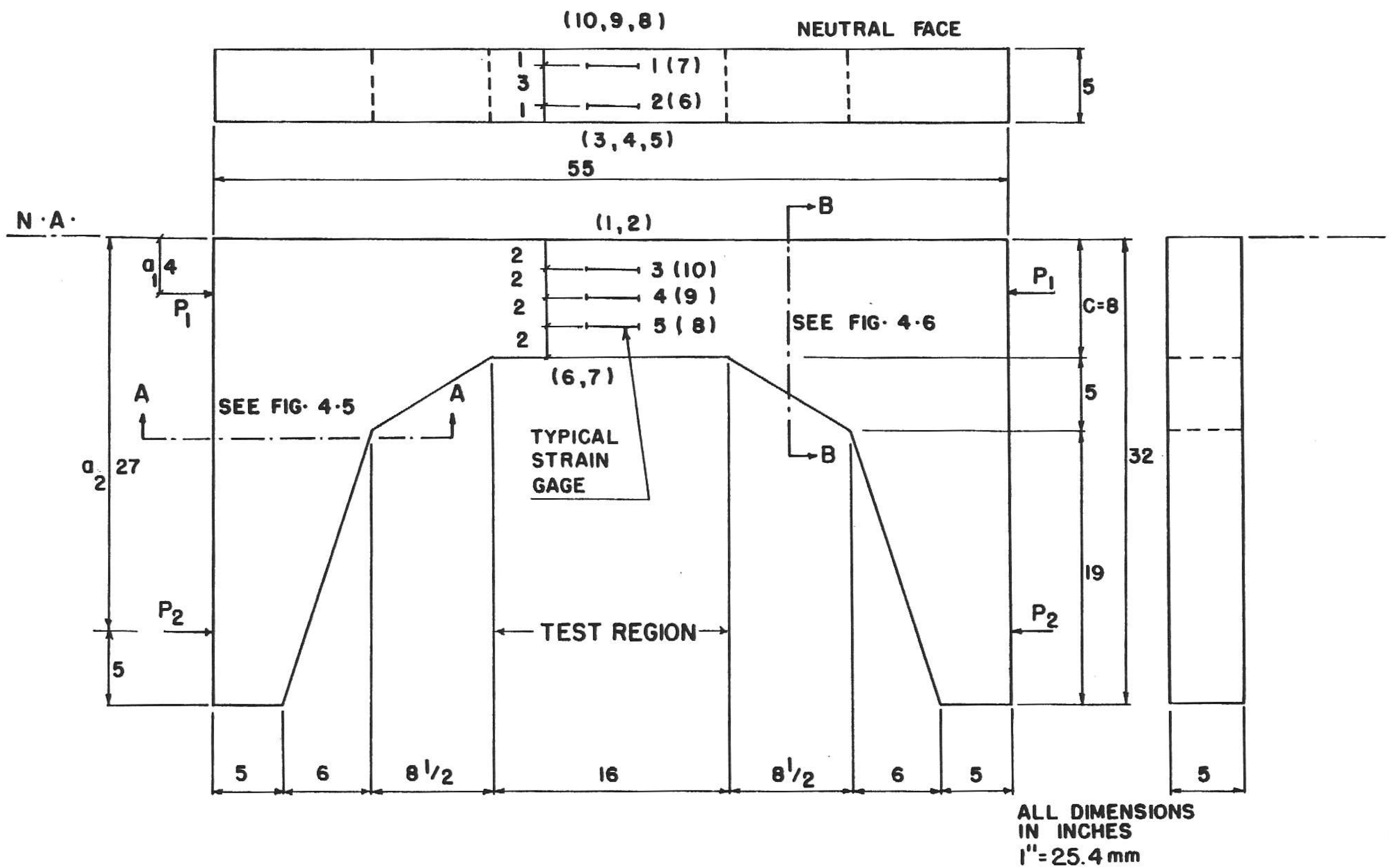

Figure 4.2: C-Shape Structural Element for Flexural Test I

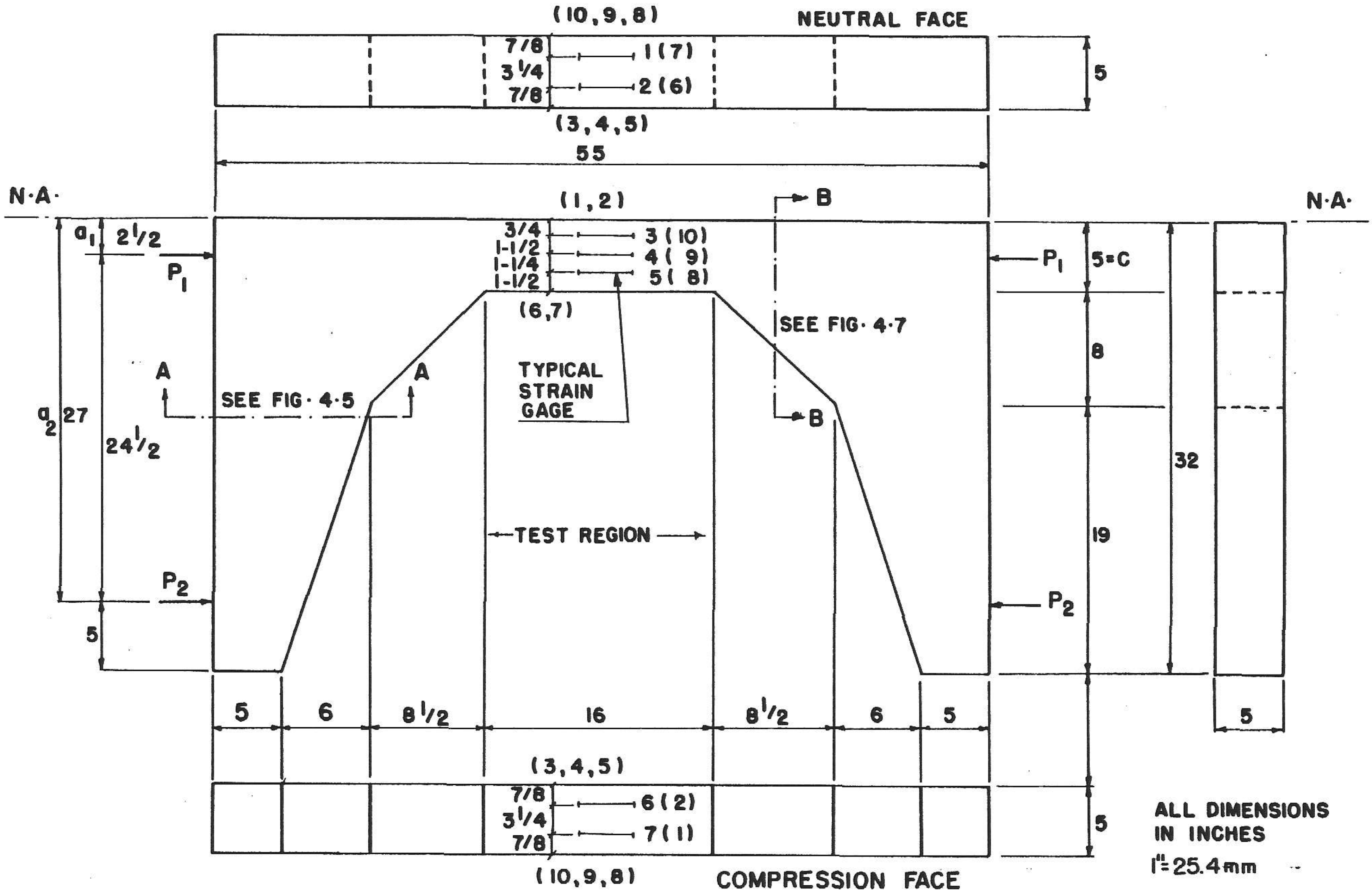

Figure 4.3: C–Shape Structural Element for Flexural Test II

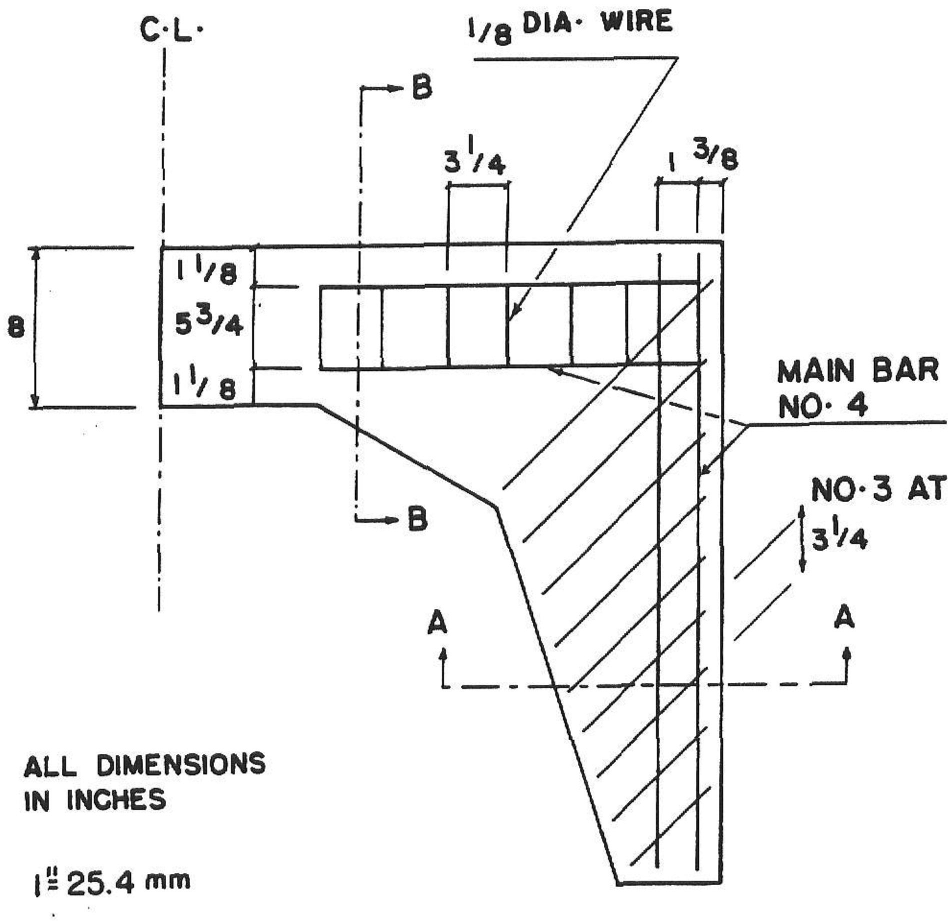

Figure 4.4: Reinforcement Layout for Specimen I (Specimen II is similar to I except area of test region is smaller, see Figure 4.3)

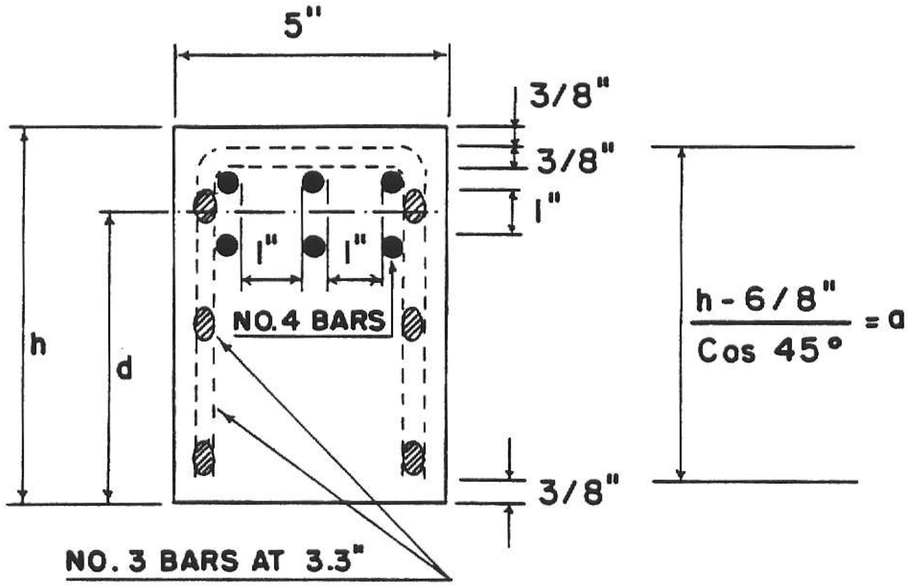

SECTION A-A (SEE FIG. 4.2, 4.3, 4.4)
1" = 25.4 mm

a = the leg size of stirrup

Figure 4.5: An Arbitrary Section A-A With Rebar Arrangement at Each Leg

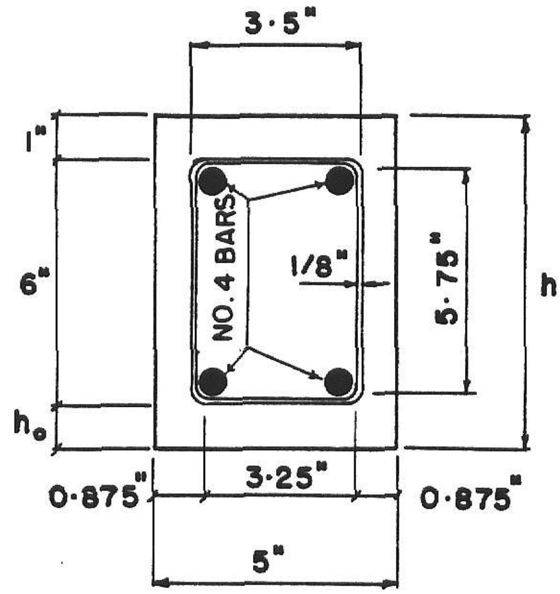

SECTION B - B
(SEE FIG· 4·2)
1" = 25.4 mm

Figure 4.6: An Arbitrary Section of Column Part With Rebar Arrangement for Specimen I

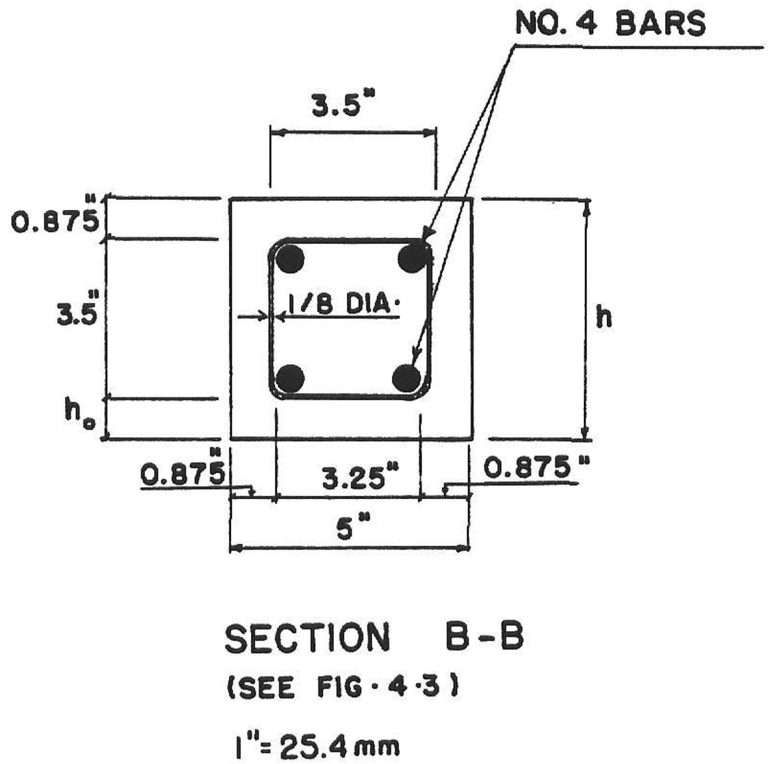

Figure 4.7: An Arbitrary Section of Column Part With Rebar Arrangement for Specimen II

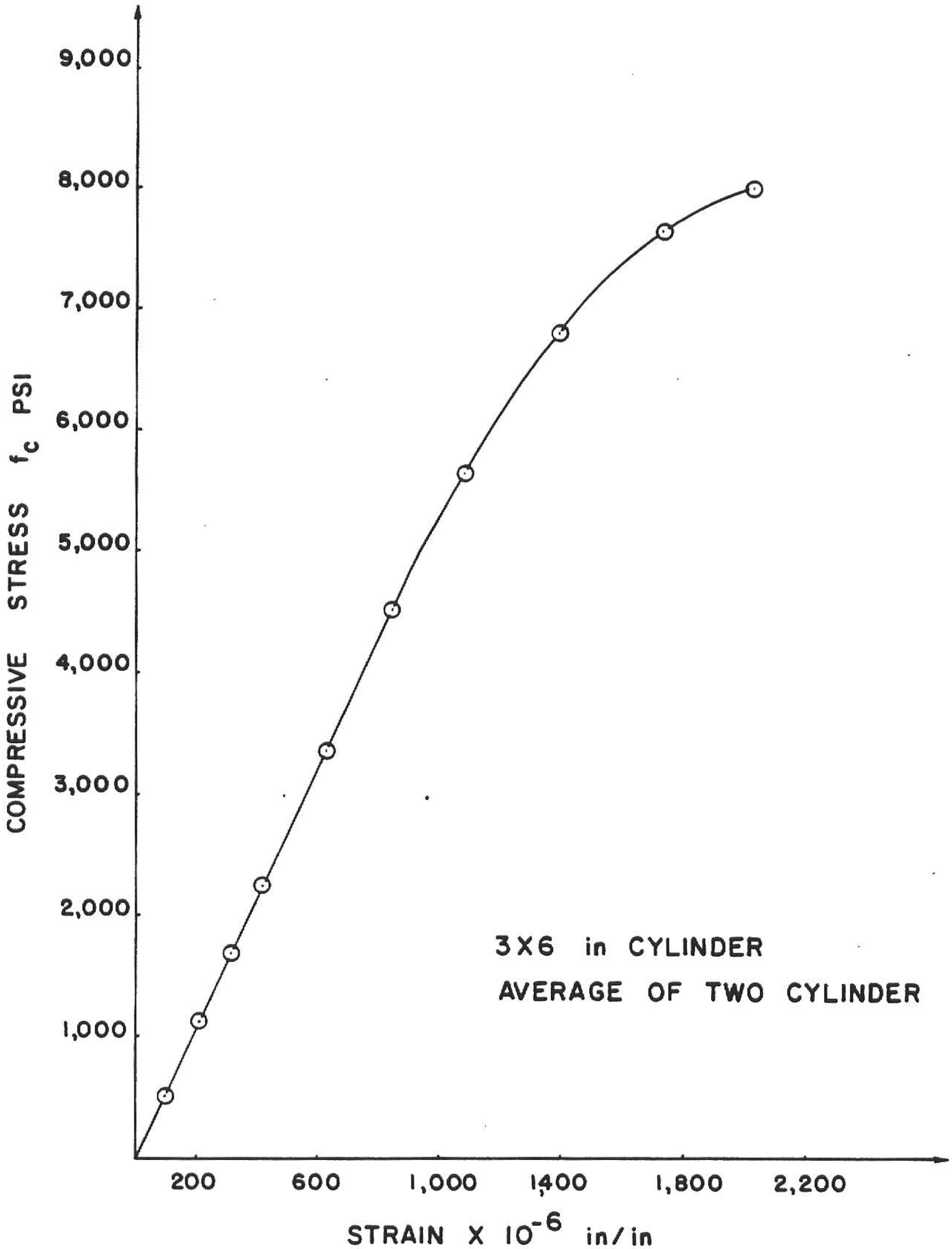

Figure 5.1: Compressive Stress-Strain Curve - Cylinder Test for Specimen I

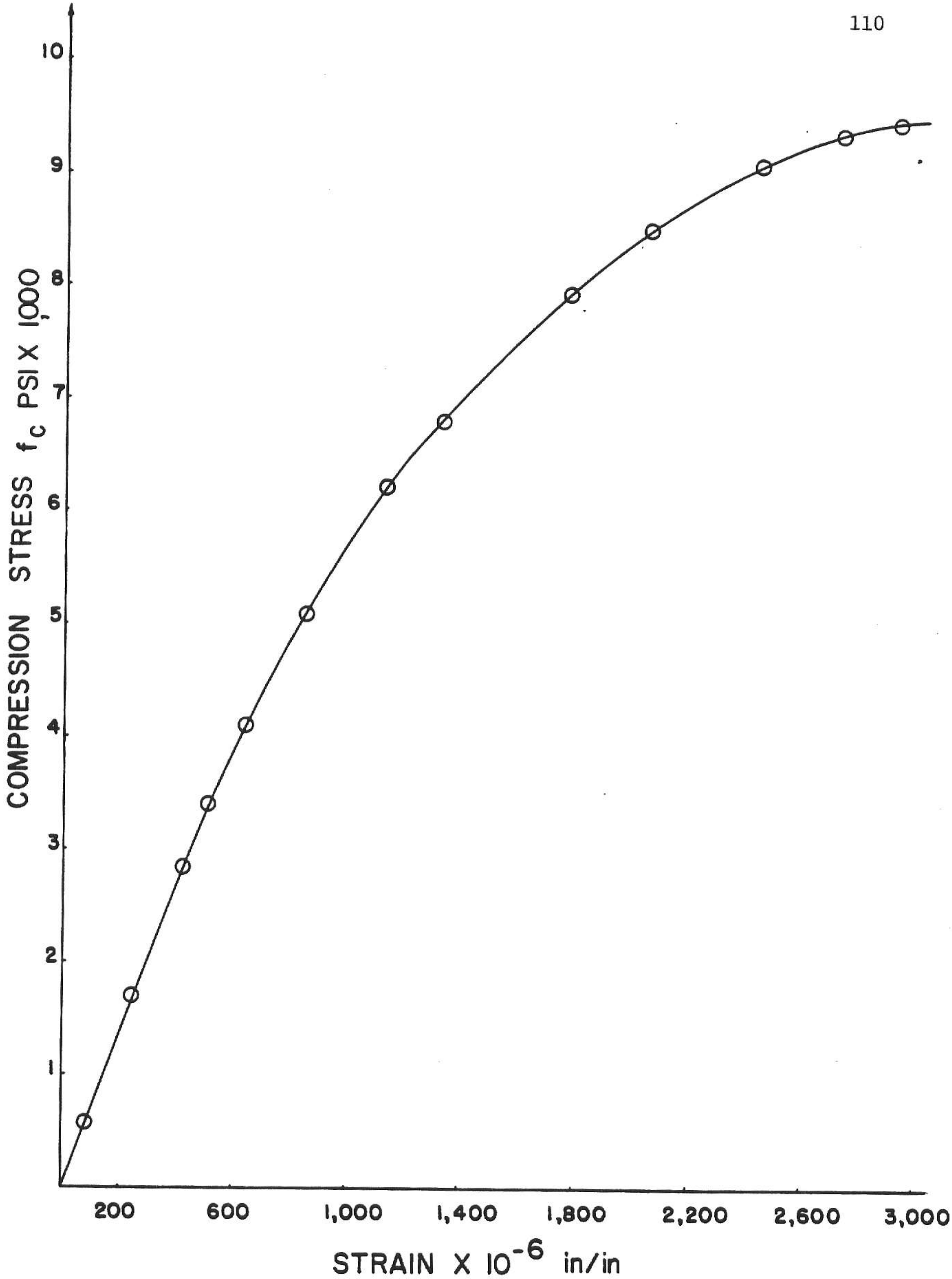

Figure 5.2: Cylinder Compressive Stress-Strain Curve for Specimen II

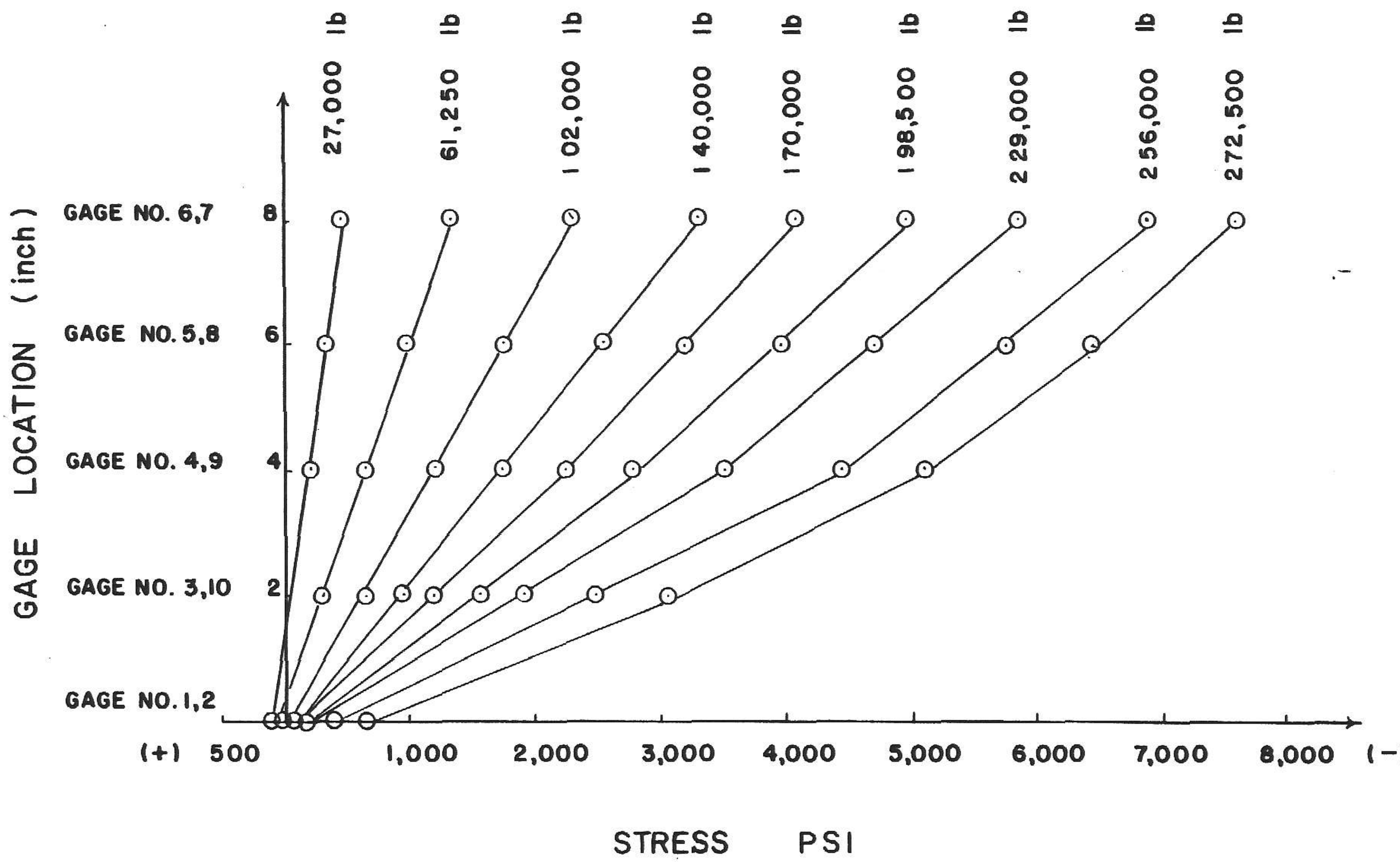

Figure 5.3: Stress Block of Specimen I

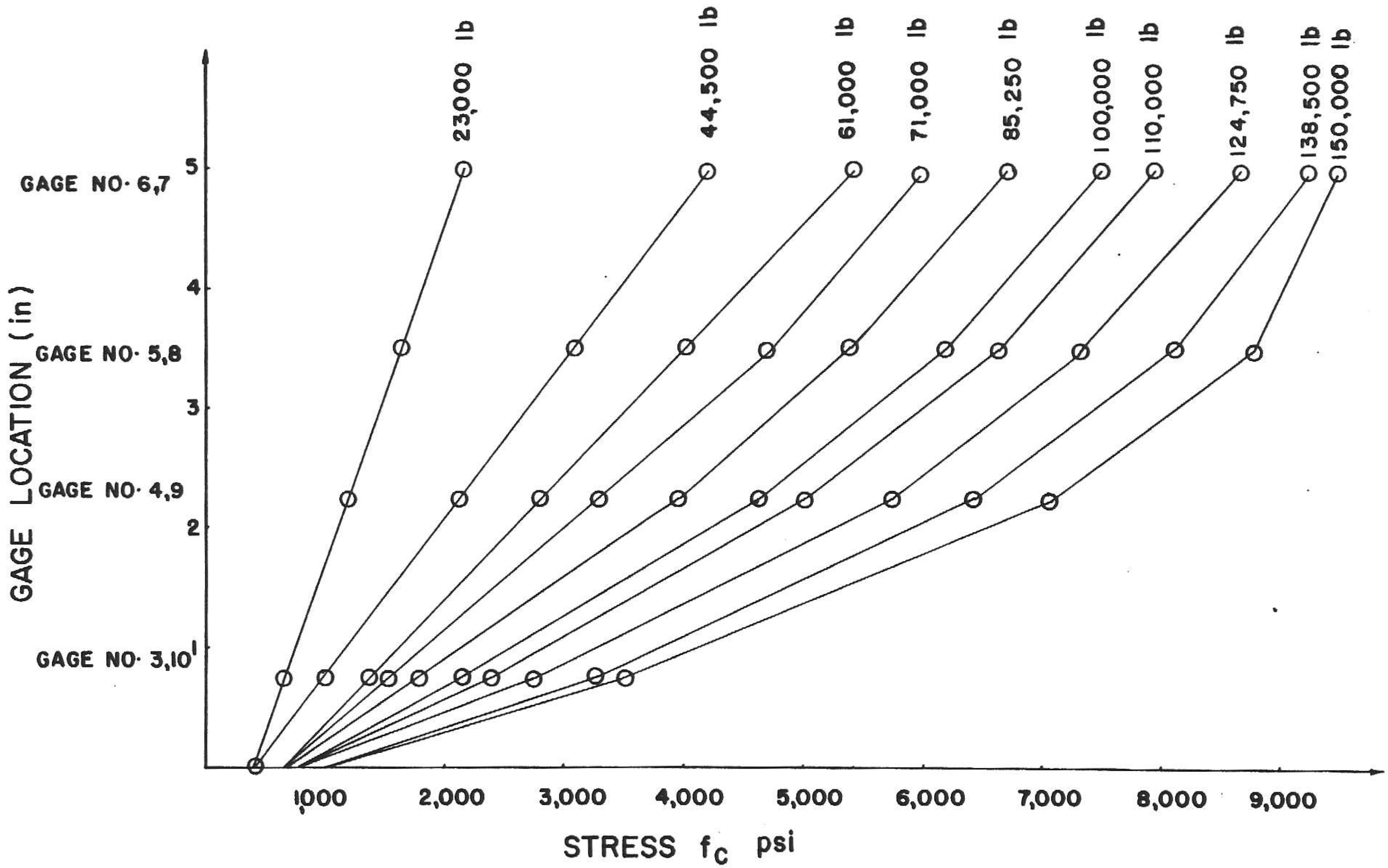

Figure 5.4: Stress Block of Specimen II

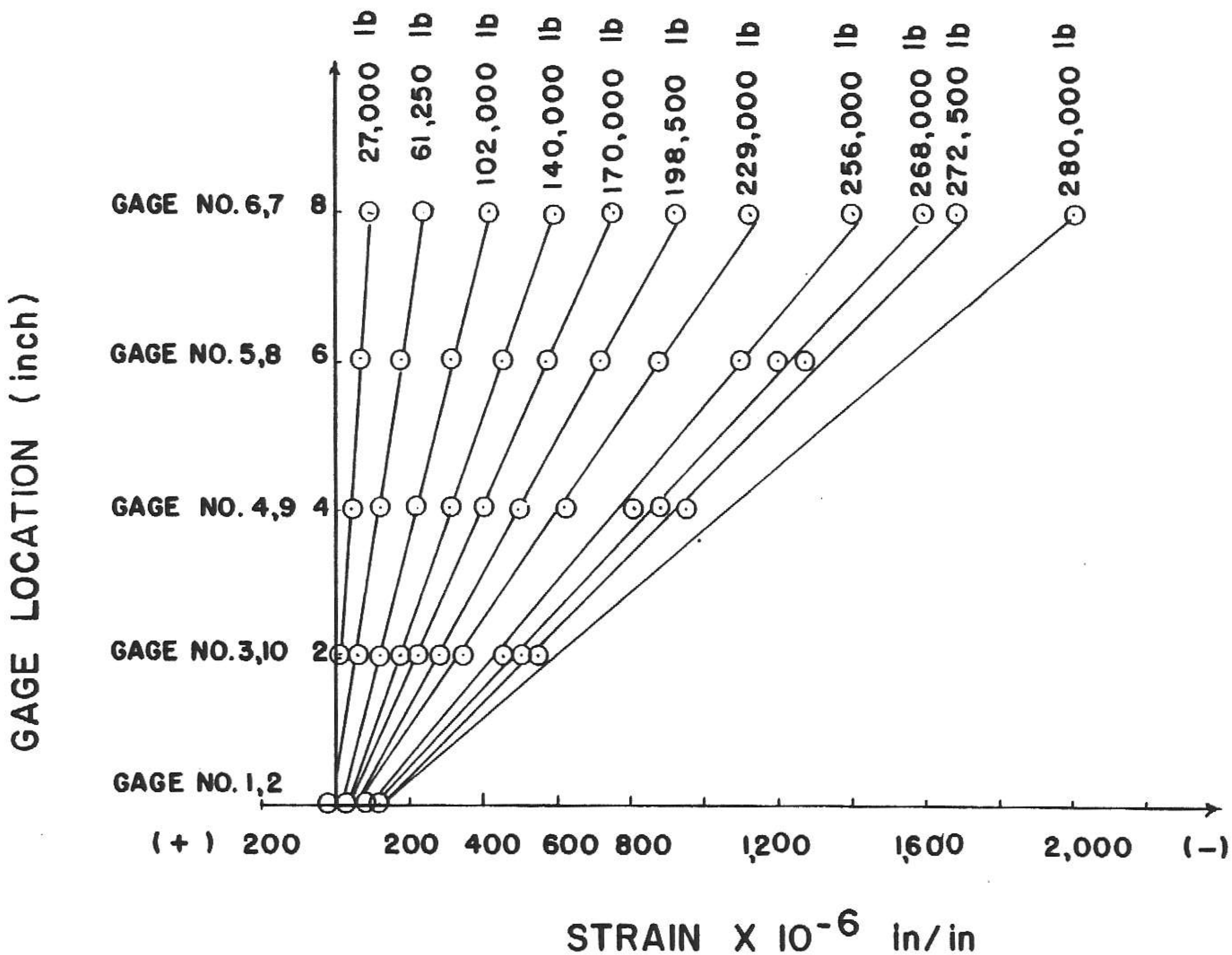

Figure 5.5: Location of Strain Gages vs. Strain for Specimen I

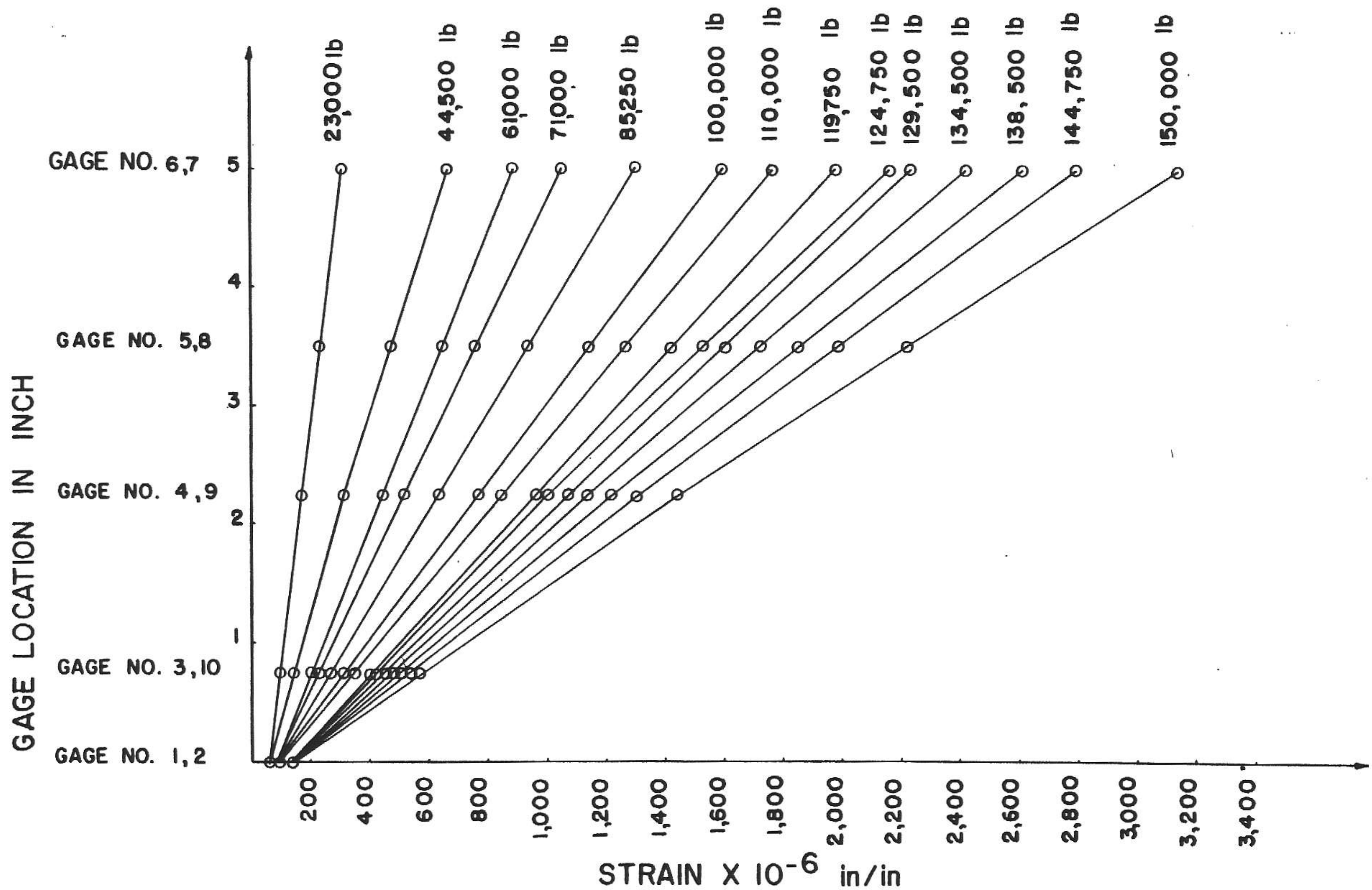

Figure 5.6: Location of Strain Gages vs. Strain for Specimen II

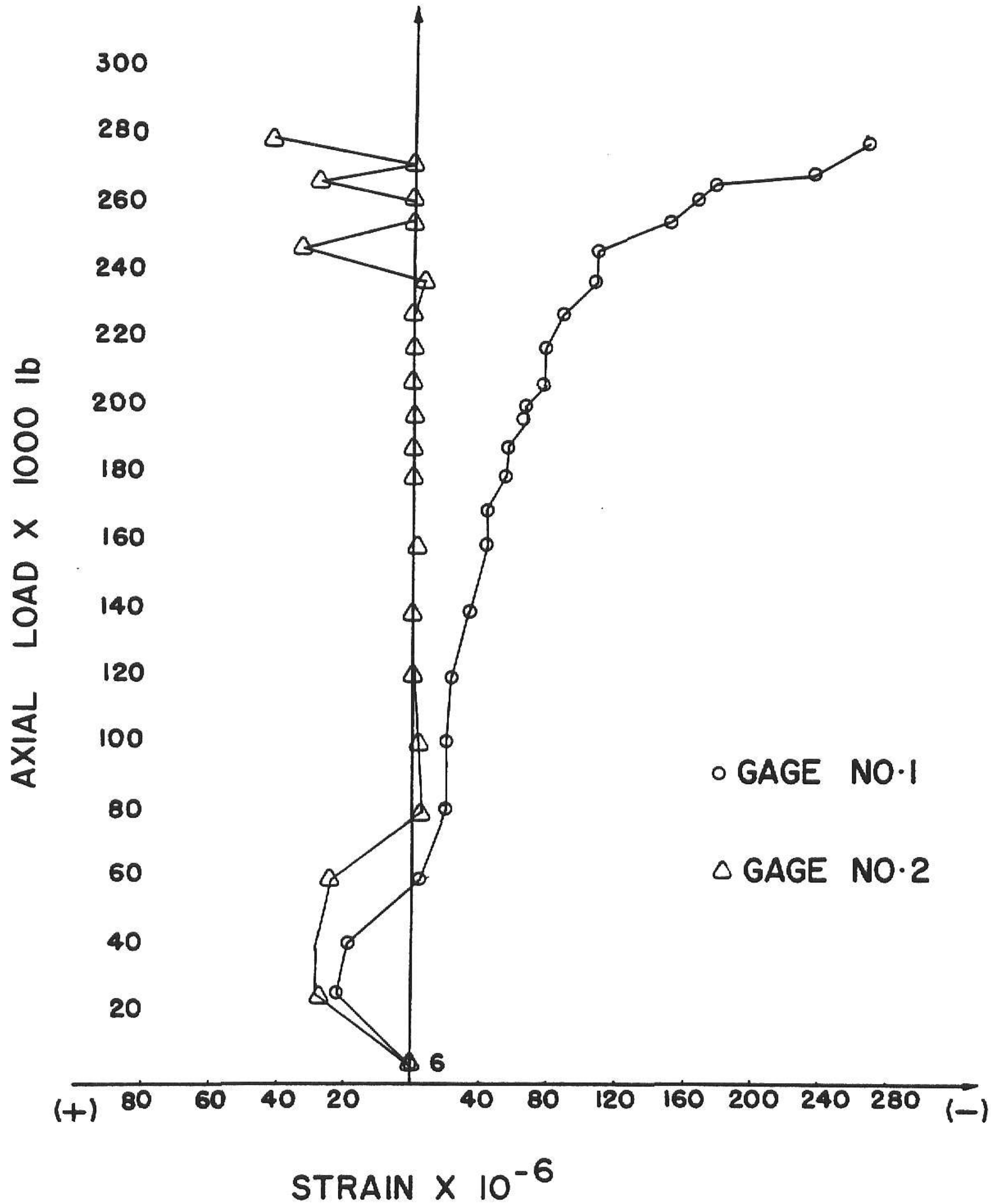

Figure 5.7: Axial Load vs. Strain for Gages 1 and 2 (neutral face) for Specimen I

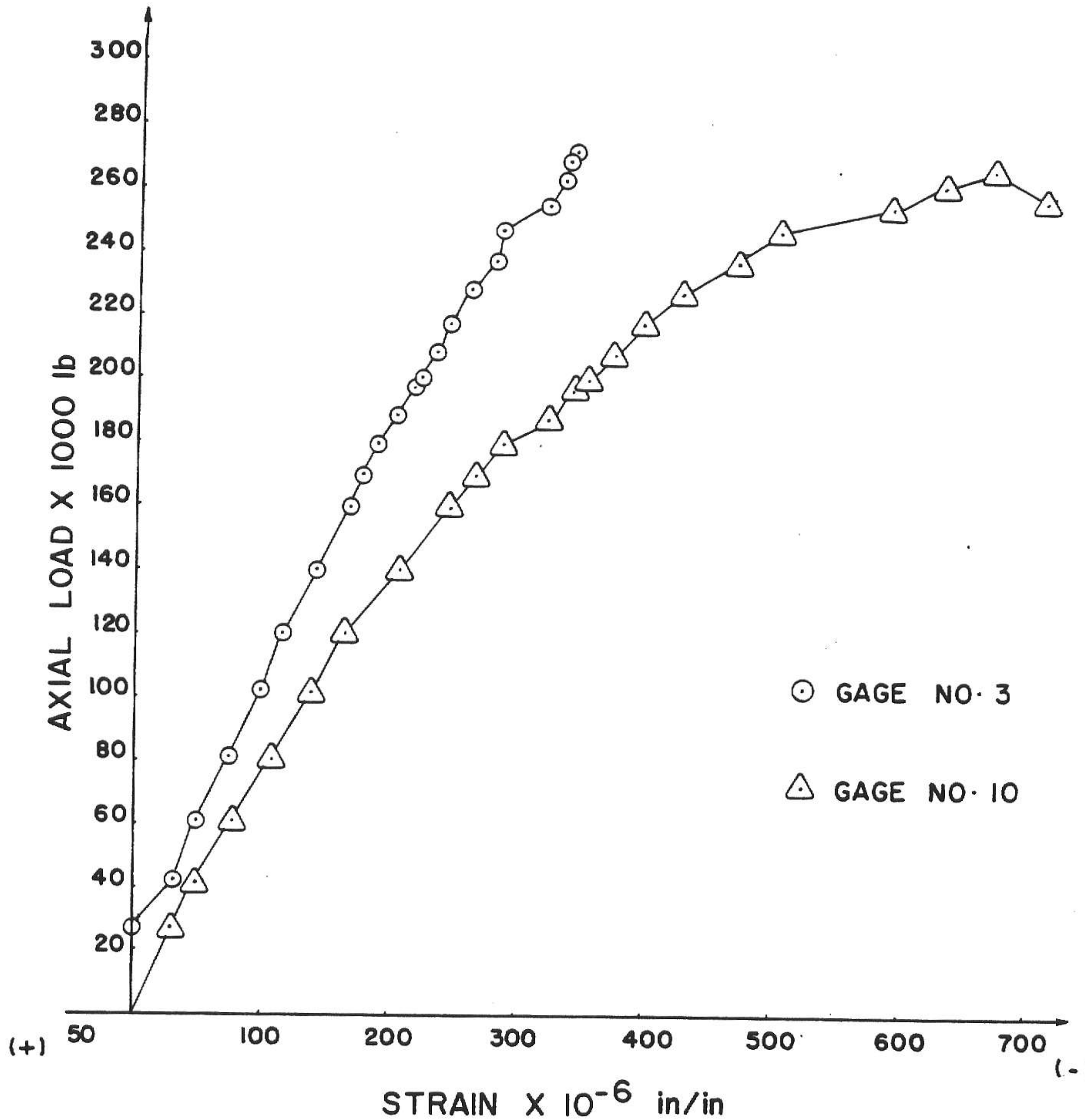

Figure 5.8: Axial Load vs. Strain for Gages 3 and 10 for Specimen I

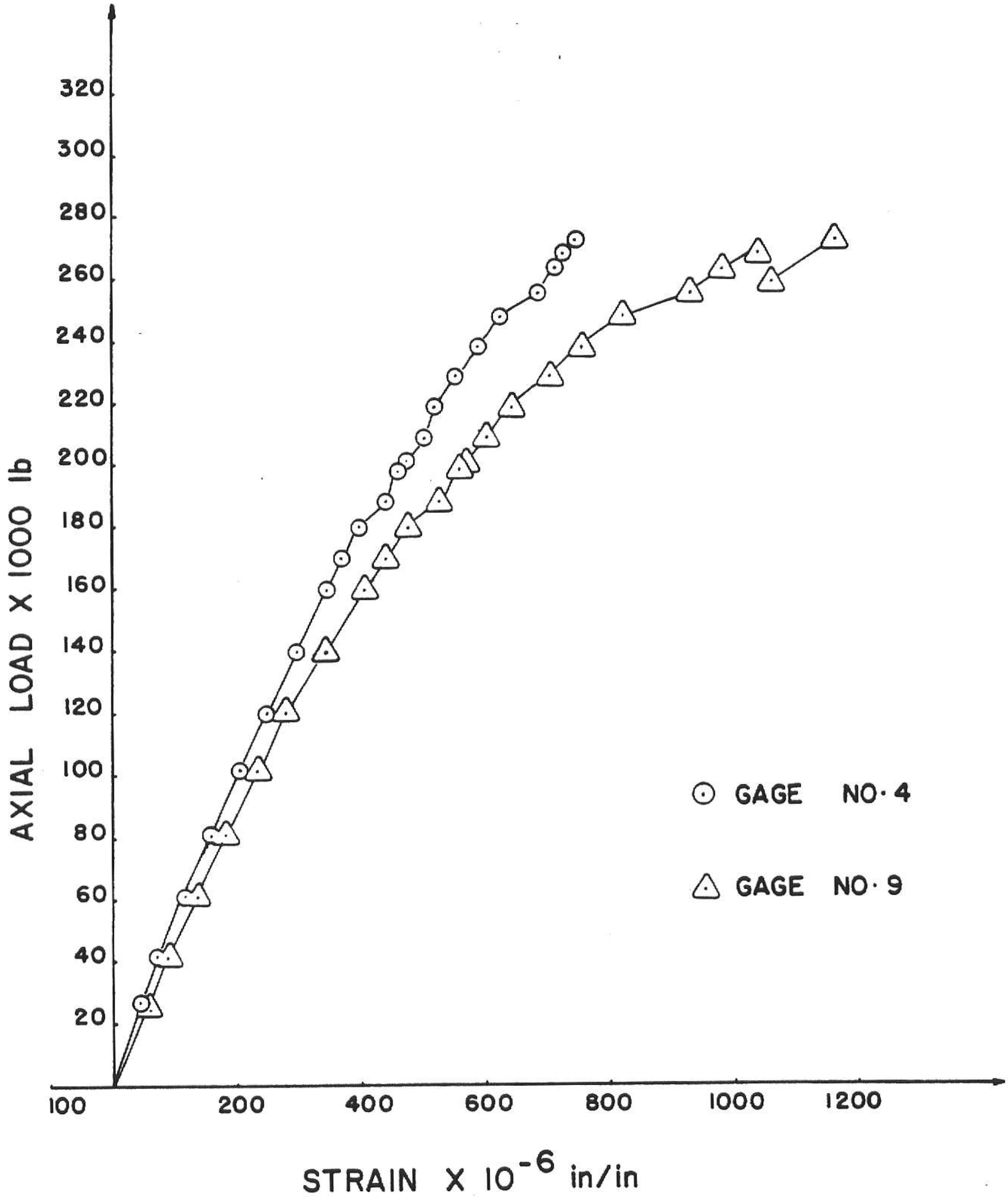

Figure 5.9: Axial Load vs. Strain for Gages 4 and 9 for Specimen I

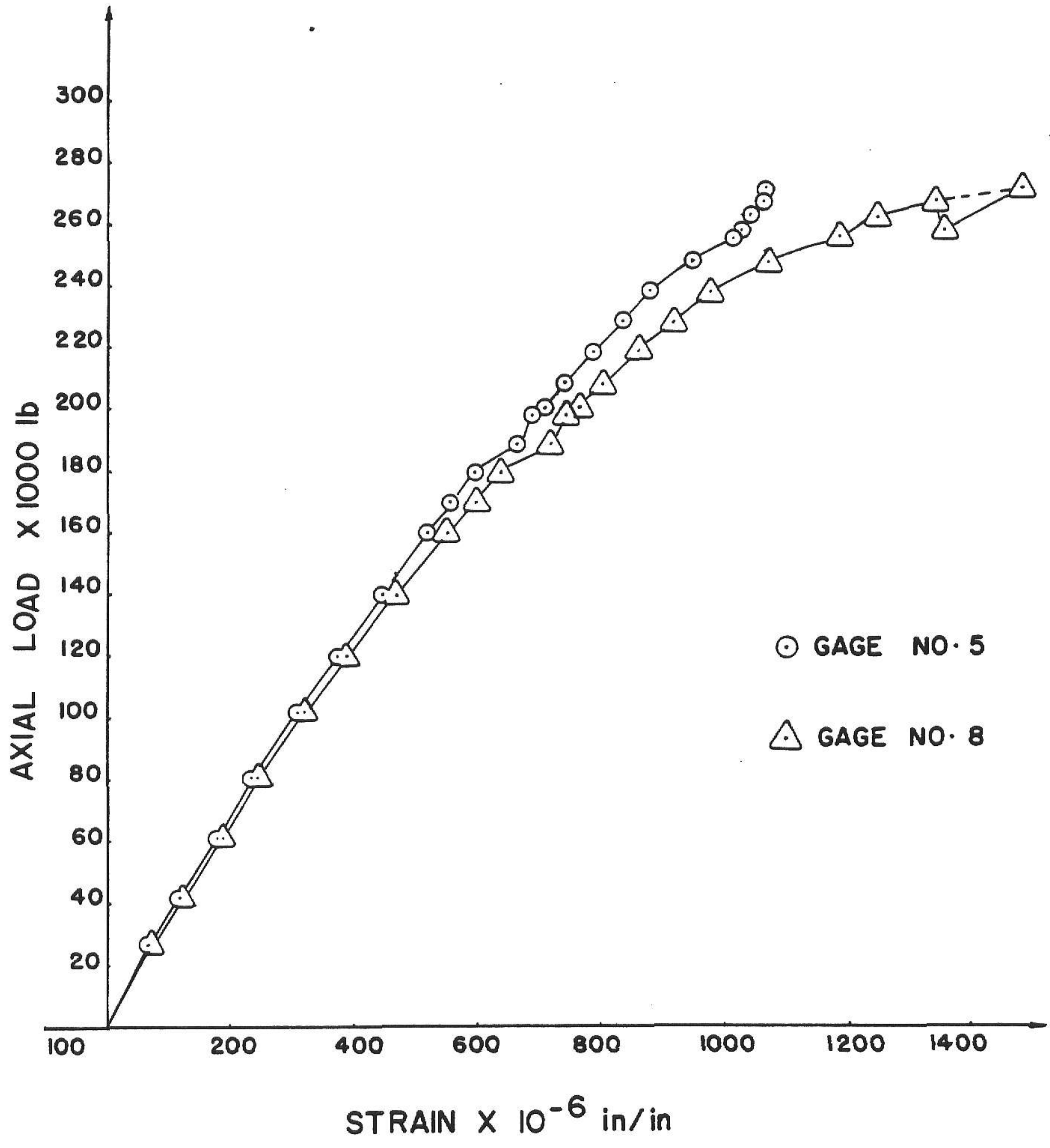

Figure 5.10: Axial Load vs. Strain for Gages 5 and 8 for Specimen I

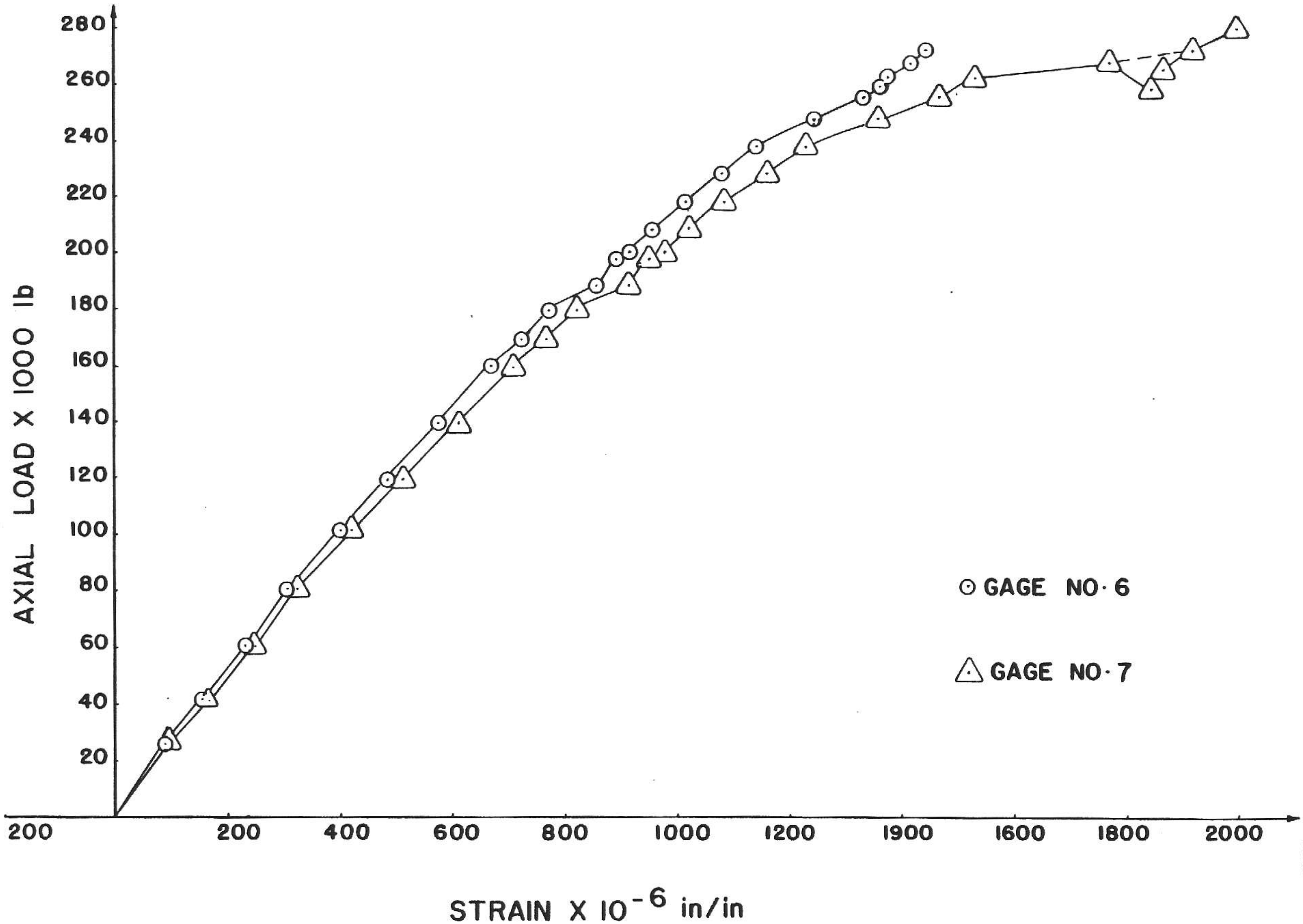

Figure 5.11: Axial Load vs. Strain for Gages 6 and 7 (Compression Face), for Specimen I

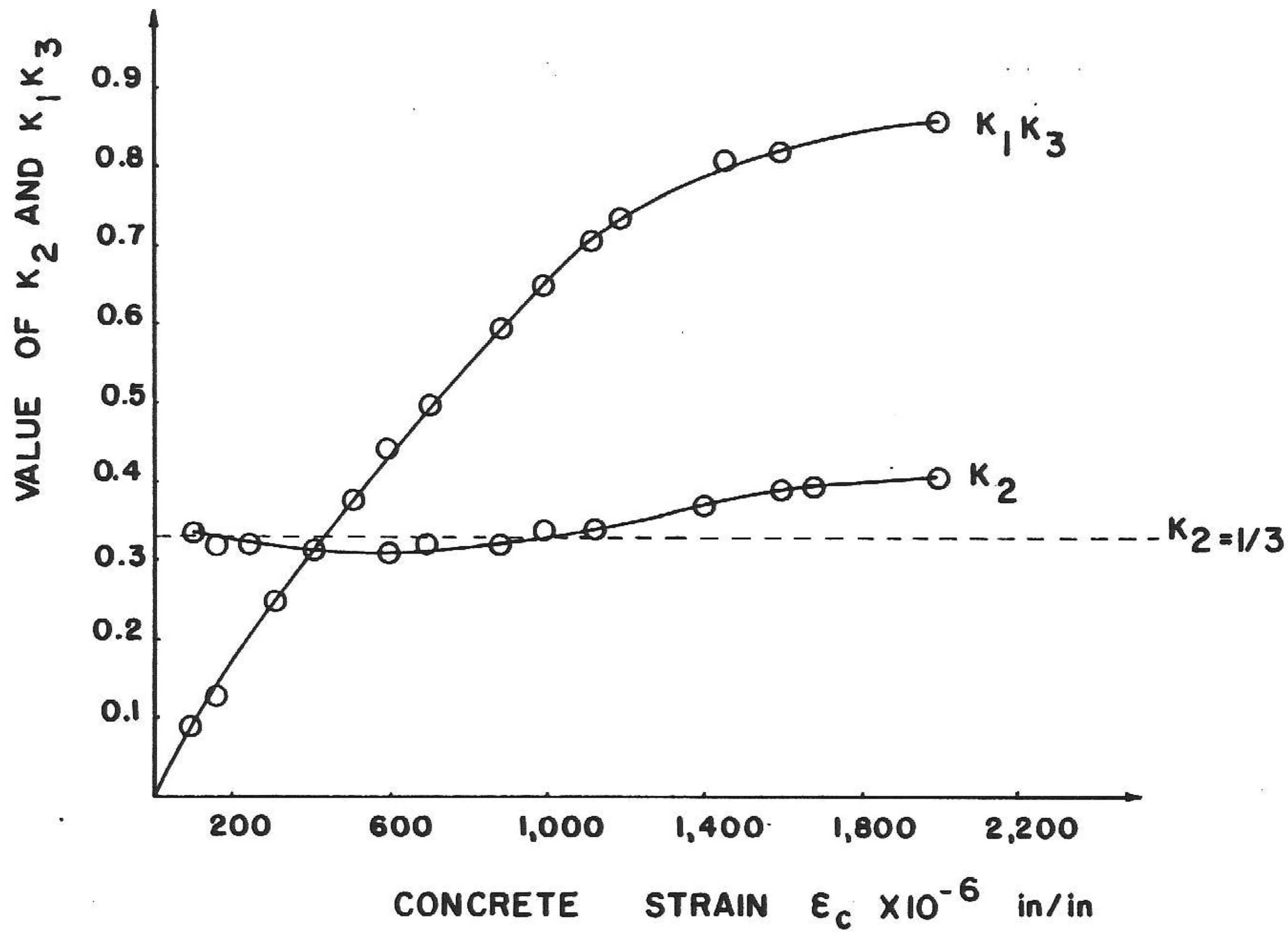

Figure 5.12: K_2, K_1K_3 Value vs. Concrete Strain for Specimen I

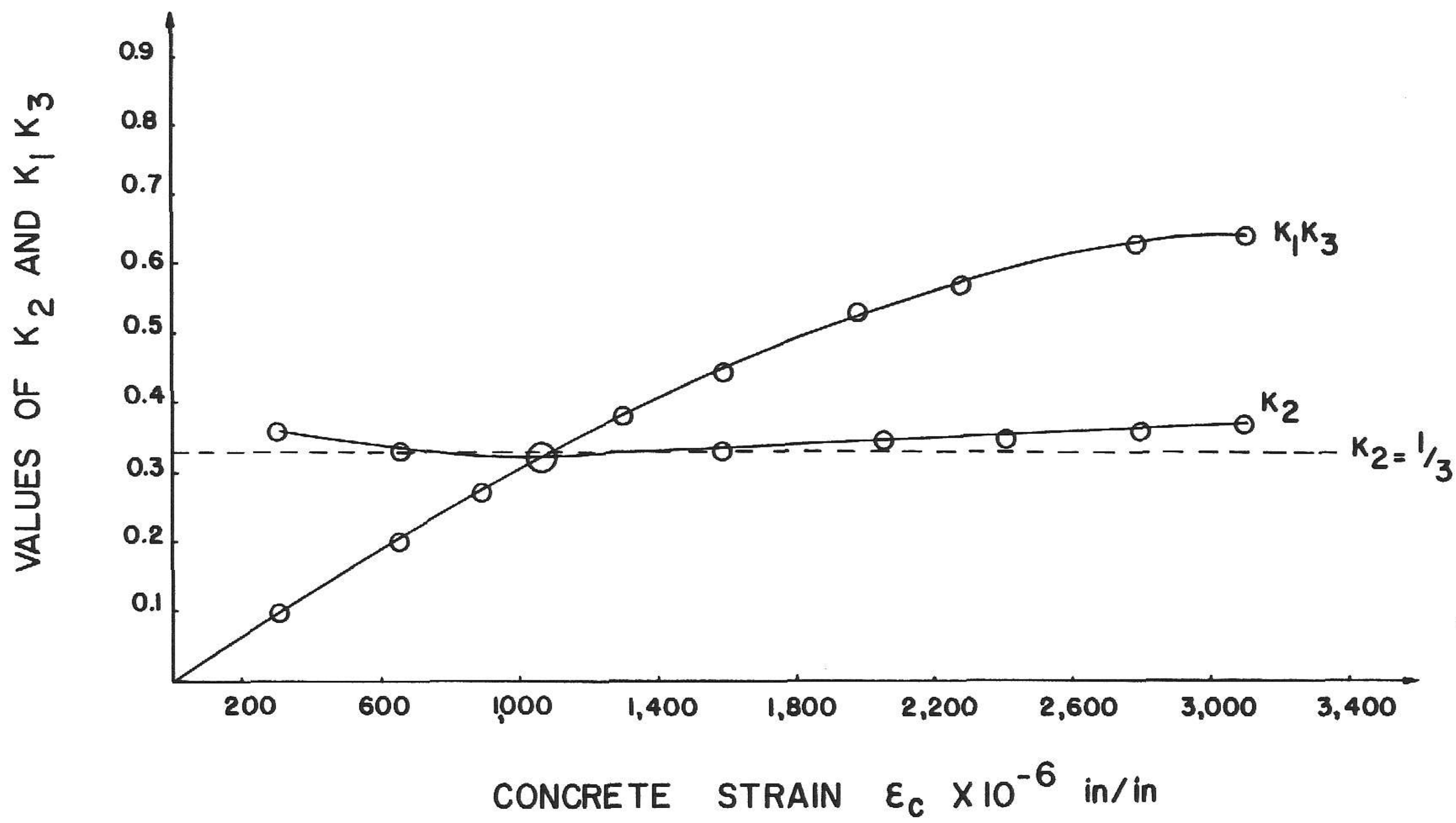

Figure 5.13: K_2 and K_1K_3 Value vs. Concrete Strain for Specimen II

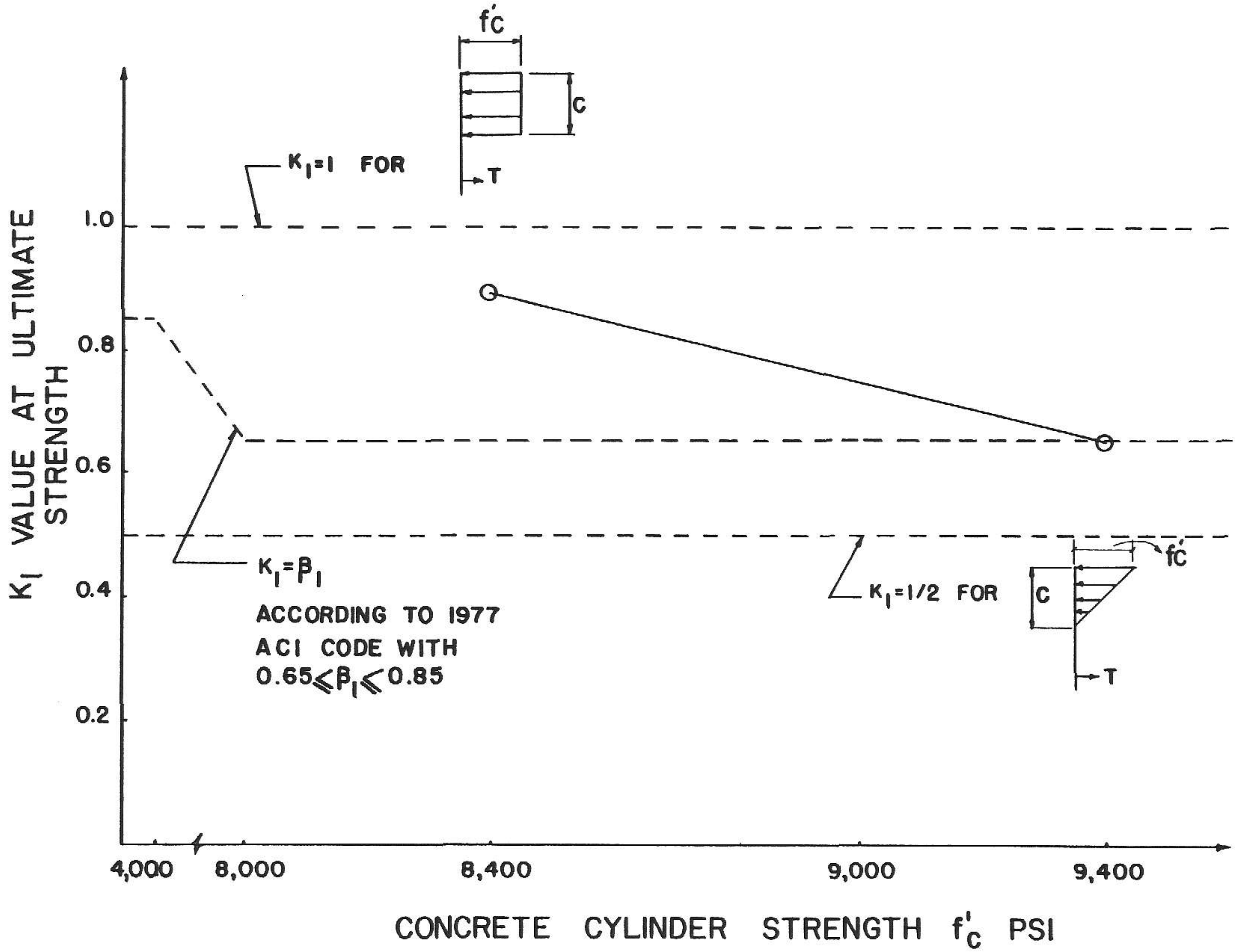

Figure 5.14: K_1 Values at Ultimate vs. Concrete Cylinder Strength

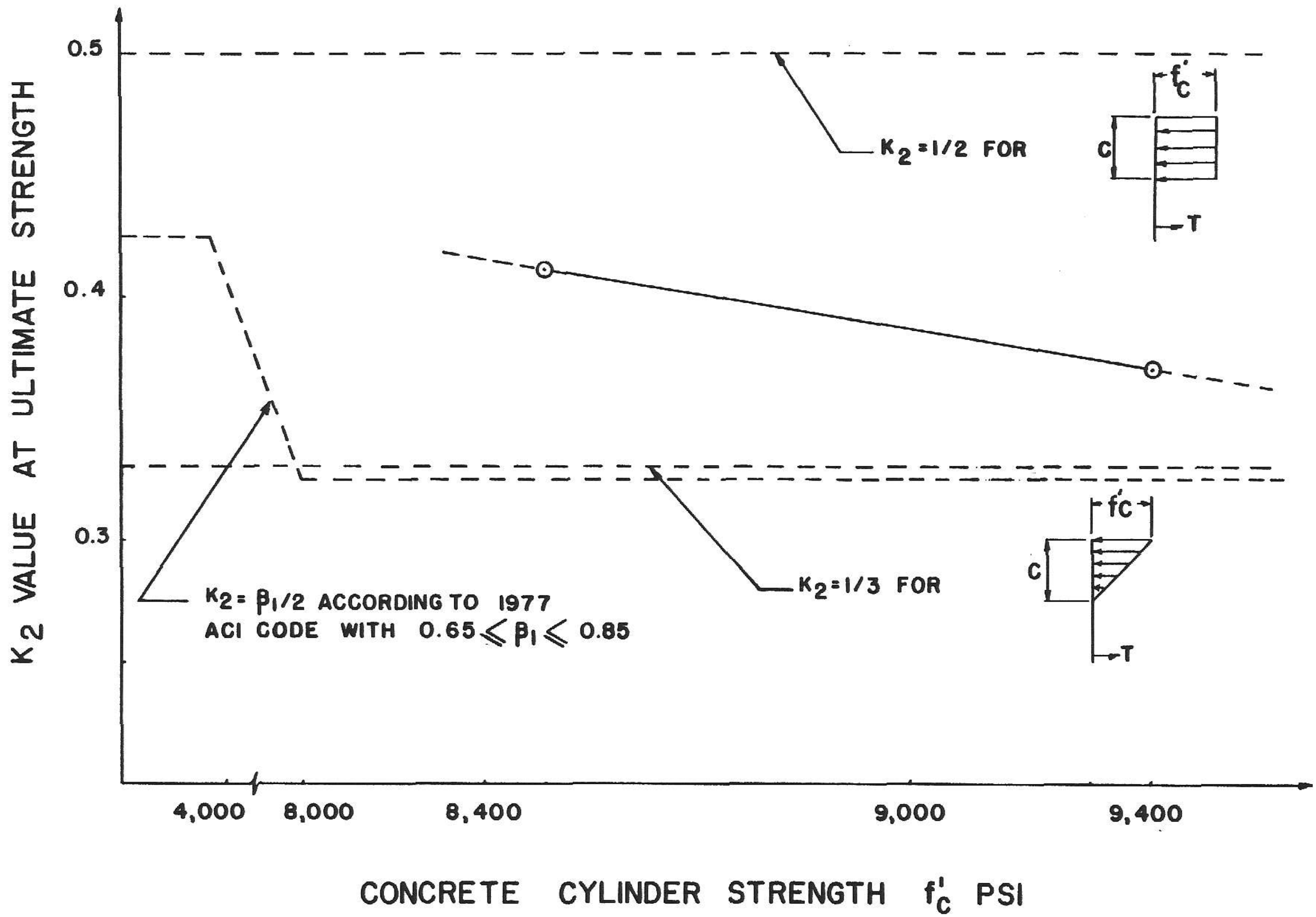

Figure 5.15: K_2 Values at Ultimate vs. Concrete Cylinder Strength

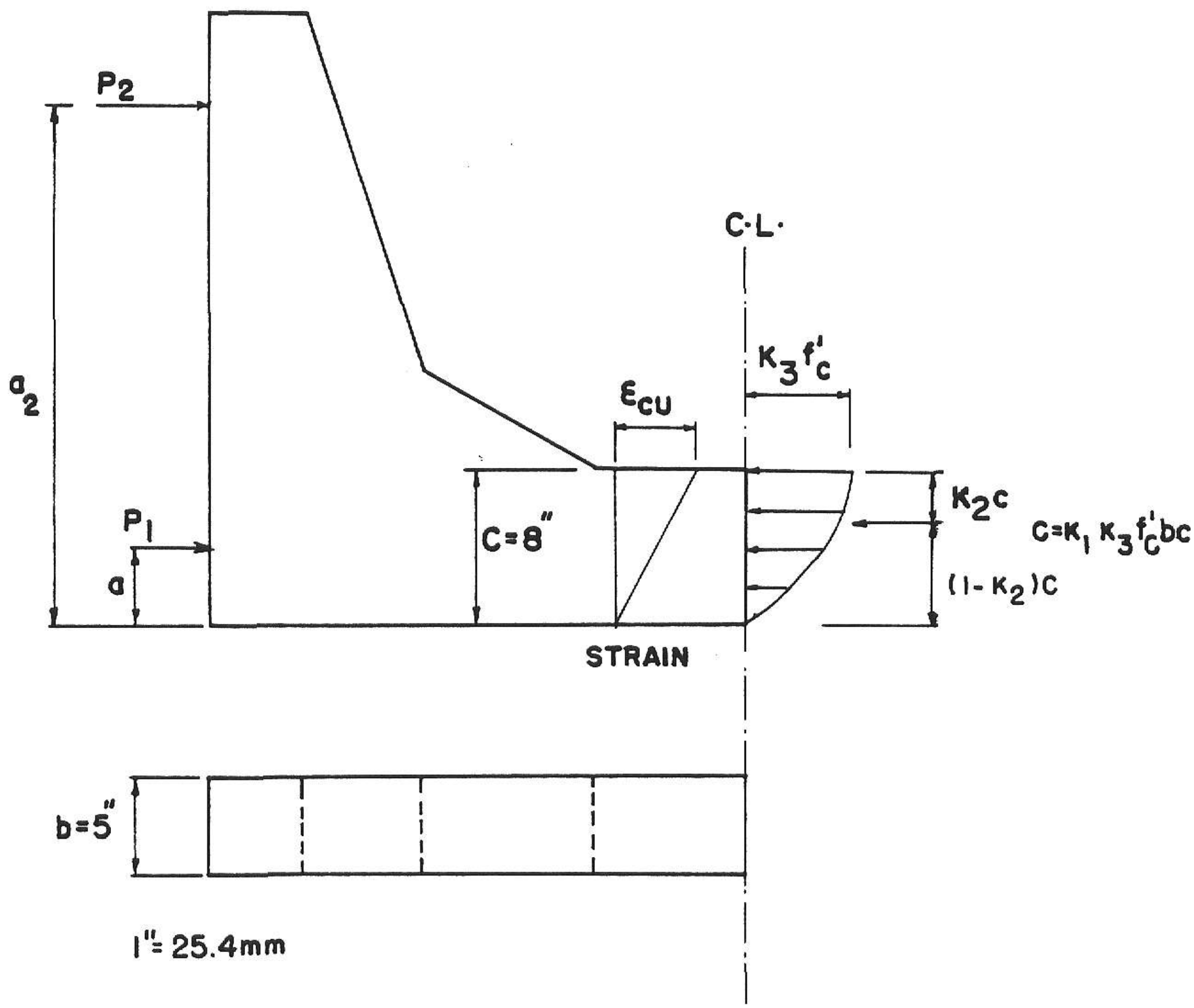

Figure 5.16: Condition at Ultimate Load in Test Specimen

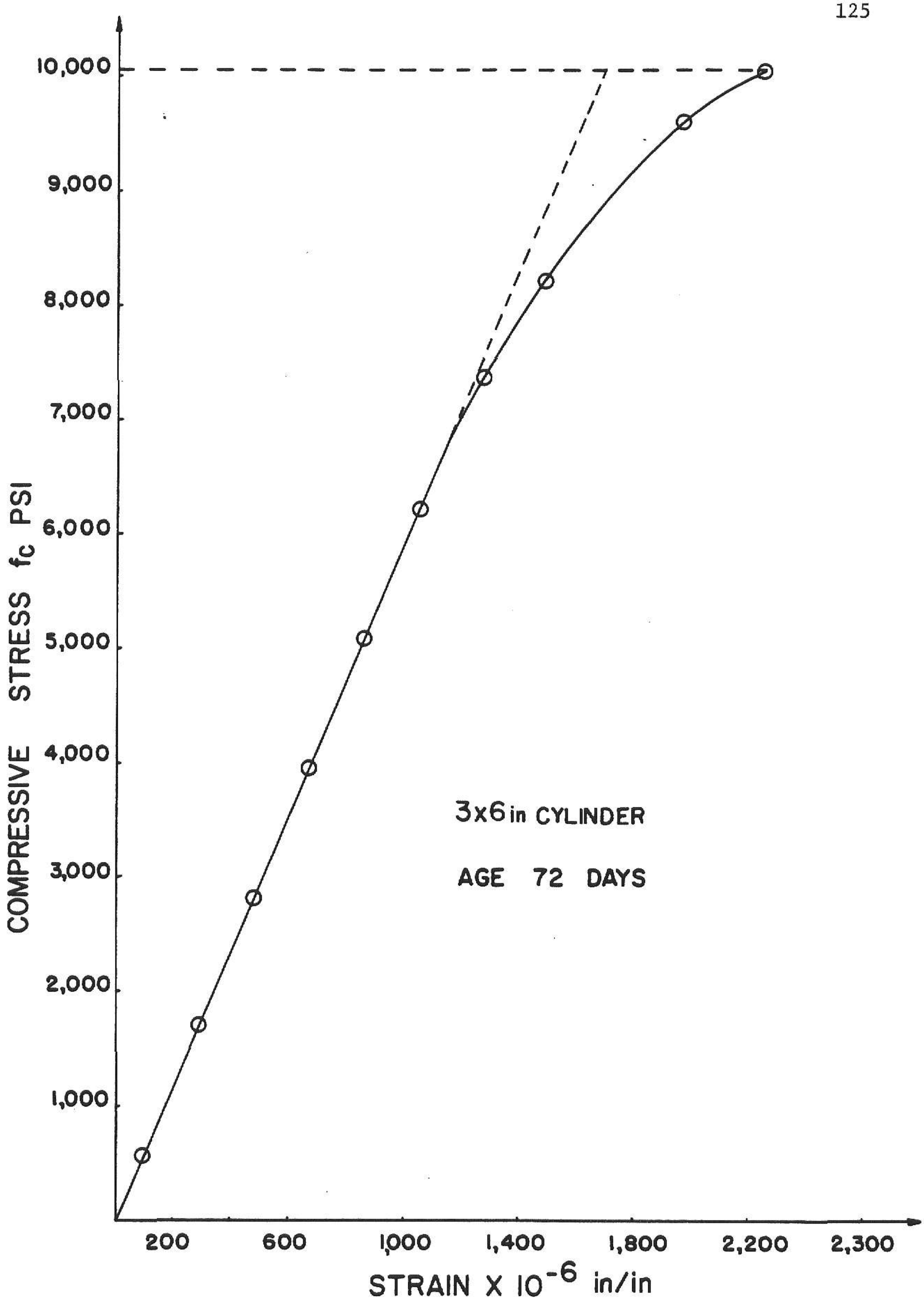

Figure 5.17: Cylinder Compressive Stress-Strain Curve for Specimen II

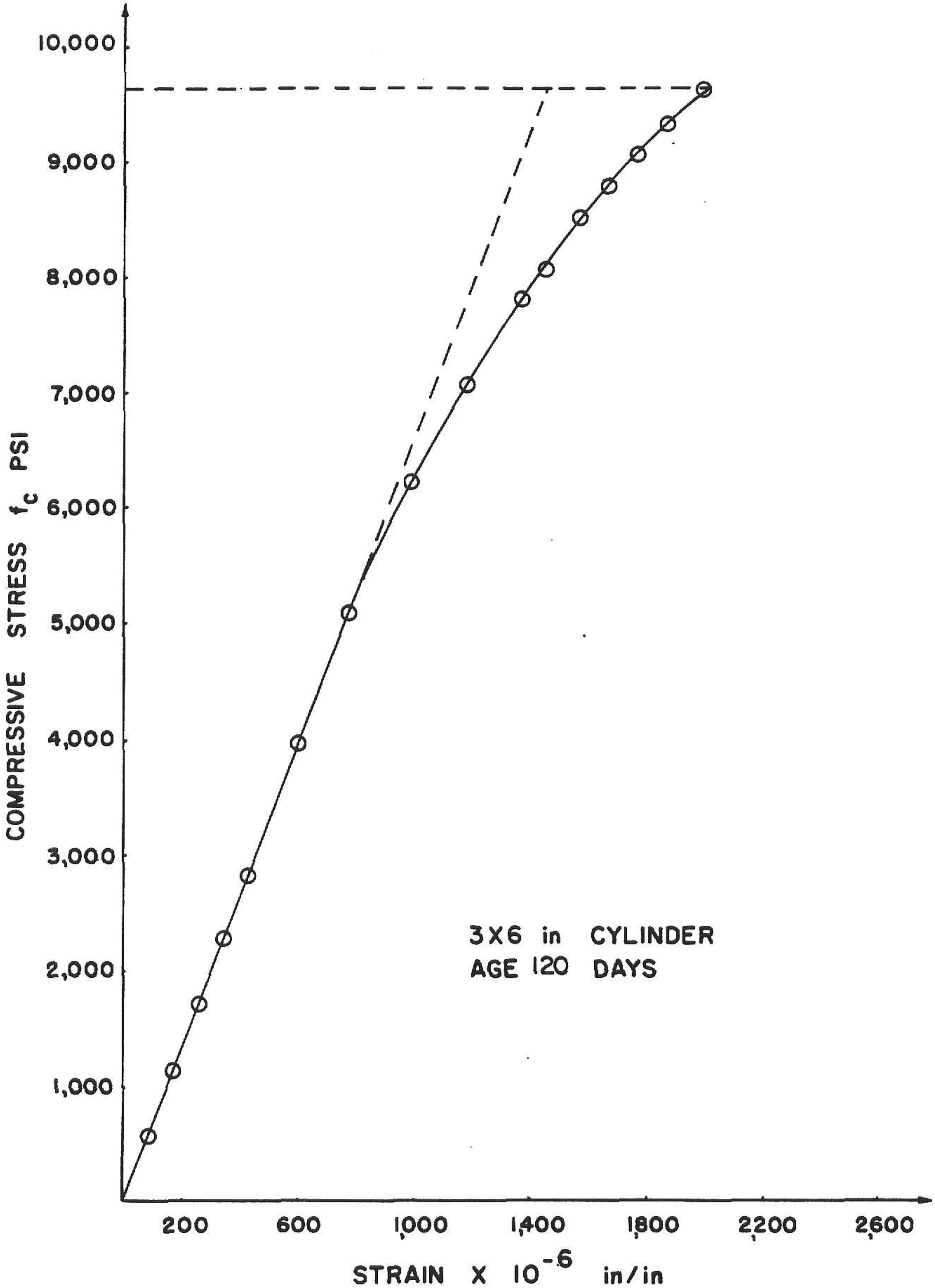

Figure 5.18: Cylinder Compressive Stress-Strain Curve

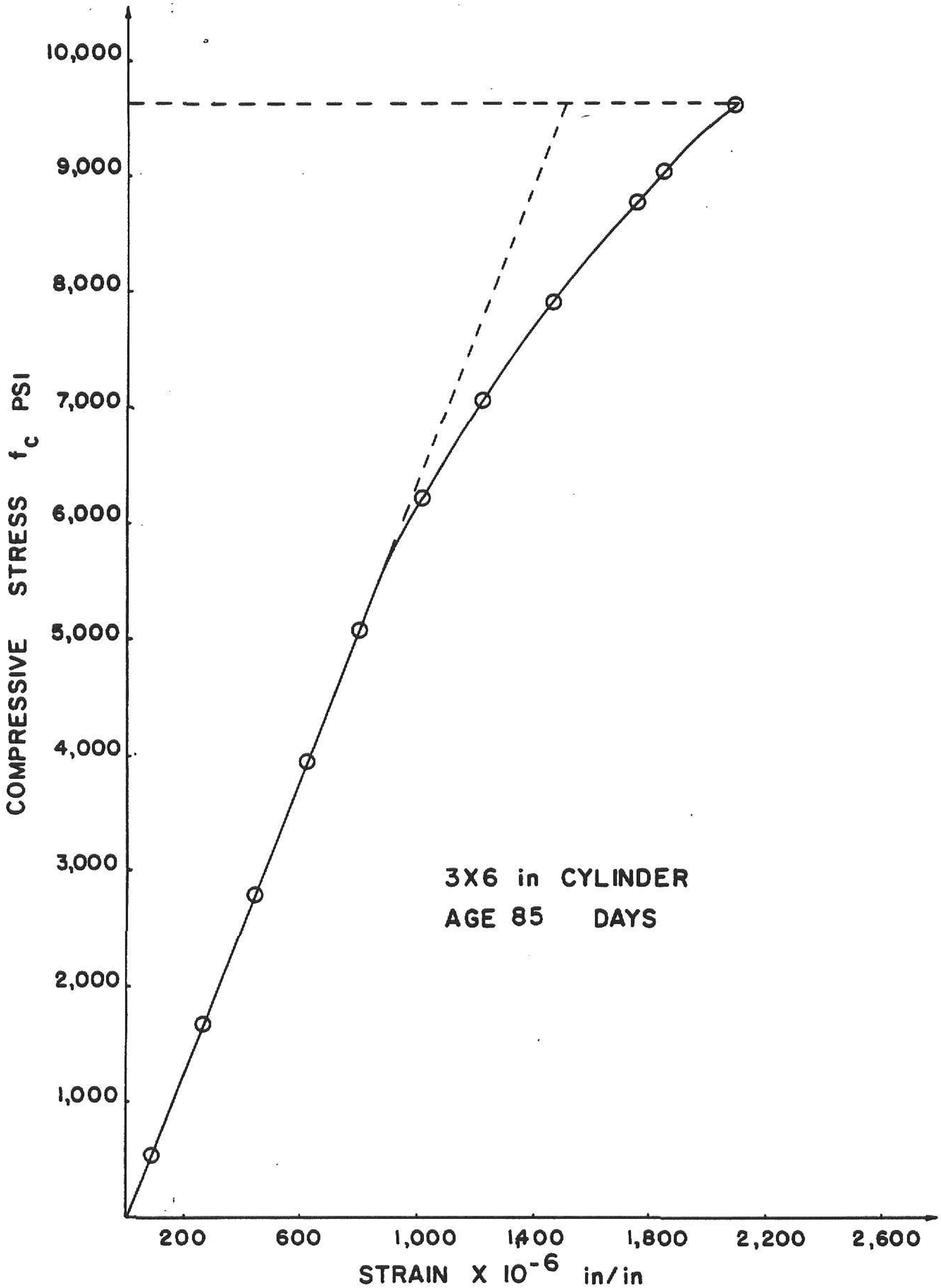

Figure 5.19: Cylinder Compressive Stress-Strain Curve

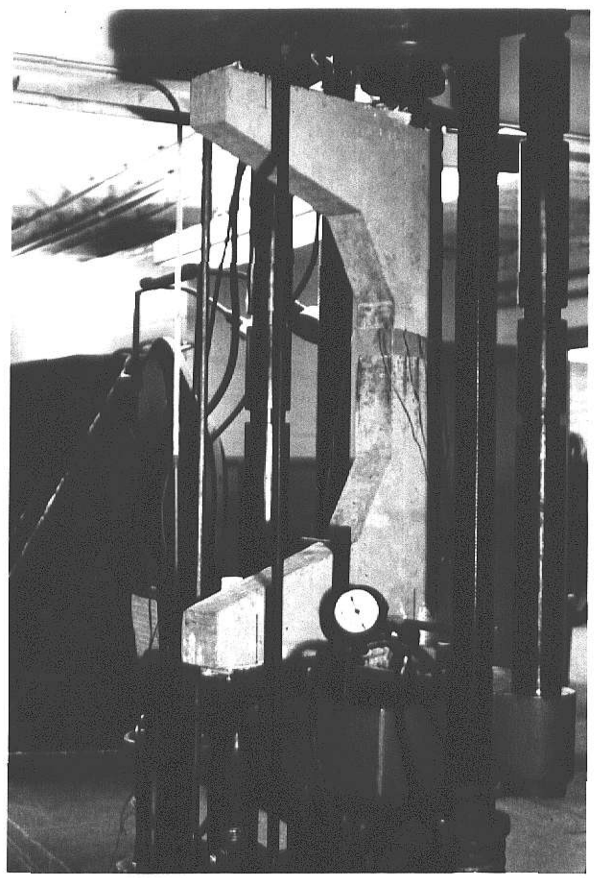

Figure 5.20: The Set-up of Element in Testing Machine

Figure 5.21: The Failure Mode

APPENDIX IV

NOTATION

W_c = weight of cement

W_s = weight of sand

W_w = weight of water

W_a = weight of coarse aggregate

γ_a = density of coarse aggregate

γ_s = density of sand

V_w = volume of water

V_c = volume of cement

V_A = volume of air content

V_s = volume of sand

V_a = volume of coarse aggregate

C.F. = cement factor

$\frac{W}{c}$ = water-cement ratio

γ_o = optimum density

P_1 = axial load applied by testing machine (i.e., major thrust)

P_2 = eccentric load applied by hydraulic ramp system (i.e., minor thrust)

M = moment

a = lever arm

T = force carried by reinforcement

C = concrete internal force

A_s = area of reinforcement

f_y = estimated allowable strength in reinforcement

f'_c = concrete cylinder strength

f_c = stress in concrete at different levels of loading

$\bar{y}$ = depth of stress block

d = distance for outermost fiber to center of gravity of steel

ϕ = reduction factor (i.e., for shear ϕ = 0.85)

A_b = area of one bar

A_v = cross-section of two legs in stirrup

V_u = applied shear force

V_c = shear force carrying by concrete

F_y = ultimate strength in rod

A = area

r = radius of rod

D = diameter of rod

K_1, K_2, K_3 = ultimate strength factor (K_1, K_2 are shape factors and K_2 is the position of concrete internal force from outermost compression fiber

M_u = ultimate moment

b = width of beam

c = depth of beam

h = height of beam

ε_c = strain at compression face

ε = strain

f_o, m_o = cross-section stress parameter

ACKNOWLEDGMENTS

The author is greatly indebted to his major professor, Dr. Stuart E. Swartz, for invaluable advice and guidance during his study at Kansas State University and carrying out this investigation.

Sincere thanks are due to Dr. Robert R. Snell, Head of the Department of Civil Engineering, for providing financial support for this project. Sincere thanks are also extended to Dr. Cecil Best for his guidance and help in developing high-strength concrete. Special thanks to Dr. Kuo-Kuang Hu and Dr. Peter B. Cooper for their guidance. Appreciation is also due to the other committee member, Dr. Leonard E. Fuller.

Special thanks to Mr. Abe Fattaey and my other Iranian friends who helped me in this project.

Special appreciation is expressed to Russell L. Gillespie, Civil Engineering Technician, for his guidance and help in using the facilities.

Special thanks also to Mrs. Peggy Selvidge, Secretary of the Civil Engineering Department, for typing this thesis.

The Production and Structural Behavior of High-Strength Concrete

by

ALI NIKAEEN

B.S.C.E., Kansas State University, 1979

AN ABSTRACT OF A MASTER'S THESIS

submitted in partial fulfillment of the

requirements for the degree

MASTER OF SCIENCE

Department of Civil Engineering

KANSAS STATE UNIVERSITY
Manhattan, Kansas

1982

ABSTRACT

High-strength concrete has been defined as that which has a compressive strength in the range from 6000 psi (41 MPa) to 12000 psi (83 MPa). The purpose of this report is to present results of a study of technique for production of high-strength concrete, the method for selecting materials and their proportions for mix design and the suitability of Kansas aggregate.

In addition, the compressive and flexural behavior of high-strength concrete made with the Kansas aggregates was studied in order to verify assumptions for certain stress-strain relations and the shape of the compressive stress block in bending.